PHD DISSERTATION 3|2017 | Forest Fragmentation in Space and Time...

Mateus Dantas de Paula

Forest Fragmentation in Space and Time – New perspectives from remote sensing and forest modelling

3|2017

HELMHOLTZ
CENTRE FOR
ENVIRONMENTAL
RESEARCH – UFZ

OSNABRÜCK 2016

Forest Fragmentation in Space and Time

NEW PERSPECTIVES FROM FOREST MODELLING AND REMOTE SENSING

Mateus Dantas De Paula

Cumulative Thesis for the degree of Doctor of Natural Sciences (Dr.rer.nat)

Forest Fragmentation in Space and Time – New Perspectives from Forest Modelling and Remote Sensing

Ph.D. Thesis

Mateus Dantas De Paula

Helmholtz Center for Environmental Research GmbH – UFZ

Department of Ecological Modelling

University of Osnabrück

Department of Mathematics/Computer Science

August 2016

Advisors

Prof. Dr. Andreas Huth (UFZ Leipzig/ University of Osnabrück)

Dr. Jürgen Groeneveld (Technische Universität Dresden/ UFZ Leipzig)

Publications part of this Thesis

Dantas de Paula, M., J. Groeneveld, et al. (2015). "Tropical forest degradation and recovery in fragmented landscapes - Simulating changes in tree community, forest hydrology and carbon balance." Global Ecology and Conservation 3: 664-677.

Dantas de Paula, M., Groeneveld, J., & Huth, A. (2016). The extent of edge effects in fragmented landscapes: Insights from satellite measurements of tree cover. Ecological Indicators, 69, 196-204. doi: 10.1016/j.ecolind.2016.04.018.

Additional publications:

Pütz, S., Groeneveld, J., Henle, K., Knogge, C., Martensen, A. C., Metz, M., Metzger, J. P., Ribeiro, M. C., **Dantas de Paula, M.**,Huth, A. (2014). Long-term carbon loss in fragmented Neotropical forests. Nat. Commun., 5, 5037. doi: 10.1038/ncomms6037

Fischer, R., Bohn, F., **Dantas de Paula, M.**, Dislich, C., Groeneveld, J., Gutiérrez, A. G., . . . Huth, A. (2016). Lessons learned from applying a forest gap model to understand ecosystem and carbon dynamics of complex tropical forests. Ecological Modelling, 326, 124-133. doi: 10.1016/j.ecolmodel.2015.11.018
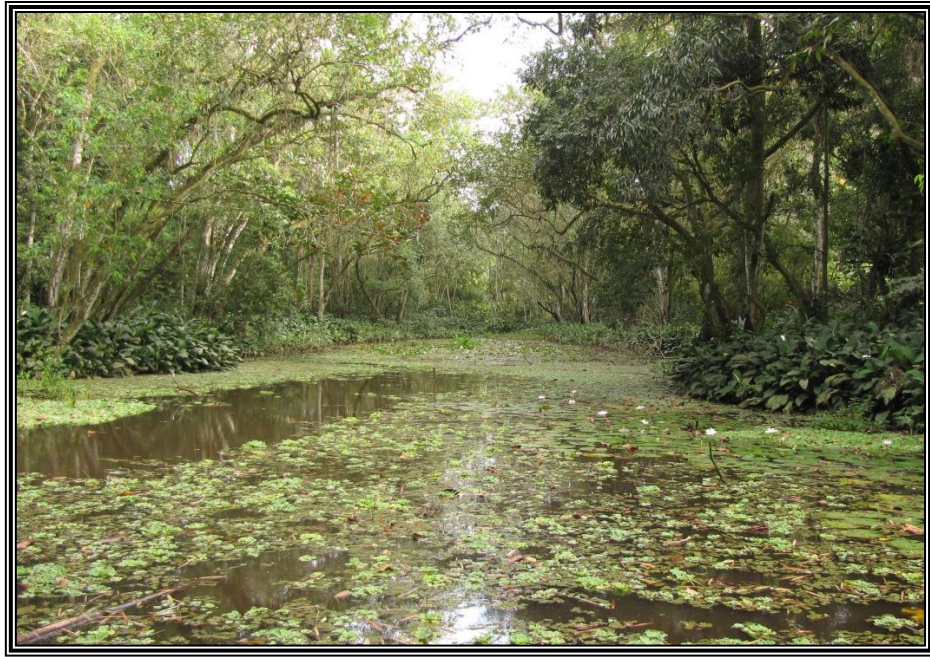
Under the tongue root a fight most dread,
and another raging, behind, in the head.

The alders in the front line began the affray.
Will and rowan tree were tardy in array.

The beech, though very noble, armed himself but late;
A sign not of cowardice but of high estate.

Some of them were cast away on the field of fright
Because of holes torn in them by the enemy's might.

In shelter linger privet and woodbine,
Inexperienced in warfare, and the courtly pine.

I have plundered the fern, through all secrets I spy.
Old Math ap Mathonwy knew no more than I.

For with nine sorts of faculty God has gifted me,
I am fruit of fruits gathered from nine sorts of tree

But I, although slighted because I was not big,
Fought, trees, in your array on the field of Goddeu Brig.

Cad Goddeu (The Battle of the Trees, Medieval Welsh Poem)

Understanding the mechanisms behind the functioning of Tropical forests represents one of the most interesting scientific challenges of our times. Extensive and dedicated field work and statistical analysis on the four continents where tropical forests are present have revealed an increasingly complex system where almost all biological groups present a very high level of interdependence and specialization in comparison with other forest types. This high level of specialization also means that tropical forests are very species-rich, and understanding why they have such high biodiversity is in itself a line of research (Wright 2002, Leigh et al. 2004, Rosindell et al. 2011).

The tree community composes most of the structure and provides most of the habitats for other biological groups in tropical forests, which are related to the species composition it has for a particular region (Gibson et al. 2011). Due to high level of interdependence and specialization, typical of tropical forests, this species composition will depend ultimately on the interaction with other biological groups. Tropical tree species depend greatly on animals for their life cycles through pollination and seed dispersal, and for their survivorship through herbivory, therefore animal species composition has also a great influence on tree species composition, closing the feedback loop.

Finally, thanks to technological breakthroughs in the field of environmental sensors, large spatial and temporal scale patterns of the biological processes in tropical forests are starting to be unraveled. Recent studies have revealed the profound influence tropical forests have in abiotic processes such as regional climate patterns (Spracklen et al. 2012), watershed dynamics (Trancoso et al. 2010) and soil composition (Camargo and Kapos 1995).

By using the individual based forest gap model FORMIND and data from remote sensing, complex forest dynamics and large scale patterns were investigated, under the context of forest fragmentation. In the first manuscript consequences of forest fragmentation to forest structure, carbon and hydrological cycles were investigated by using the FORMIND model; in the second, remote sensing data of tree cover was analyzed in order to observe large scale patterns of edge effects in different regions of the world. In the third and final chapter, the FORMIND model was again used to study the effects of animal loss in seed dispersal and eventually biomass retention of forests. At the time of the publication of this thesis, both the first and second chapters are published in peer reviewed journals.

ABSTRACT

Empirical studies on severely fragmented regions suggest that decades after fragmentation, forest edges located near human-modified areas exhibit the structure of early successional states, with lower biomass per area and higher mortality compared to non-edge areas. These habitat changes (edge effects) can also have a considerable impact on ecosystem processes such as carbon and water balance, which in turn have a major impact on human activities. Also, the disruption of ecological interactions caused by the loss of animals (defaunation) has the potential of impacting human influenced fragmented landscapes much deeper than only through the microclimate-induced increased tree mortality caused by edge effects. Since large animals are most vulnerable in these landscapes, large tree seeds which are dispersed by them become more vulnerable to pre-dispersal seed predation, reducing tree recruitment in latter stages. Also, the loss large animals which predate on smaller animals can cause relaxation of top-down controls of this small seed-eating animal group, further impacting tree recruitment. Even though detailed and long term studies were developed on the topic of edge effects at local scale, understanding edge effect characteristics in fragmented forests on larger scales and finding indicators for its impact is crucial for predicting habitat loss and developing management options.

Using field data from a long-term fragmented landscape in the Brazilian Northeastern Atlantic Forest, and the Forest Model FORMIND, we were able to visualize the time scale in which edge effects influence tropical forests by performing 500-year simulations. We observed changes in community composition, aboveground biomass, total evapotranspiration and total runoff, and evaluate the consequences of defaunation on biomass retention of a Brazilian Northeastern Atlantic Forest tree community by varying pre- and post-dispersal seed predation pressures in fragmented and intact scenarios. Finally, we evaluate the spatial and temporal dimensions of edge effects in large areas using remote sensing by using tree cover as an indicator of habitat quality and in relation to edge distance.

FORMIND simulations show forest biomass degradation lasting around 100 years. If edge effects cease, recovery of biomass lasts around 150 years. Carbon loss is especially intense during the first five years after fragmentation, resulting in a decline of over 5 Mg C ha^{-1} y^{-1}. Finally, edges of large fragments face an evapotranspiration loss of 43% and total runoff gains of 57% in relation to core areas of large fragments. The effects of large seed loss are only notable after 80% seed reduction or 10 times higher predation rates, but can cause the extirpation of this species group and up to 29% less biomass retention for the area. Our remote sensing results show that for all 11 LANDSAT scenes pixel neighborhood variation of tree cover is much higher in the vicinity of forest edges in relation to forest interior.

Our studies suggest that fragmented landscapes can be of significantly lower value in terms of ecosystem services, and that defaunation has the potential to reduce biomass retention and species richness through dispersal collapse. Satellite based estimations of tree cover at edges suggest a maximum distance for edge effects and can indicate the location of unaffected core areas. However, tree cover patterns in relation to fragment edge distance vary according to the analyzed region, and maximum edge distance may differ according to local conditions.

ABBREVIATIONS

BNAF – Brazilian Northeastern Atlantic Forest

DBH – Diameter at Breast Height

EVI – Enhanced Vegetation Index

fAPAR - Fraction of Absorbed Photosynthetically Active Radiation

GPP – Gross Primary Production

IBM – Individual Based Model

LAI – Leaf Area Index

LIDAR – Light Detection and Ranging

LTC – Landsat Tree Cover

NDVI – Normalized Difference Vegetation Index

ODM – Organic Dry Mass

PET - Potential Evapotranspiration

PFT – Plant Functional Type

PPFD - Photoactive Photon Flux Density

SAR – Synthetic Aperture RADAR

SAVI – Soil Adjusted Vegetation Index

SLOSS – Single Large or Several Small

REDD - Reduced Emissions from Deforestation and Degradation

VCF – Vegetation Continuous Fields

CONTENTS

1. OVERVIEW

1.1. THE STATE OF THE WORLD'S TROPICAL FORESTS

Forests are one of the most important biomes on earth, being habitat of over 70% of all terrestrial species, especially in tropical areas (Gibson et al. 2011). They relate to virtually all major terrestrial matter cycles, such as carbon, water and nitrogen, as well as climate (Hawkins et al. 2003, Kleidon 2009). Forests are particularly important for the carbon cycle, being considered a sink of around 1.2 Gt of Carbon per year (Houghton 2005, Houghton et al. 2009, Beer et al. 2010, Pan et al. 2011). Tropical forests are very rich in tree species having between 40,000 and 53,000 in total, and considering that most are very rare, they are very vulnerable to deforestation (Slik 2015). Therefore, human induced changes in forest cover are expected to impact ecological and ecosystem processes, in both large and small temporal and spatial scales. Considering temperature trends for example, (Alkama and Cescatti 2016) found that 18% of the biophysical warming due to CO_2 emissions may be caused by forest loss alone. From a pre-industrial total of 5,900 million hectares, total global forest area is now just over 5,000 million hectares, having lost on average 5.2 million hectares per year between 2000 and 2010, most of which in tropical forest areas (FAO 2015). This has caused a reduction of 46% in the global tree population (Crowther et al. 2015). The recent advance of human frontiers has claimed vast amounts of tropical forests (Hansen et al. 2013, FAO 2015) and has been the main driver of the ongoing tropical biodiversity change (Sala 2000). Since tropical forests are so important for biodiversity, this land change by humans is considered to be the main cause of the recent and ongoing species extinction level event (Ceballos et al. 2015).

Although forest loss can and is being reverted in parts of the word, one third of it occurred in primary forests, areas which have never before been removed by humans (FAO 2015). In comparison to temperate or even secondary tropical forests, primary forests are especially rich in biodiversity and in woody biomass content and are considered to be irreplaceable (Gibson et al. 2011). Strong drivers of forest loss in poor and biodiversity rich areas around the world have spurred the development of the "hotspot" concept, regions of focal action for reducing species extinction and loss of local and global environmental services (de Sherbinin 2013). Recent reports on forest cover have also highlighted the importance of considering the changes in remaining forest ecosystems even after deforestation in a particular area has ceased (Sloan and Sayer 2015). As developing countries are reducing their deforestation rates in the last years, this change of remaining forests, or forest degradation has become one of the focal points of forest change research. The Forest Resources Assessment (FRA) has for the first time measured the degradation of forests, defining it as a partial canopy cover reduction (PCCR) of >20% between 2000 and 2012, presumably as a result of fire, wood removals, small clearances, insect damages and so on (Sloan

and Sayer 2015). In the tropical regions, the area that experienced PCCR between 2000 and 2012 amounted to 156 million hectares, or 9% of the total forested area (van Lierop et al. 2015). This is equivalent to 6.5 times the total area of forest loss for the same period (Sloan and Sayer 2015). Forest degradation is also a significant source of carbon emissions, being equivalent to 9-24% of the total emissions due to deforestation (Pütz et al. 2014). Total global annual carbon emissions due to deforestation for the last decade are considered to be in the range of 1 Gt of Carbon per year (Baccini et al. 2012).

Forest degradation has a very strong temporal component - although the advance of human frontiers on the landscape level occurs in the scale of months, the shift from a stable climax community into a new stable state can take several decades (Pütz et al. 2014), in the case for example, of the collapse of the dispersion and recruitment mechanisms of long-lived trees (Oliveira et al. 2008). This causes the degradation process to last up to 100 years, as the slow life cycles of trees are influenced and tree communities shift to different compositions. Several other processes (e.g. evapotranspiration) can exhibit this slow-degradation pattern (Dantas de Paula et al. 2015), which must be now considered when mapping important ecosystem services such as carbon storage.

Most studies which deal with the human impact to forest ecosystem processes are focused on the carbon cycle (Houghton 2005, Pütz et al. 2014, Chaplin-Kramer et al. 2015). This is understandable since carbon stocks can be estimated from basal area measurements or estimations from forest inventories (FAO 2014). The study of other ecosystem processes is not as straightforward. Understanding the influence of forests to the water cycle however can mean complex, expensive and long duration projects, with lower number of sampling points (Ilstedt et al. 2007). The demand for information on this subject, is growing as the role of forest cover in regular, abundant and quality water sources becomes relevant for the quantification of ecosystem services. Also, the influence of forest transpiration in climate patterns is starting to become evident with remote sensing studies. For example (Spracklen et al. 2012) linked forest transpiration to the recharge of air masses, and considering climate models in conjunction with remote sensing data, predicted a reduction between 12 and 21 percent reduction of precipitation in the amazon considering current deforestation trends. Considering the complexities involved in studying the small and large scale hydrological processes in forests, the use of individual-based computer forest models opens exciting possibilities, due to their ability to process large amounts of data under many modelled processes and predict future conditions. By coupling models such as climate and soil to the forest model, it is possible to realize scientifically sound predictions. For example, using the forest model FORMIND, (Fischer et al. 2014) estimated that forest carbon stocks in Madagascar would be altered significantly only when rainfall decline in climate change scenarios was larger than 30%.

1.2. DEFORESTATION AND EDGE EFFECTS

On top of the challenges to understand the inherent complexities of the biotic and abiotic processes of tropical forests, comes the human dimension. The advance of humans in a forested landscape occurs through the exploitation of resources – either the removal of a resource from the forests (hunted animals, wood, etc.) or the land use change for the production of a particular crop, influencing natural habitats (Tilman et al. 1994, Fahrig 2003, Villard et al. 2014, Haddad et al. 2015, Newbold et al. 2015). Any one of these influences has the potential to change the species composition and the processes that depend on them (Cochrane and Laurance 2008). Species that flourish in the human influenced landscapes are commonly called "winners" by the conservation biology community, and those that perish are called "losers" (Tabarelli et al. 2012). Studies on these groups indicate that the winner species community is similar to an early successional state (Tabarelli and Lopes 2008, Pütz et al. 2011), as can be found in areas submitted to natural disturbances such as fire (Barlow et al. 2003, Cochrane and Laurance 2008, Grace et al. 2014). Typically, a landscape under human presence retains only remnants, "fragments" of the original forested landscape (Figure 1), on which biological groups inhabit in a metapopulation condition, similar to island archipelagos (Diamond 1972, Laurance et al. 1998). The habitat conditions inside these forest fragments will largely depend on their size, since the transition area between the agricultural matrix and the fragment's interior is influenced by edge effects (Murcia 1995, Didham and Ewers 2012). These edge effects cause altered microclimatic conditions up to 60 meters from the edge, such as lower humidity, higher temperature and light levels, which in turn influence the vegetation and consequently the animal communities (Kapos 1989, Kapos et al. 1993, Camargo and Kapos 1995).

Figure 1. Tropical forest remnants of Brazilian Atlantic Forest inserted in the sugarcane plantation of Usina Trapiche S/A.

Edge effects affect major ecosystem processes such as biomass storage (Laurance 1997, Barlow et al. 2003, Nascimento and Laurance 2004), and therefore accurate assessments of a fragmented landscape's condition to represent a pristine forest and its dynamics, will depend on understanding how far these edge effects penetrate into the fragment. The maximum edge effect penetration distance is related to the biological variable being analyzed, varying from less than 10 meters in the case of reduction of fugal fruiting bodies, up to 400 meters in the case of elevated wind disturbance (Figure 2). Most of negative effects however, occur within 100 meters of the edges (Laurance et al. 2002). Some animals react positively to edges, such as certain termites, aphids, and light loving butterflies (Brown and Hutchings 1997). But the most striking and habitat-altering consequences of edge effects are sharp increased rates of mortality and damage of large trees, which are disproportionately important umbrella species, and increasingly at risk of disappearance (Oliveira et al. 2008, Dantas de Paula et al. 2011a, Lindenmayer et al. 2016). In order to understand maximum edge penetration, the time since the edge creation plays a crucial role (Kapos 1989, Kapos et al. 1997). Young edges are very open environments where light, wind and warm air masses penetrate up to 100 meters – as time passes, regrowth around edges "seals" the edges and microclimatic changes can be noted only up to 10 meters (Didham and Lawton 2001).
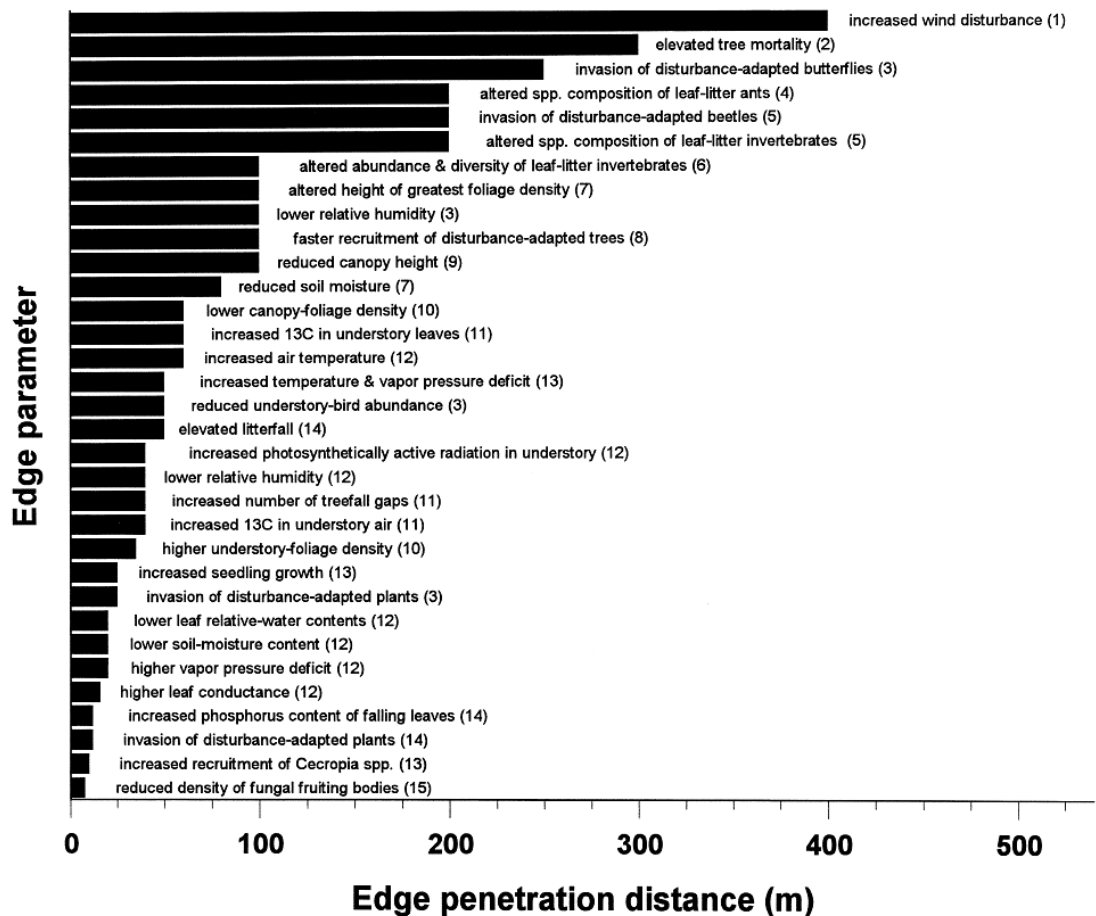
Figure 2. Penetration distances of different edge effects into the forest remnants of the Biological Dynamics of Forest Fragments Project (Laurance et al. 2002).

The wealth of field data information on forest fragmentation has also been studied in a landscape context (Hansson and Angelstam 1991, Metzger and Décamps 1997, Poiani et al. 2000), for planning and conservation purposes. The main underlying scientific challenge is to try and conciliate human landscape change, species survival and ecosystem function (Menon and Bawa 1997), which ultimately returns to human well-being in the form of ecosystem services (Menzel and Teng 2010). In the light of this, studies have modelled the condition of species in human landscapes drawing parallels with island biogeography theory (Laurance 2008)(i.e. forest fragments are islands supporting emigrating and extinction communities, proportional to fragment size and distance). This has sparked the SLOSS debate, in which a single large or several small forest fragments are preferred (Baz and Garcia-Boyero 1996, Ovaskainen 2002). The use of island biogeography theory to understand species dynamics in fragmented landscapes been met with general unfavorable field sampling follow up results, mostly reaching the conclusion that human landscapes are much more dynamic and permeable than water-isolated islands (Laurance 2008).

These human-natural landscape representations also incorporate edge effects in order to evaluate total natural available habitat (Zheng and Chen 2000). The edge definitions are generally a fixed distance from the human-forest border, defining fragments which are too small or with shapes which deviate too much from circles as completely dominated by edges (Sanderson et al. 2002). This concept too has been challenged with follow-up field results, which found variable edge distances in highly heterogeneous landscapes (Zheng and Chen 2000, Pinto et al. 2010), and very small fragments with particularly good mature-forest microclimate conditions (Götmark and Thorell 2003). This leads us to conclude that human-natural landscapes are highly context dependent, and at the moment edge effect generalizations can't be applied without accessing local conditions. Finally, changes in natural landscapes take time to reach a new equilibrium in terms of species composition and ecosystem processes. Therefore recent fragmented areas exhibit "debts" which will be "paid" in time, and to not reflect the actual condition to support biological groups (Tilman et al. 1994, Helm et al. 2006, Vellend et al. 2006). For example, in the Kansas fragmentation experiment, changes in succession patterns were only detectable after 12 years (Haddad et al. 2015). Studying the long term impacts of fragmentation is thus adamant for understanding and acting on the ongoing human induced species loss.

Apart from edge effects and deforestation, the loss of large and medium animals is one of the most striking consequences of human induced landscape change (Dirzo et al. 2014). This process, defaunation occurs due to the fact that large predators require extensive home ranges and food resources in order to survive in fragmented habitats, and are the first to disappear. In severely fragmented habitats such as the Brazilian Northeastern Atlantic Forest, only 19% of the large and medium mammals are present, in most of the habitat (Mendes Pontes et al. 2016). In the case of birds, large fruit eating birds are most vulnerable (Silva and Tabarelli 2000). This has two important indirect effects on tree communities. First, many tree species with large seeds are dispersed by large fruit eating birds and mammals, therefore in the absence of these animals their seeds remains undispersed and are very quickly attacked by bruchids. (Janzen 1969) noted that undispersed seeds are practically unviable ones. Second, the loss of large predators provokes a relaxation of top down seed consumer control, and predation rates can increase manifold (Dyer and Letourneau 1999). Considering that large seeds are not dispersed due to the lack of the seed disperser, and that smaller seeds escape predation satiating the predators with large numbers (Janzen 1969), there is an expectation that defaunated landscapes will be dominated by small seeded tree species (Silva and Tabarelli 2000). Since this tree group has also on average lower adult wood density (Chave et al. 2006), it is reasonable to expect that these communities will retain also less biomass. This has indeed been observed considering both the loss of birds in the Atlantic Forest (Bello et al. 2015), and the loss of large mammals in the Amazon (Peres et al. 2016).

1.3. FOREST MODELS

Due to the extraordinary life span of trees, studying forest dynamics using conventional experimental biology in the field becomes an arduous if not impossible task, easily surpassing project durations (Shugart 1984). This is why mathematical representations of forests and their processes are needed, fostering the field of forest modelling (Pretzsch 2009). Already in the 18th century the use of mathematical equations was proposed in order to predict future properties of tree populations (Pretzsch 2009). This was done at the time using Yield Tables, a tabular statement which summarizes per unit area basis all essential data relating to the development of a fully-stocked and regularly thinned even-aged tree crop at periodic intervals. Yield tables were mostly used for planning and taxation purposes, as well as predicting wood production in managed stands. Model development then progressed to sub-regional and site-specific yield table stands, and culminated in early 20th century in the construction of computer growth simulators for the evaluation of stand development under different management schemes (Botkin et al. 1972, Bugmann 2001). These earlier models were more focused on yield, therefore inputs and results were more aggregated, and details on individual trees lost. This made sense also because the field sites were generally monocultures or mixed stands with few species. With the expansion in computer processing in the 1960s, these models could now incorporate the influence of direct and indirect eco-physiological factors such as climate and soil properties, and then scientific questions on the ecology of natural and disturbed environments started to be made (Pretzsch 2009). For this a higher level of detail was needed on forest stands, therefore the concept of individual based modelling (IBM) was incorporated into tree models (Liu and Ashton 1995). Individual based ecology is a concept (and is the main tool to work with this paradigm) in which system properties emerge from individuals with adaptive behavior (Grimm and Railsback 2005). Tree succession, a common process in natural stands through which trees colonize un-forested habitats, and that also occurs after mortality of older trees, could now be much better analyzed with individual tree models (Shugart 1984, Shugart 1998). The constant succession state of mature stands caused by the death of older trees, creating gaps of light in the forest, was the basis behind one particular case of individual tree models, the gap models, which became the most important model class for studying the dynamics of natural forests (Bugmann 2001). The very first of these models, JABOWA (Botkin et al. 1972), was developed by Daniel Botkin and was able to successfully simulate the temperate Hubbard Brook forest with 13 species, by incorporating gap dynamics and competition for light and growth limitations caused by soil properties. This work made way for myriad other models, which rely on the same general principle of defining the simulation area as a collection of patches or plots (Shugart 1984, Bossel and Krieger 1991, 1994). These patches are generally

independent of each other, and most processes occur within one patch. Although sharing the same principle, in this early phase of development, models were developed for each forest type, generally adapting to the existing field data such as FORET (Appalachian deciduous forests (Urban et al. 1991)), BRIND (Australian Alps (Shugart and Noble 1981)), FORAR (mixed oak-pine forests of Arkansas (Mielke et al. 1978)), OUTENIQUA (mixed evergreen forests of the southern Cape, South Africa (van Daalen and Shugart 1989)), FORSKA (Norway spruce-dominated forests of central Sweden (Prentice and Leemans 1990)), FORCLIM (temperate forests of Europe (Bugmann and Solomon 2000)) and SIBBORK (boreal forests (Brazhnik and Shugart 2016)).

Applying the gap model concept to tropical forest types provides a higher level of complexity, due to the sheer amount of tree species, and the multi-tiered height structure. One of the first gap models to take on this challenge was the FORICO model (Doyle et al. 1982), based on the FORET, which was applied in a lower montane rainforest in Puerto Rico. Major modifications included the recomputation of all model parameters and the incorporation of a model subroutine to consider the disturbance effects of hurricanes which are common to forests in the West Indies. The FORICO simulated 36 tree species, each with its own parameter set, but model structure remained virtually the same as FORET. A later model applied to the forests of southeast Asia (Huth and Ditzer 2000), FORMIX brought the concept of plant functional types into the gap model approach, which became an interesting strategy to aggregate new species properties with similar functional role. This model was used extensively to investigate different logging (Kürpick et al. 1997, Huth and Ditzer 2001, Kammersheidt et al. 2002, Huth et al. 2004) and more recently climate change scenarios (Fischer et al. 2014), focusing on biomass results. The temperate forest pedigree of early individual based forest gap models is certainly one of the explanations for a limited approach when simulating tropical forests. Unlike temperate types, the great interdependence of tropical tree communities on other biological groups means that seed dispersal and predation, pollination and herbivory reach a much higher level of influence on species survivorship, and must be incorporated in the simulations. With very few exceptions (Köhler et al. 2002), the incorporation of those interactions of trees and other biological groups has been non-existent in forest models. This is unfortunate, since forest models have great potential in analyzing ecological interactions and cascades such as defaunation, which is being studied for its consequences to the carbon cycle through tree loss (Peres et al. 2016).

FORMIND (Köhler and Huth 1998), a version of FORMIX with a continuous height layer structure, became very successful in tropical forest simulation, for being used in several tropical forest types and even some temperate areas. Its continuous use for 25 years in 19 reference study sites around the tropical belt have confirmed its importance as one of the most prominent local scale forest simulation models (Fischer et al. 2016). Within FORMIND, physiological processes such as

photosynthesis and respiration are simulated at the tree level, and the simulation area is a composite of 20-m × 20-m patches that can interact via seed dispersal and the falling of large trees (Figure 3). Light falling on the top of the forest canopy is the main driver of the FORMIND model. As light travels to the forest floor, it is attenuated according to the light extinction coefficient and the Leaf Area Index (LAI) of tree crowns on each height layer. The closing (through regrowth) and opening (through mortality) of canopies will allow light to reach the forest floor which in turn regulates seedling establishment. Tree growth and response to light are typical tree properties which attempt to simulate real forest species composition by grouping trees into plant functional types (PFTs). Most studies in FORMIND consider light response and maximum height as functional grouping approaches. Geometric properties of trees, such as height, crown size and shape, are determined by the trunk diameter at breast height, a common field measurement, using allometric relations. This allows for a simpler initialization of FORMIND with field data, and result comparison. Photosynthesis determines diameter growth, which in turn provides height increments and chances to reach higher light levels at the top of canopy. In addition to light responses, limitations to photosynthesis can also be implemented using environmental factors such as water use efficiency in the soil, and temperature variations. The life cycle of trees is also implemented in detail, with seeds being thrown from adult trees of each PFT according to pre-defined dispersal kernels, and falling into seed banks. Surviving seeds germinate according to the light conditions at the forest floor, and become seedlings which face high diameter dependent mortality. Once reaching the adult phase, trees grow according to their predetermined PFT growth rates and die according to mortality rates, either standing or falling causing damage to neighboring trees. For each tree a so-called carbon balance (photosynthesis – respiration) is calculated. FORMIND can output a wealth of results for each year of simulation, with the most common being basal area, biomass, stem number, carbon flux, stem diameter distribution, number of falling trees, fire damages, leaf area index, logging, mortality, seed numbers, seedling numbers, and soil-water results. A full model description and up to date publication list can be found in (Fischer et al. 2016) as well as in the FORMIND website (www.formind.org). In FORMIND's parameterization, it is possible to choose from several equations in order to simulate ecological processes and tree properties. For the simulations executed in this Thesis, I use the equations described in the appendix (Equations A1).
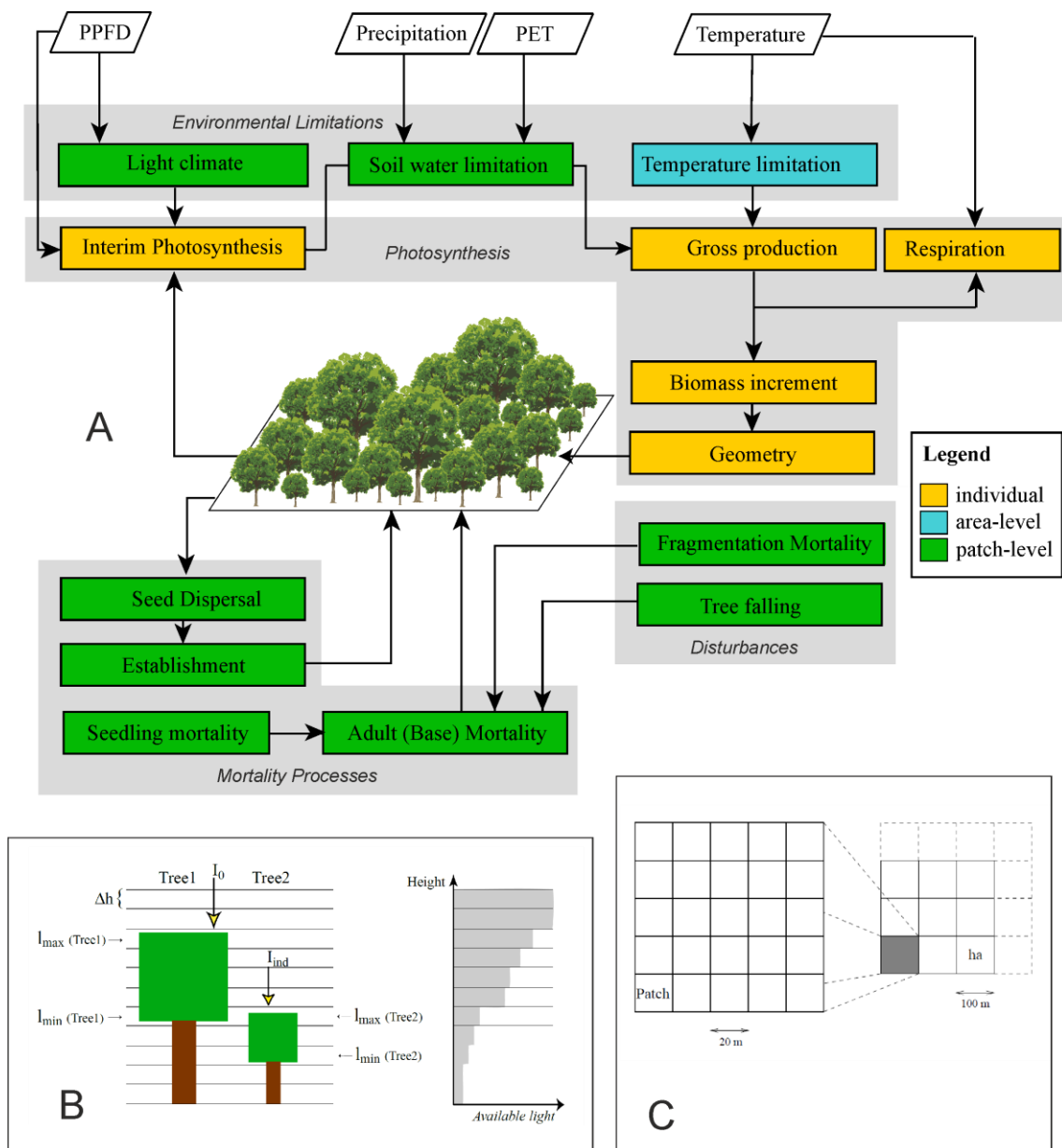
Figure 3. Overview of the FORMIND model. A. Block diagram of the modelled processes in FORMIND. Different colors indicate the spatial scale on which each process is calculated (blue = area, green = patch, orange= individual). Rhombuses indicate climatic input parameters with the following abbreviations: PET (potential evapotranspiration), PPFD (photoactive photon flux density). B. Simulated light response in tree canopy, depending on I0 (incoming radiation) and its value for each height (h) layer, light varies for each tree in relation to top (Imax) and bottom (Imin) of canopy. C. spatial structure in which the model operates (Köhler 2000). Based on graphs from the FORMIND handbook (www.formind.org).

The main power of FORMIND is its modular approach, developed through the various application studies using the model, and that can raise its complexity level. Several aspects of tree ecology have

been studied by FORMIND. These have analyzed questions in relation to tree community dynamics (Groeneveld et al. 2009), and the effect of functional group richness and neutral theory implementations in correctly predicting ecosystem properties (Kazmierczak et al. 2014). The effect of disturbances in forests has been a popular topic in FORMIND studies, for example logging (Huth and Ditzer 2001, Kammersheidt et al. 2002, Huth et al. 2004), fire, and landslides (Dislich and Huth 2012). Forest fragmentation in particular has been studied since the original implementation of the FORMIND fragmentation module by (Köhler 2000), based on higher tree mortality rates for patches on the edge of the simulation area. Expanding on this, (Pütz et al. 2011) analyzed different simulation areas and studied different external seed input values, and conclude that forest fragments below 25 hectares suffer substantial structural changes, with up to 60% reduction in biomass, and external seed rain was only able to compensate for about 30% of the fragmentation effects. A follow up study integrated these results with remote sensing (Pütz et al. 2014), and highlighted the importance of forest edge degradation to total carbon emissions due to deforestation, being between 9 and 24% of the total. Recent studies are showing that local models such as FORMIND have a large role to play in increasing the mapping accuracy of several ecosystem processes, for example carbon content (Shugart et al. 2015). Comparisons between models and remote-sensing products allow detailed models to be tested, fueling a hypothetic-deductive approach to ecological research. For example, relatively simple regression models using LiDAR metrics can provide predictions of aboveground biomass of tropical forests at hectare scales over a wide range of conditions (Shugart et al. 2015). The model is managed by a team of interdisciplinary researchers from the Helmholtz center for environmental research – UFZ, in a subversion framework, which allows for the consistency of recent changes in relation to past applications of the model. Finally, FORMIND is being prepared to become available online in an open source format, which can increase the number of users and aggregate to its applicability, precision and complexity. It has then the potential to become a broad platform in which tropical forests can be simulated.

1.4. REMOTE SENSING OF FORESTS

Remote sensing is a relevant tool for studying the spatial, spectral and temporal aspects of forest, and is particularly useful in its ability to acquire large quantities of data in short time (Menon and Bawa 1997). The data is produced by passive or active light sensors, boarded on aerial or space borne, manned or unmanned platforms (Ustin 2004), as can be seen in Figure 4 and in the list in Table 1. Passive sensors collect light reflected from the sun in the visible and invisible spectra, known to be useful in mapping forest extent and photosynthetic productivity (Carson and Ripley

1997). Active sensors beam electromagnetic energy to earth and measure its return properties, commonly using Synthetic Aperture Radar (SAR) sensors (Ustin 2004). These systems are particularly useful in measuring canopy height, an important measurement to determine forest structure (Neumann and Reigber 2010).
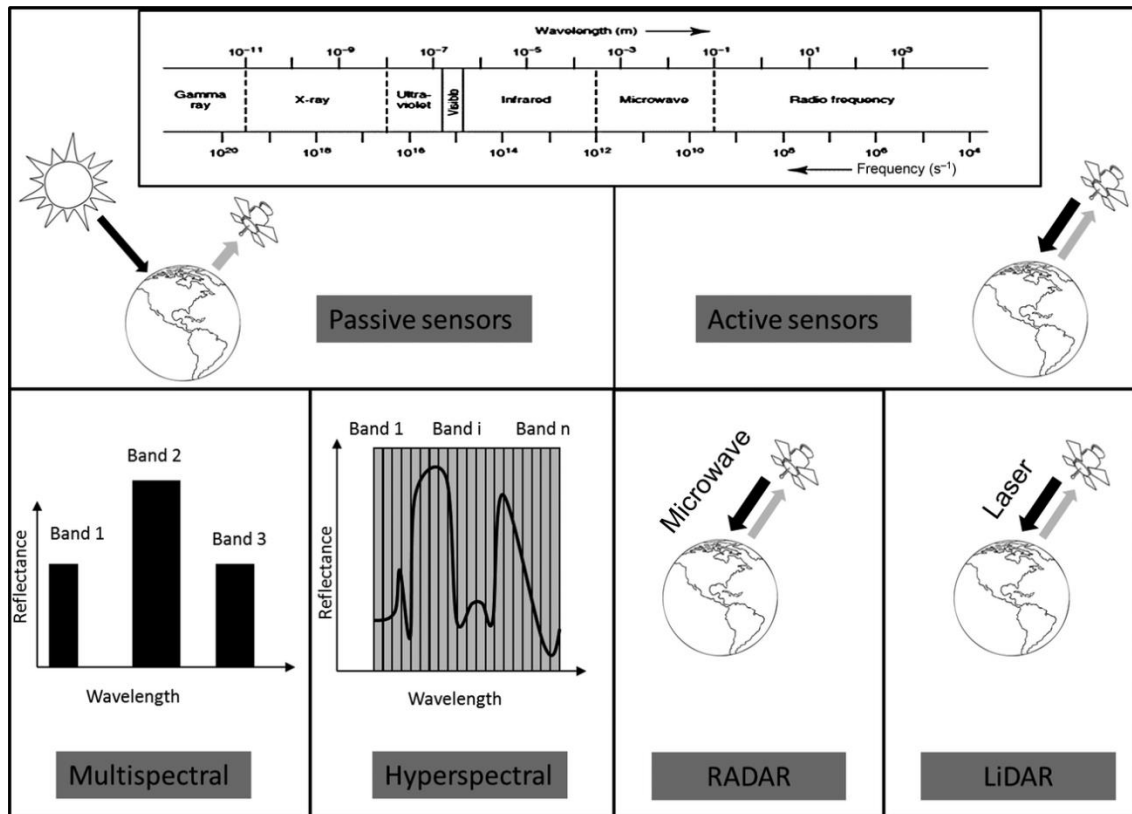

Figure 4. Main types of sensor aboard remote sensing platforms (Pettorelli et al. 2014).

The spatial aspect of satellite data refers to the resolution of the acquiring sensor, which suggests the detail available in terms of pixel size. For georeferenced digital images pixels have a size in meters or degrees, and this determines the range of applications the data is able to be used in. For regional to global studies, 100-1000 m coarse resolution sensors are used, while for tree to stand-level observations fine (<10 m) data are needed (Ustin 2004). An important limitation of the coarse spatial resolution however, is that detail is lost at a rate dependent on the dimensions of ground features (Niemann et al. 1997), therefore errors are scaled and information may become too imprecise. This aspect of coarse resolution data can be highlighted by recent attempts to map global tropical biomass using diverse remote sensing products, such as (Saatchi et al. 2011) with 1 km resolution and (Baccini et al. 2012) with 500 m resolution. These global biomass maps unfortunately provide conflicting results when comparing to ground plots, with whole regions being over or under estimated by >25% (Mitchard et al. 2014). A more recent attempt in biomass

mapping has promised improved results (Avitabile et al. 2016), but remains at a coarse resolution of 1 km.

Multi-temporal observations of forests are necessary in several studies which aim to evaluate seasonal changes in forest properties (Huang et al. 2009), analyze human land use change (Hansen et al. 2013), or obtain images which are free from adverse atmospheric conditions such as clouds (Seddon et al. 2016). The temporal resolution of satellites is the time between successional observations of a particular area, and is also known as "revisit time". Therefore, sensors designed to acquire data on a daily basis (e.g. MODIS) are able to record well the presence of forest fires (Hansen et al. 2008b), and others with a lower acquisition frequency (e.g. 16 days for LANDSAT) are most suitable for land use change studies (Huang et al. 2009).

Since remote sensing relies on capturing electromagnetic radiation data from objects, when considering measurements from vegetation, photosynthesis and leaf water content becomes the most important ecological processes for studying vegetation remotely (Ponzoni and Shimabukuro 2007). Satellite-boarded sensors contain cameras which are sensitive to different spectral intervals. These intervals, or bands, are chosen in order to be sensitive to different regions of the landscape, such as water, soil, or vegetation. Considering that plants absorb solar radiation within the range of 0.55 to 0.67 μm, and water absorbs radiation in the short wave infrared region (1.3 – 2.50 μm), evaluating reflective patterns of the landscape inside this ranges provides most information of vegetation properties and conditions (Ustin 2004). Recent advances in satellite and sensor technology have further enhanced our capabilities in forest remote sensing. Hyperspectral sensors such as HYPERION aboard the EO-1 observe in 50 or more bands are able to create a contiguous spectral signature of the reflected forest cover, offering the opportunity to study data from satellites in a similar manner to chemical spectroscopy (Ustin 2004). This offers a huge potential for differentiating tropical forest species, as differences in their biochemical composition, structure and water content are reflected (Clark et al. 2005, Asner and Martin 2008, Townsend et al. 2008, Asner 2009, Asner and Martin 2009, Asner et al. 2011, Asner et al. 2014). However, attempts to identify species composition with hyperspectral satellite data (Clark et al. 2005, Alonzo et al. 2014, Dalponte et al. 2014), in high diversity areas remains a technical challenge. Active remote sensing system explores with Synthetic Aperture Radars (SAR) the three-dimensional structure of forest by beaming down radiation at different wavelengths and measuring the distance of the return signal (Neumann and Reigber 2010). The longer the wavelength (or lower frequency) of the SAR sensor, the more it penetrates into the canopy. Therefore X (3 cm wavelength) or C (5.6 cm wavelength) Band SARs operating at 10 and 5.3 GHz respectively are more adequate to measure canopy height, while L (23.5 cm wavelength) and P (74 cm wavelength) Band SARs operating at 1.25 and 0.4 GHz respectively reflect at the ground or at more dense elements such as tree trunks, providing

estimates of biomass (Ustin 2004). LIDAR, another active remote sensing concept, typically uses Near Infrared laser pulses to estimate tree heights, and provide currently the best predictions of forest structural parameters (Zolkos et al. 2013). However, LIDAR measurements are currently limited to aerial platforms (with the exception of the GLAS/ICEsat satellite, unfortunately no longer in operation), which entail high cost and limited areas (Su et al. 2016). Although active sensors show a promising future role in

Table 1. Selected space borne missions with sensors relevant for the study of vegetation.

Provider	Mission	Acquisition Period	Sensor	Type	Spectral Resolution (No. Bands, Wavelength Range in μm)	Temporal Resolution (Days)	Spatial Resolution (m)	Access
NASA	LANDSAT 9	2023	-	Optical Passive	-	16	-	Free
ESA	-	2020	BIOMASS	P-Band SAR	1	-	50 to 200	Free
ESA	Tandem-L	2020	SAR-L TandemL	L-Band SAR	1	8	1	Free
ESA/DLR	EnMAP	2018	HSI	Optical Passive	232 (0.42-2.45)	4	30	Free
Digital Globe	WorldView-4 (GeoEye-2)	2016-	GIS-2	Optical Passive	5 (0.45-0.92)	1	0.31 to 1.24	Private
ESA	Sentinel 3A and 3B	2016-	OLCI	Optical Passive	21 (0.4-1.02)	1	300	Free
ESA	Sentinel 2A and 2B	2015-	MSI	Optical Passive	12 (0.443-2.19)	5	10 to 60	Free
Digital Globe	WorldView-3	2014-	WV-3 CAVIS, MSS, PAN, SWIR	Optical Passive	16 (0.405-2.365)	<1	0.31 to 1.24	Private
ESA	Sentinel 1A and 1B	2014-	SAR-C Sentinel1	C-Band SAR	1	12	5	Free
JAXA	ALOS-2	2014-	PALSAR-2	L-Band SAR	1	14	3	Free
NASA	LANDSAT 8	2013-	OLI, TIRS	Optical Passive	11 (0.43-12.51)	16	15 to 100	Free
EUMETSAT	Metop-B	2012-	AVRRH/3	Optical Passive	6 (0.58-12.5)	0.5	1,090	Free
EADS/Astrium	PLEIADES 1A and 1B	2011-	HiRI	Optical Passive	5 (0.45-0.89)	26	0.7 to 2.8	Private
Deimos Imaging	Deimos	2009-	HiRAIS	Optical Passive	5 (0.45-0.89)	2	0.75 to 5	Private
Digital Globe	WorldView-2	2009-	WV110	Optical Passive	8 (0.45-1.04)	1.1	0.41 to 2.4	Private
Digital Globe	GeoEye-1	2008-	GIS-MS, GIS-PAN	Optical Passive	5 (0.45-0.92)	1	0.41 to 1.65	Private
Canadian Space Agency	RADARSAT-2	2007-	RADARSAT-1	C-Band SAR	1	24	1 to 100	Private
Digital Globe	WorldView-1	2007-	WV	Optical Passive	1 (0.4-0.9)	1.7	0.4	Private

Provider	Mission	Acquisition Period	Sensor	Type	Spectral Resolution (No. Bands, Wavelength Range in µm)	Temporal Resolution (Days)	Spatial Resolution (m)	Access
ESA	TerraSAR-X/Tandem-X	2007-	SAR-X	X-Band SAR	1	11	1	Free
JAXA	ALOS	2006-2011	AVNIR-2	Optical Passive	4 (0.42-0.89)	46	10	Free
JAXA	ALOS	2006-2011	PALSAR	L-Band SAR	1	46	10	Free
EUMETSAT	Metop-A	2006-	AVRRH/2	Optical Passive	6 (0.58-12.4)	0.5	1,100	Free
NASA	ICESat	2003-2010	GLAS	LIDAR	2 (0.532 and 1.064)	183	70	Free
ESA	ENVISAT	2002-2012	MERIS	Optical Passive	15 (0.41-0.9)	3	300	Free
ESA	ENVISAT	2002-2012	ASAR	C-Band SAR	1	-	30	Free
Digital Globe	Quickbird	2001-	Quickbird	Optical Passive	5 (0.45-0.9)	2.4 to 5.9	0.61 to 2.44	Private
NASA	EO-1	2000-	Hyperion	Optical Passive	220 (0.4-2.5)	16	30	Free
NASA	EO-1	2000-	ALI	Optical Passive	10 (0.48-2.35)	16	10 to 30	Free
CRESDA/INPE	CBERS1-4	1999-	PAN, WFI, MUXCam, IR-MSS	Optical Passive	5 (0.45-0.73)	52	5 to 10	Free
Digital Globe	Ikonos	1999-	OSA	Optical Passive	5 (0.45-0.9)	3	1 to 4	Private
NASA	LANDSAT 7	1999-	ETM+ (obs. SLC failure)	Optical Passive	8 (0.45-0.9)	16	15 to 60	Free
NASA	Terra	1999-	MODIS	Optical Passive	36 (0.62-14.385)	2	250 to 1,000	Free
NASA	Terra	1999-	ASTER	Optical Passive	15 (0.52-11.65)	16	15 to 90	Free
EADS/Astrium	SPOT4-5	1998-	VEGETATION	Optical Passive	4 (0.43-1.75)	1	1,000	Free
EADS/Astrium	SPOT4-7	1998-	HRG,HRVIR,NAOMI	Optical Passive	5 (0.45-0.9)	1 to 5	1.5 to 20	Private
NOAA	NOAA15-19	1998-	AVRRH/3	Optical Passive	6 (0.58-12.5)	0.5	1,090	Free

Provider	Mission	Acquisition Period	Sensor	Type	Spectral Resolution (No. Bands, Wavelength Range in µm)	Temporal Resolution (Days)	Spatial Resolution (m)	Access
Canadian Space Agency	RADARSAT-1	1995-2013	RADARSAT-1	C-Band SAR	1	24	10 to 100	Private
JAXA	JERS-1	1992-1998	SAR	L-Band SAR	1	44	18	Free
JAXA	JERS-1	1992-1998	OPS	Optical Passive	8 (0.52-2.4)	44	18	Free
ESA	ERS 1 and 2	1991-2011	AMI	C-Band SAR	1	3	30	Free
NOAA	NOAA10-14	1986-2007	AVRRH/2	Optical Passive	6 (0.58-12.4)	0.5	1,100	Free
EADS/Astrium	SPOT1-3	1986-1996	HRV	Optical Passive	4 (0.5-0.73)	4	10 to 20	Private
NASA	LANDSAT 5	1984-2013	MSS	Optical Passive	4 (0.5-1.1)	16	60	Free
NASA	LANDSAT 4	1982-2001	TM, MSS	Optical Passive	7 (0.45-2.35)	16	30 to 120	Free
NASA	LANDSAT 1-3	1979-1983	MSS	Optical Passive	5 (0.5-12.6)	18	79	Free

remote sensing of vegetation, the use of optical sensors is still more widespread in forest research due to the huge amount of freely available data in long temporal intervals (Huang et al. 2009).

Some remote sensing products are particularly useful for mapping land vegetation properties, and are generated by integrating multiple spectral and field reference data. For example the vegetation indexes are created by summing or multiplying image pixels according to ecologically relevant spectral bands (Bannari et al. 1995). These indexes such as Normalized Difference Vegetation Index (NDVI), Enhanced Vegetation Index (EVI) or Soil Adjusted Vegetation Index (SAVI) using mainly the red and infrared bands, have been known to correlate to a number of vegetation processes. NDVI has been particularly studied (Pettorelli 2013), and known to relate significantly with: Plant richness, with both positive (Gould 2000, Bawa et al. 2002) and negative (Oindo et al. 2000) correlations; Plant community patterns, in order to inform species distribution (Pérez-Hoyos et al. 2010) and composition (He et al. 2009); Plant attributes such as Leaf Area Index (Wang et al. 2005), net primary production (Schloss et al. 1999) and fraction of photosynthetically active radiation absorbed by the photosynthesizing tissue in a canopy (Myneni and Williams 1994, Carson and Ripley 1997); and plant physiological status, for example stress under herbivory (Dantas de Paula et al. 2011b). The vegetation index approach is however fraught with limitations especially for areas with very high leaf density (Bannari et al. 1995, Pettorelli et al. 2005). Tree cover in particular is also an important forest descriptor (Sexton et al. 2015), being especially related to canopy openness, which is one of the main properties of forest edges in fragmented forests (Muraoka and Koizumi 2005, Köhler and Huth 2007, Neumann and Reigber 2010). Although links with ground based information are fundamental, many of these characteristics can be obtained through remote sensing. Vegetation continuous fields (VCF) is one of those, and represents each point in the land surface into three different components: percent tree cover, non-tree cover and bare (non-vegetation) cover, with all three summing up to 100% (DeFries et al. 1995, DeFries et al. 1999). It was originally developed for the MODIS (Moderate Resolution Imaging Spectroradiometer) satellite (Hansen et al. 2005), and is generated with an algorithm which receives as input 1. Training data generated mainly from orthorectified Landsat Geocover maps; 2. 16-day MODIS surface reflectance composite (bands 1-7) and brightness bands 20, 31, 32; and 3. MODIS Global 250 meter Land/Water map. The resulting tree cover pixel values, generated by averaging 30 independent regression trees, represent light penetration to the ground, as opposed to simple "crown" cover. The 30 meter LANDSAT VCF dataset is a further improvement of the original MODIS product, and was created using 2000 -2005 LANDSAT images and MODIS' own Cropland Layer in order to increase the accuracy of agricultural areas (Townshend et al. 2011).

Remote sensing has been considered also particularly useful for biodiversity monitoring and invaluable in order to revert the global biodiversity loss. Initiatives such as GEO BON (Group on Earth Observations Biodiversity Observation Network), endorsed by the CBD (Convention on Biological Diversity of the United Nations) are developing and seeking consensus on essential

biodiversity variables (EBV), which incorporate strong remote sensing components. EBVs help prioritize by defining a minimum set of essential measurements to capture major dimensions of biodiversity change, and the variables selected as EBVs harness remote sensing (RS) to measure continuously across space (e.g., habitat structure), or local sampling schemes that can be integrated to enable large-scale generalizations (Skidmore and Pettorelli 2015). Examples of variables that currently meet EBV requirements are tree cover, leaf area index, fraction of absorbed photosynthetically active radiation, soil moisture, fire disturbance and inundation (Pettorelli et al. 2016). Most relate to forest measurements, since forests are home to the largest number of terrestrial species (Gibson et al. 2011).

1.4.1. ANALYSIS OF FOREST CHANGE AND DEGRADATION USING REMOTE SENSING

The analysis of remote sensing data can provide us with important insights on the impacts of human land use change in forests (Menon and Bawa 1997, Kerr and Ostrovsky 2003, Huang et al. 2009). The PRODES project in the Amazon forest constantly monitors with satellite images the forest cover, providing yearly estimates of loss and fire occurrences (Hansen et al. 2008b). Global forest change maps, such as (Hansen et al. 2013) can now offer us a very precise picture on forest loss and gain, offering solid basis for decisions on management by countries. Satellite data has been also integrated with other land and aerial based information, allowing for the mapping of not only forest cover but also carbon stocks (Saatchi et al. 2011) and tree density (Crowther et al. 2015). Categorical forest-non forest maps have been the most common data in evaluating deforestation, and its binary concept allows for the integration of data from multiple sources, even historical maps (Petit and Lambin 2002). Detailed historical forest change has been studied in local and regional scale for North America (Foster 1992) and Europe (Kozak 2003), as well as understanding historical change of tropical forests in relation to probable original extents (Ribeiro et al. 2009). These digital forest maps are created by defining a forest cover threshold and classifying the landscape in a manual or automatized way (Forman 1995). In fragmented forests, the result is a forest remnant archipelago containing biological populations which interact by dispersing through a human influenced "matrix". This mixed human-natural arrangement has been thoroughly studied within the biological conservation community aiming to evaluate scenarios in which biodiversity loss was mitigated (Hansson and Angelstam 1991, Menon and Bawa 1997, Metzger and Décamps 1997, Poiani et al. 2000). Considering data from edge effect extent and animal movement within human landscapes, geometric properties of the fragments such as size, shape and proximity to

neighbors were analyzed (Sanderson et al. 2002), and concepts such as single large or several small forest reserves were debated (Ovaskainen 2002).

However, categorical approaches have the downside of considering only in the best case indirect quantification of forest conditions inside the fragments. The edge effect penetration is also considered at a fixed distance, even though several field experiments point to the fact it is largely influenced by landscape and climatic heterogeneity (Camargo and Kapos 1995, Didham and Lawton 2001, Pinto et al. 2010). As forest degradation and carbon emissions become relevant topics, researchers intensify efforts to quantify internal changes of ecological processes in fragments. Using biomass map data (Baccini et al. 2012) and estimations of biomass using forest models, researchers have evaluated patterns of global tropical aboveground carbon stocks, finding that global carbon calculations may be overestimated in tropical fragmented areas due to loss in edges (Pütz et al. 2014, Chaplin-Kramer et al. 2015). Considering the hydrological conditions of fragmented forests, (Briant et al. 2010) used the SWIR band of the MODIS satellite to produce a shortwave infrared water stress index to analyze the desiccation of forest canopies in fragmented forests. They concluded that reduced water estimations penetrated up to 2.7 km inside the forest fragments. Although both studies point in the right direction of studying fragmented landscapes by quantifying internal fragment conditions, the spatial resolutions used (500 and 250 meters respectively) relate poorly to the scale in which edge effects are known to occur, which are around 100 meters (Laurance et al. 2002, Dantas de Paula et al. 2016).

1.5. CHAPTERS

In this Thesis I use the individual based forest gap model FORMIND and remote sensing to expand in the understanding of the consequences of forest fragmentation to forest dynamics and the processes that depend on them indirectly. These new tools make use of computer simulations in order to approach the complexity of tropical ecosystem dynamics under human influence, and allow a glimpse into large spatial and temporal scales. Furthermore, unmeasured properties such as changes in the hydrological cycle, and tree mortality can be estimated by relating to known equations and parameters. The studies presented here were grouped into 3 chapters:

1.5.1. CHAPTER 1. TROPICAL FOREST DEGRADATION AND RECOVERY IN FRAGMENTED LANDSCAPES - SIMULATING CHANGES IN TREE COMMUNITY, FOREST HYDROLOGY AND CARBON BALANCE

In the first chapter, using forest edge, fragment and interior field data plots as reference, I parameterize a forest model in order to understand the dynamics of ecosystem processes in each of these fragmented forest conditions. The main processes studied were carbon (storage and emission) and water (evapotranspiration and surface runoff, using local climate and soil information). The degradation time, from a mature forest to edge conditions was also estimated through the simulations, as well as the time to recovery into mature conditions. This work was published in the journal Global Ecology and Conservation.

1.5.2. CHAPTER 2. THE EXTENT OF EDGE EFFECTS IN FRAGMENTED LANDSCAPES: INSIGHTS FROM SATELLITE MEASUREMENTS OF TREE COVER

It is common in fragmented landscape planning, to consider a fixed edge distance and estimate areas under edge influence and those which are not. This approach was noted to be limited, due to the complexity of edge effect penetration in heterogeneous landscapes. In this second chapter, I make use of remote sensing to evaluate habitat conditions inside fragments of human modified landscapes around the world, in order to evaluate the penetration and nature of edge effects. For this I use as proxy for habitat conditions the LANDSAT Tree Cover product, for 11 scenes in tropical and temperate forest types. This work was published in the journal Ecological Indicators.

1.5.3. CHAPTER 3. DISPERSAL COLLAPSE OF LARGE SEEDED TREE SPECIES – A MODELLING EXPERIMENT ON ITS CONSEQUENCES TO FOREST BIOMASS RETENTION.

Finally, I return to forest simulation in order to study the effects of local animal extinction in fragmented landscapes for the tree community. Since larger animals are most vulnerable in small fragments, and many are responsible for dispersing large seeds, trees with this propagule characteristic are not able to disperse as far, and become vulnerable to seed predation due to their lower seed production numbers. Here I use FORMIND coupled with a spatial seed predation module in order to observe how total and per functional group biomass is affected when pre- and

post- dispersal seed predation rates increase and reduce the amount of seeds for the large seeded plant functional types.

Tropical Forest Degradation and Recovery in Fragmented Landscapes - Simulating Changes in Tree Community, Forest Hydrology and Carbon Balance

Authors: Dantas de Paula, M[1,a], Groeneveld, J[1], Huth, A[1,2,3]

2.1. INTRODUCTION

Land use leaves behind patches of natural areas which are often inaccessible due to the topography or the lack of road infrastructure (Angelsen and Kaimowitz 1999, Laurance et al. 2002, Freitas et al. 2010). The vegetation remnants in these forest fragments typically go through several changes resulting in a community that differs from the original natural vegetation, before arriving in a new "relaxed state" (Diamond 1972), or so-called dynamic equilibrium. This transition process drives the fragment to a different stable state in relation to its primary condition (Santos et al. 2008, Tabarelli and Lopes 2008), which we will define here as "anthropogenic climax community" (ACC). This degradation process has also been called "retrogressive succession" (Tabarelli and Lopes 2008). In a recently fragmented forest, many species are expected to go extinct. Thereafter, it takes a long time for original species abundance distributions to be restored and so ecological restoration activities are required if original levels are to be reached (Melo et al. 2013a). The restoration of these forests, completing the cycle of the "forest transition" concept, also depends strongly on individual stakeholders and are frequently hindered when short-term economic benefits influence the decision making (Satake and Rudel 2007).

Because human advances in tropical regions are fairly recent, most tropical forest fragments are not considered to have reached their final ACC. Loss of species and changes in their relative abundances occur at differing rates: fragments of up to 1000 hectares experience half of their expected bird community extinctions in 50 years (Brooks et al. 1999), many of which are seed dispersers for numerous tree species (Silva and Tabarelli 2000). A delay is thus expected between habitat changes and the number of future lost species (extinction debt), and this time interval has been estimated to be more than a century for trees in fragmented landscapes (Helm et al. 2006, Vellend et al. 2006). Since some species can have a disproportional effect on ecosystem function (Walker et al. 1999), we can also expect a delay in changes to measurements such as biomass, or processes such as evapotranspiration.

The degradation or retrogressive succession of the fragments has two main components. Besides being thrown into marked metacommunity dynamics, forest fragments exhibit striking changes in the vicinity of their borders, known as edge effects (Laurance 1997). These effects are mainly driven by microclimatic changes which occur in forest edges, such as decreased humidity and increased light availability (Pinto et al. 2010). These microclimatic changes in turn cause a general increase in mortality in plant communities, as well as increased turnover and growth (Laurance et al. 2002). An empirical study lasting 32 years on forest edges in the Amazon has suggested that increased tree mortality in the first 100 meters of forest fragment edges might be one of the most important processes driving the change of species abundance distributions and forest structure in

forest fragments (Laurance et al. 2011). Other empirical studies have found that changes in species composition are related to their functional type, with late-successional, shade-tolerant species showing a decline in abundance at forest edges, and early-successional, shade-intolerant species showing increased abundance (Oliveira et al. 2008). Very large trees (emergent) are also especially vulnerable in small edge-effect dominated areas, and their loss contributes significantly to a reduction in average per hectare biomass values (Dantas de Paula et al. 2011a). The spatial extent of edge effects have also been researched and debated: Although in the 32-year Amazon fragmentation experiment the main effects could be detected up to 100 meters from the forest edge, in studies on long-term fragmented forests, edge effects on the tree community have been detected at up to 300 meters in larger, preserved fragments, while in smaller ones (up to 300 meters) the whole area could be considered to be in an edge state (Santos et al. 2008). Finally, understanding how much area in a landscape is affected by edge effects depends largely on the resolution used to map the forest area. Considering a 1000-meter edge distance, using a 1 km^2 resolution satellite (AVHRR), in Africa 18%, in Asia 48%, in Australia 30% and in South America 14% of forests are affected by edge effects (Wade et al. 2003). This scale of analysis leaves out smaller fragments, which can compose a large part of a landscape's forests. Based on 30-meter resolution LANDSAT data, a fragment size of at least 5 ha, and an edge distance of 300 meters, 92% of fragments in the Brazilian Atlantic Forest were found to be affected by edge conditions (Dantas de Paula et al. 2011a).

The shift in tree community and structure caused by edge effects can have a significant effect on the ecosystem processes occurring in forest fragments. One study on Amazonian forest fragments (Laurance 1997) identified a significant loss of 36% biomass up to 100 meters from the forest edge in 17-year-old forest fragments. In the Brazilian Northeastern Atlantic Forest (BNAF) with 200-year-old fragments, however, a loss of up to 60% biomass was found (Dantas de Paula et al. 2011a). This loss produces carbon emissions amounting to 0.2 Pg C y-1 or 9-24% of the annual global C loss due to deforestation, but are still not considered in global carbon accounting (Pütz et al. 2014). Another disruption caused by edge effects in forest fragments happens in forest hydrology. Trees pump soil water and return it to the atmosphere through transpiration, allowing 25-56% of rainfall to be recycled within the ecosystem (Aragão 2012). On the local scale, cleared forest areas have been known to present larger precipitation values than forested areas, but this has been demonstrated to be caused by a convectional process, which due to warmer conditions in the clearings, draws cool humid air from forests and sends it to the atmosphere, causing localized thunderstorms (Laurance et al. 2011). This process also causes further drier conditions at distances of up to 1.0-2.7 km from the forest edge, which exacerbate edge effects and increase the forest's vulnerability to fire (Cochrane and Laurance 2008). On the regional scale, however, precipitation is reduced, as demonstrated by a study (Spracklen et al. 2012) which used satellite data to analyze the

rain pattern of air masses that travel over forested regions. They found that for each leaf area index (LAI) increase of 1, there is an increase of 0.3-0.4 mm of daily rainfall. Air masses traveling over sparsely vegetated surfaces, however, lose moisture during continental transport because of reduced water recycling. Water also exits forests through surface runoff into streams and rivers. Preserved forests typically have less surface runoff than cleared areas because rainwater is better able to infiltrate the soil there, and takes much longer to saturate (van Dijk and Keenan 2007). Therefore streams in fragmented landscapes experience greater temporal variation in flow, being exposed to more flooding events in the wet season, flow failure in the dry season, as well as increased sediment input (Nessimian et al. 2008, Trancoso et al. 2010). Understanding impacts of land-use changes on the hydrology of forests is vital for areas such as the BNAF, which is considered a climate change hotspot and can be expected to experience water-related socio-climatic impacts in the future (de Sherbinin 2013).

Although much attention is given to the degradation process of primary forests in fragmented landscapes, forests trapped in an ACC can recover and go back to dynamic states similar to the original condition (Laurance et al. 2011, Melo et al. 2013a). The recovery process has been considered to be relatively fast (taking a decade or two) if protected from external disturbances, and a secondary forest will soon emerge surrounding a forest fragment, minimizing edge effects, and bringing the microclimatic conditions back into pre-edge values (Laurance et al. 2011). Depending on the level of degradation, however, this process can only be accomplished through human interventions, such as institutional, economic and technical measures. Large-scale forest restoration initiatives, such as the Atlantic Forest Restoration Pact (AFRP), offer hope that in the near future many tropical landscapes will contain recovering and not degrading forests (Pinto et al. 2014).

While empirical studies have delivered important insights into forest fragmentation, the inherent challenges encountered when dealing with the time scales of forest dynamics (i.e. trees are long-living individuals) have led to the development of new approaches to processing field data, one of which is ecological modeling (Shugart 1984, Grimm and Railsback 2005). Forest models, which describe the main properties of ecosystems and their underlying processes, are also able to replicate the general behavior of a system in a time scale of several centuries, thus providing valuable insights. Our approach uses an individual-based forest gap model (FORMIND), that incorporates different plant functional types (PFTs) characterized by shade tolerance or growth form (Köhler and Huth 1998, 2004, Köhler and Huth 2007). The model is also responsive to different soil and climate conditions, and has been used to simulate impacts of climate change to tropical forests (Fischer et al. 2014). FORMIND has been parameterized to different tropical forest types in Central and South America (Köhler et al. 2003, Rüger et al. 2008), to Asian dipterocarp

lowland rain forest (Köhler and Huth 1998, Huth and Ditzer 2000, Huth et al. 2004), and to the Brazilian Atlantic Forest (Groeneveld et al. 2009, Pütz et al. 2011). Both studies in the Brazilian Atlantic Forest used field data from a large preserved primary forest fragment (10,000 ha) and several smaller fragments in the proximity of Sao Paulo, with ages ranging between 40 and 80 years. Data has also been used to parameterize the FORMIND model, and to simulate the impact of edge effects on forest community and structure by increasing the mortality in the edge (up to 100 meters) of simulated areas of various sizes. Those investigators found a strong trend towards lower biomass in fragments smaller than 25 ha in size, driven mainly by tree mortality in the edges, and highlighted the importance of density regulation of seedlings in explaining realistic patterns of observed biomass distribution, long-term coexistence and a realistic speed of the forest succession (Groeneveld et al. 2009). However, a limit of 25 ha contrasts with empirical findings in the much older landscape from the Brazilian Northeastern Atlantic Forest (BNAF), which finds completely edge-dominated fragments of up to 300 hectares in size (Santos et al. 2008, Tabarelli and Lopes 2008). This somehow suggests that edge effects creep slowly into the forest fragment up to a certain fragment size, over a time frame of more than 100 years.

The present study uses data from a very old (>200 y) fragmented landscape in the BNAF to model and investigate the consequences in terms of tree community and structure of transitions between the interior (core) of large fragments, edges of large fragments, and small fragments in relation to stem number, basal area and biomass. Using the modeled BNAF we aim to answer the following questions: a) How do different plant functional types respond in the transitions? b) How long do the transitions last? c) How do the transitions affect the following ecosystem processes: carbon balance, evapotranspiration and runoff?

2.2. MATERIALS AND METHODS

2.2.1. STUDY AREA

This study models forest located in the landscape of the Serra Grande sugar mill property, located in the BNAF of the state of Alagoas, Brazil (Figure 5). The property comprises approximately 9000 ha of forest, entirely surrounded by a stable, uniform and inhospitable matrix of sugar-cane monoculture. It is located in a low-altitude plateau (300-400m a.s.l.), characterizing the remnants as lowland terra firme tropical forest. In relation to its phenological behavior, the fragments represent two types - evergreen and semi-deciduous forests, containing 219 species according to

the field data, distributed among 5 main families: Leguminosae, Lauraceae, Sapotaceae, Chrysobalanaceae and Lecythidaceae. (Pôrto et al. 2006). The local climate is classified as *Aw* (Peel et al. 2007), with a 3-month dry season (<60 mm/month) from November to January, and an annual rainfall of 2000 mm. The Serra Grande landscape contains two dystrophic soil types with high clay content, yellow-red podzols (70%) and yellow-red latosols (30%) (IBGE 1985, ZAAL 2009), according to the Brazilian soil classification system. Sugar cane cultivation and forest clearing in the Serra Grande landscape started in the 19th century, and to ensure watershed protection and water supply for sugar-cane irrigation, forest fragments have been strictly protected against disturbances such as wildfires and logging. Only 9.2% of forest cover is left, including the 3500-ha Coimbra Forest – considered to be the best preserved large forest fragment in the region (Oliveira et al. 2008). Coimbra still retains a full assemblage of plant species, although large mammals such as tapirs and white-lipped peccaries have been extirpated throughout the region due to overhunting. Although this is a single unreplicated tract of forest, samples from it have been used successfully as 'control' sites to assess the long-term effects of habitat fragmentation on the structure of tree assemblages (Santos et al. 2008).
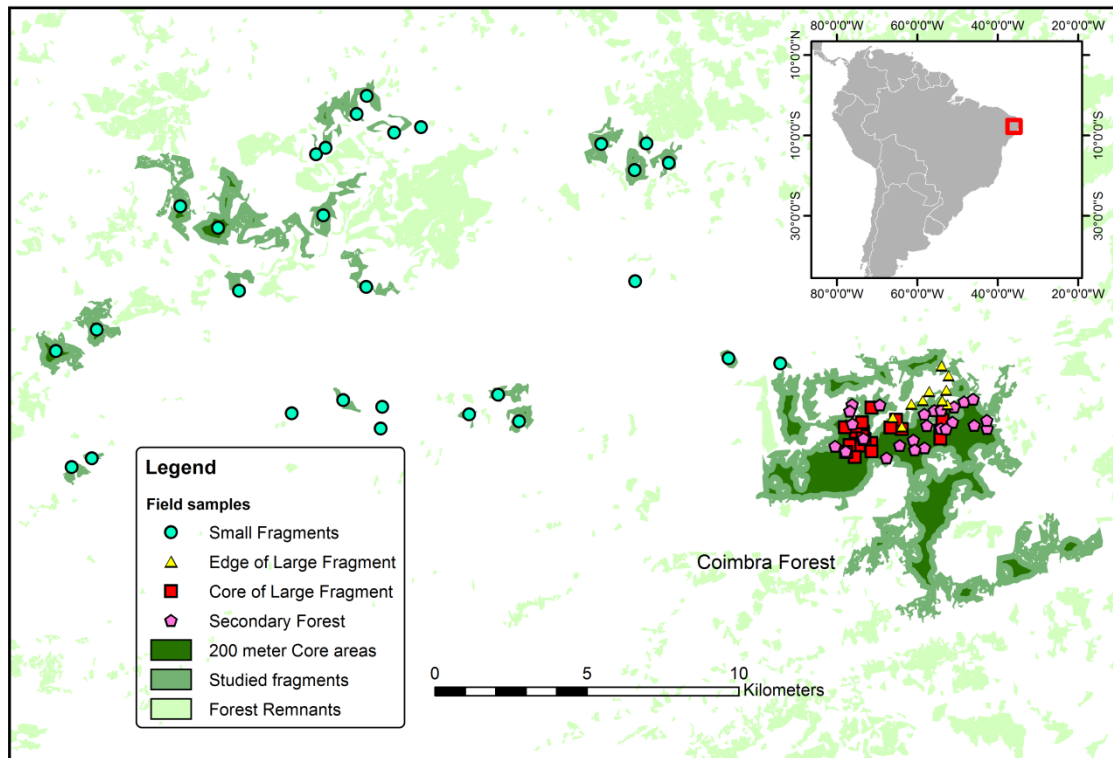
Figure 5. Location of the field plots in the Serra Grande Landscape, Alagoas, Brazil.

To parameterize the FORMIND model, we use a databank on forest inventories from 75 field plots in the Serra Grande landscape (Santos et al. 2008), each of 0.1 ha (10x100m) where all trees >10 cm diameter at breast height (DBH) where identified to species level, and measured for height and DBH. We used plots from 4 different habitat types: 1. Edge of large fragment – 10 random samples (1 hectare) located in peripheral areas within 100 m of the border of the Coimbra Forest; 2. Core of large fragment - 20 random samples (2 hectares) randomly placed at >200m from the Coimbra Forest edge; 3. Small fragments – 30 plots (3 hectares) located in the geometric center of 30 fragments ranging between 3.4 and 295.7 ha. To avoid confusion, we define "small fragments" in this work as continuous areas of forest of less than 300 ha in size (being Coimbra referred to as "large fragment"). In order to find important parameters such as maximum yearly DBH growth, we used as a reference 25 secondary forest plots (2.5 hectares) placed within 25 different secondary forest patches (one plot per patch), with known ages varying from 5-65 years of natural succession following slash-and-burn subsistence agriculture (maize, cassava, beans). It is important to note that due to the favorable fragment shape and size, several fragment plots were located inside the

>200 meter range. However, due to the complexities of edge penetration by microclimatic effects (Pinto et al. 2010) and isolation, these samples were still statistically considered as fragments, and not core areas (Melo et al. 2006, Santos et al. 2008, Tabarelli and Lopes 2008). To illustrate this, we separated the small fragment plots into edges and core, with the same criteria as used for the large fragment Coimbra (200 meter edge) and compared the biomass values (Figure A 4) in an ANOVA analysis. Statistical similarities were only found between the edges of Coimbra and the small fragments, with the core areas being significantly different (Coimbra core: Mean 38.1 Mg/0.1 ha ODM, ±16.34 SD; small fragment core: Mean 21.98 Mg/0.1 ha ODM, ±11.14 SD). The difference between small fragment core and fragment edge depends on one outlier (LSD post-hoc test p = 0.013753; fragment core: Mean 21.98 Mg/0.1 ha ODM, ±11.14 SD; fragment edge: Mean 12.05 Mg/0.1 ha ODM, ±5.69 SD). Therefore we had no strong support to differentiate core and edges of fragments plots into different categories and treated both as small fragment habitats. Another reason for including the small fragment plots in the analysis is that their tree community may represent a very significant portion of the BNAF, since 92% of its total remaining forest is located at less than 300 meters from the closest edge (Dantas de Paula et al. 2011a). Forest fragments smaller than 400 hectares (depending on shape) are considered to be significantly influenced by edge habitats, and so our samples are representative of such a landscape (Laurance et al. 1998). Tree communities, however, vary greatly between small fragments and also in our samples, therefore our reference scenario can be considered only an "average small fragment tree community".

Each individual tree was categorized according to plant functional type (PFT), considering shade tolerance (shade-tolerant or shade-intolerant species), maximum attainable height (0-19 m = understory; 19 – 27 m = canopy; 27 – 40 m = emergent), and two extra PFT's representing very large trees with maximum DBH larger than 150 cm (Magnanini and Magnanini 2002), resulting in eight plant functional types (maximum diameters can be seen in Table A 2). The extra-large tree category was included, because it is probably most affected by edge effects (Oliveira et al. 2008, Dantas de Paula et al. 2011a) and is particularly important for carbon storage – in our field data, single individuals of *Ficus guaranythica* (220 cm DBH) and *Sloanea obtusifolia* (200 cm DBH) were able to store up to 10% of the whole aboveground biomass in one hectare of forest. We randomly selected 10 samples (10 x 0.1 ha) from each habitat condition (in the case of the edge, all of them) as input for the FORMIND model.

2.2.2. THE FOREST MODEL FORMIND AND ITS PARAMETERIZATION

FORMIND is a process-based, individual-oriented, spatially explicit forest growth simulation model. It was developed to study the long-term spatial and temporal dynamics of uneven-aged species-rich

rain forest stands for continuous forest or forest fragments. FORMIND is initialized either empty, representing the situation after clear cut, or based on 1 hectare inventory data, with DBH measurements of individuals and their PFT categories. Yearly seedling ingrowth per hectare is defined. FORMIND then models yearly tree growth calculating stem diameter increments, and translates this diameter growth into height and crown growth using pre-determined stem diameter-to-height equations, and form factor values. It is assumed that light availability and space are the main limiting factors for individual tree growth and forest succession in tropical regions (Bugmann 2001). Within each forest patch all trees compete for light and space following the gap model approach (Botkin et al. 1972), which means that forest dynamics are mainly driven by gaps created by large toppling trees where recruitment rates and growth rates are substantially increased, especially for shade-intolerant species. A complete overview of the model can be found in (Köhler 2000, Dislich et al. 2009) and at www.formind.org.

The parameterization of the FORMIND model is carried out by defining environmental, establishment, mortality, geometry and biomass production parameters. For this study, only the allometry relations for tree geometries (diameter-height relationships) where defined from the actual field samples – all others were chosen from the literature, giving preference to forest formations similar to the BNAF. In order to better reproduce each PFT's growth dynamic, the secondary forest plots were used as a control point during a succession simulation, in order to adjust the diameter growth speed parameters. This was done to find a parameter set which not only ended in a stable field plot condition, but also replicated the natural succession from an initial empty plot. This allowed for a more realistic reproduction of the temporal behavior of the model in relation to stem number and biomass changes. Using this core of large forest fragment parameterization, we modified the mortality and establishment parameters and executed simulations with FORMIND, seeking to reproduce edge of large fragment and small fragment stem number and biomass field conditions. These two parameters are considered to be most affected by edge effects (Laurance et al. 2002, Melo et al. 2006, Laurance et al. 2011). Finally, we had 3 different parameterizations, each simulating stable core of large fragment, edge of large fragment and small fragment tree communities. The parameter values and graphics showing the behavior of each plant functional type can be seen in the appendix in Table A 1 and Figure A 8.

To simulate changes in forest hydrology, we used FORMIND's climate module, and parameterized it with daily precipitation and potential evapotranspiration from historic averages measured around 60 km from the Serra Grande landscape, and kept constant for the entire duration of the simulation (Figure A 3). We chose the dominant soil type (yellow-red podzols) for simplification, and detailed soil data collected from regional 1:100.000 soil classifications (ZAAL 2009), and local studies (Lima

et al. 2008). Additional soil parameters were calculated based on (Maidment 1993). For more details on the main processes of FORMIND's Water Module, see (Fischer et al. 2014).

2.2.3. CALCULATING BIOMASS, TOTAL RUNOFF AND EVAPOTRANSPIRATION

The FORMIND forest model calculates biomass from tree diameter values in each time step and derives from the diameter other geometric tree measurements that compose the biomass equation presented in the appendix (Equation A1). FORMIND's biomass equation takes into account diameter, height, specific wood density for each PFT, and a form factor which considers the deviation of the tree's trunk from a perfect cylinder. Photosynthetic production (which may be limited by several factors in the model such as light availability and soil water content) brings diameter growth which is translated by the equation into biomass change.

Evapotranspiration and total runoff for each patch are calculated based primarily on daily precipitation, potential evapotranspiration, forest structure and soil characteristics. Individual trees take up soil water resources to fulfill the requirements for their gross primary production (GPP), which is calculated by multiplying the photosynthetic rate of a tree per year (P_{ind}) by the limitation factors related to soil water content (ϕ_W) and temperature (ϕ_T, inactive in our simulation):

$$GPP = P_{ind} \cdot \varphi_W \cdot \varphi_T$$

Both factors range between 0 and 1 and thus only reduce GPP when conditions are unfavorable. The water reduction factor is related to the soil water content, and is calculated using the approach by (Granier et al. 1999).

In our experiment evapotranspiration (ET) equals the sum of transpiration (TR) and interception (IN) in relation to time (t):

$$ET(t) = TR(t) + IN(t).$$

Where transpiration is dependent on gross primary production (GPP) and the water use efficiency (WUE) parameter:

$$TR(t) = \frac{1}{A_{patch}} \sum_{All\ trees} \frac{GPP(t)}{WUE},$$

And interception is dependent on the leaf area index (LAI) of the patch:

$$IN(t) = min\left(K_L \cdot \left(\sum_i LAI_i\right), PR(t)\right)$$

where K_L [mm/h] is the interception constant and PR [mm/h] denotes the precipitation.

Total runoff is calculated as the sum of surface runoff ($RO_\rightarrow$) and subsurface runoff ($RO_\downarrow$):

$$RO(t) = RO_\rightarrow(t) + RO_\downarrow(t),$$

Where surface runoff is defined in relation to the soil porosity parameter (POR [-]), soil water content (θ_{soil} [mm]), and precipitation (PR [mm]).

$$RO_\rightarrow(t) = max(0, \theta_{soil}(t) + PR(t) - IN(t) - POR),$$

And subsurface runoff is calculated according to the approach by (Liang et al. 1994):

$$RO_\downarrow(t) = K_s \cdot \left(\frac{\theta_{soil}(t) - \theta_{res}}{POR - \theta_{res}}\right)^{\frac{2}{\lambda}+3}.$$

Where K_s [mm/h] is the fully saturated conductivity, θ_{res} [mm/h] the residual water content, and λ [-] the pore size distribution index [-].

We determine an individual's uptake of soil water based on its demand and on the total available soil water. In FORMIND, soil water content (θ_{soil}) is computed by subtracting from the precipitation (PR(t)) the interception (IN(t)) and runoff (RO(t))):

$$\frac{d\theta soil}{dt} = PR(t) - IN(t) - RO(t).$$

More details on the advanced climate module and water limitation can be found in the FORMIND handbook, available at http://formind.org/.

2.2.4. SIMULATION SCENARIOS

In order to reproduce the transitions with the FORMIND model, we changed the seedling ingrowth and mortality parameters for each habitat. For the *degradation transitions* (core of large fragment to edge of large fragment, and core of large fragment to small fragment) we initialized the model with core of large fragment field samples, but executed it with edge of large fragment or small

fragment parameters, simulating the sudden change in core conditions during a degradation process caused by edge effects. For the *recovery transitions* (edge of large fragment to core of large fragment, and small fragment to core of large fragment), we initialized the model with edge of large fragment or small fragment field samples, and executed it with core of large fragment habitat parameters (Figure 6). The aim is to simulate the ceasing of edge conditions through the recovery or restoration of forest around the simulation area. For each transition, 10 simulation runs of 4 hectares each were run, with the average then calculated. Furthermore, through this simulation it was possible to explore the time scale involved in the fragmentation degradation and recovery effects in individual PFTs, as well as in the whole community. Aboveground carbon emissions and sequestration were simply calculated using the yearly variation in biomass values (biomass/2) during the four transitions. For the forest hydrology we decided to simulate the change in per hectare evapotranspiration and total surface runoff, which are important for determining changes in regional rain patterns and watershed dynamics respectively.
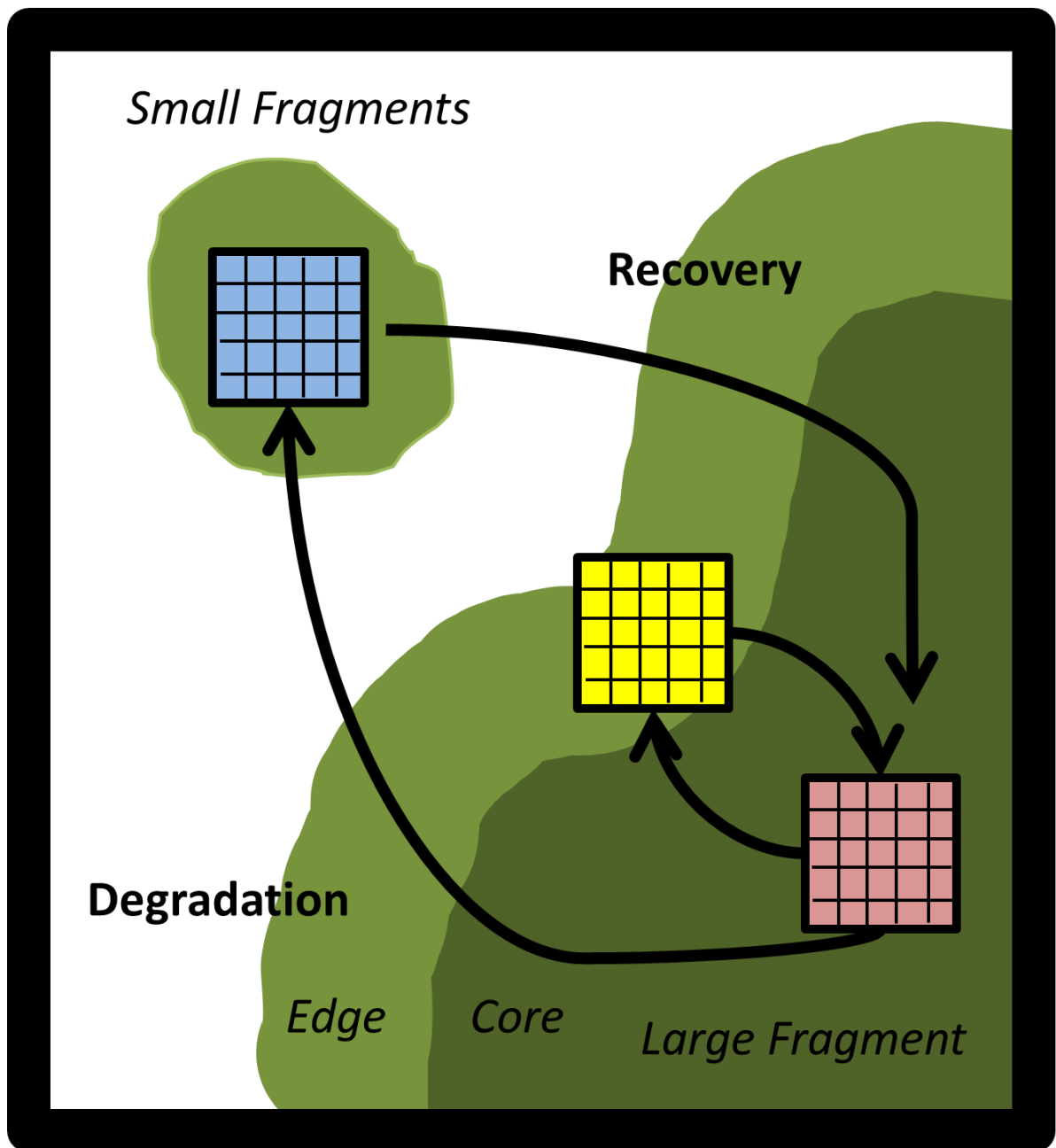
Figure 6. Diagram showing the forest transitions. Blue: Small fragment; Yellow: Edge of large fragment; Red: Core of large fragment.

2.2.5. DATA ANALYSIS

Given our aim to understand the dynamics of the forest transitions, we searched for time points from which the forest reaches a stable state, using the average curves for all measurements

generated in the 10 simulations of 4 hectares. It is important to note that the position of stable points in a curve can be arbitrary, and change according to the definitions of stability. However, in most cases it is easy to identify the point from which a function reaches a stable state, even visually. We decided to define stability by comparing the mean and standard deviation of 50-year intervals between a point in time and the last 50 years of simulation (years 450-500, where the model has reached a dynamic equilibrium). A time point (x axis) is considered stable if the difference to the y value's mean is lower than 20% and standard deviation is lower than 5 times the values of the last 50 years. Finally, to verify statistical differences of evapotranspiration and runoff between the three habitat types, we conducted an ANOVA comparing the final 50 years of all 10 runs between the three habitat types.

2.3. RESULTS

Our PFT species groupings showed a familiar pattern of higher species richness, biomass and stem count for shade-tolerant and emergent species for the field data in the core of large fragments, and a higher representation of shade-intolerant canopy/understory species in edge of large fragment and small fragment areas (Table 2). Although biomass values between edge of large fragment and small fragment habitats seem to be distinct, in reality they are statistically similar, and both differ from core of large fragment habitats (Figure A 4). Comparing the same dataset in terms of aboveground carbon we observed this lack of significant differences between these two habitats, since the variation of carbon in small fragment samples is high.

Table 2. Field sample or initial simulation conditions for the three habitat types. Total values represent 1 hectare of simulated area; 1 and 2 = understory; 3 and 4 = canopy; 5 – 8 = emergent. Additionally, 7 and 8 represent trees able to grow beyond 150 cm in diameter. Gray lines are shade-tolerant trees . Total field sampled area in core of large fragment areas were 2 hectares, in edge of large fragment samples 1 hectare, and in small fragment areas 3 hectares – values shown are 1 hectare averages.

	PFT	Biomass (Mg ODM)	Change (%)	Stem Number (N)	Change (%)	Species Richness	Change (%)
	1	0.12	-	3.5	-	1.5	-
	2	0.1	-	1.5	-	1	-
	3	5.38	-	60.5	-	20.5	-
Core of	4	11.83	-	70.5	-	16	-
large	5	53.83	-	248	-	31.5	-
Fragment	6	140.75	-	459	-	19.5	-
	7	35.155	-	82.5	-	8	-
	8	91.64	-	92	-	10	-
	Total	338.805	-	1017.5	-	108	-
	1	1.87	1458.3%	40	1042.9%	2	33.3%
	2	0.4	300.0%	3	100.0%	1	0.0%
	3	9.48	76.2%	93	53.7%	24	17.1%
Edge of	4	1.9	-83.9%	26	-63.1%	7	-56.3%
large	5	45.9	-14.7%	341	37.5%	18	-42.9%
Fragment	6	1.91	-98.6%	19	-95.9%	4	-79.5%
	7	13.09	-62.8%	69	-16.4%	3	-62.5%
	8	0.28	-99.7%	3	-96.7%	1	-90.0%
	Total	74.83	-77.9%	594	-41.6%	60	-44.4%
	1	0.79	558.3%	15	328.6%	7.3	388.9%
	2	0.54	440.0%	6	300.0%	3.7	266.7%
Small	3	38.97	624.3%	177.33	193.1%	32.7	59.3%
Fragments	4	47.22	299.2%	51.33	-27.2%	9.0	-43.8%
	5	45.14	-16.1%	280	12.9%	22.0	-30.2%
	6	44.3	-68.5%	94.33	-79.4%	12.7	-35.0%

7	24.45	-30.5%	122	47.9%	4.0	-50.0%
8	7.56	-91.8%	19.67	-78.6%	6.0	-40.0%
Total	208.97	-38.3%	765.66	-24.8%	97.3	-9.9%

The parameterization of the FORMIND model allowed for a consistent representation of the forest dynamics and behavior of the modelled functional groups, allowing for differences in maximum height and light responses. Seed input, and mortality rates were adjusted to reflect the succession sequence and time scale of the secondary forest plots (Figure 7). Further testing with a sensitivity analysis shows that the chosen parameter values are robust, for a maximum parameter change rate of p = 50% (see appendix Figure A 2). To recreate edge of large fragment and small fragment stem number and biomass values from the core area parameterization, mortality and seed input parameters were altered accordingly (Table 3), resulting in mortality rates of shade-intolerant species as high as 35 times (from 0.2% to 7%) the core values. Seed input was also altered, mostly by raising the values for shade-intolerant species and lowering for shade-tolerant species.
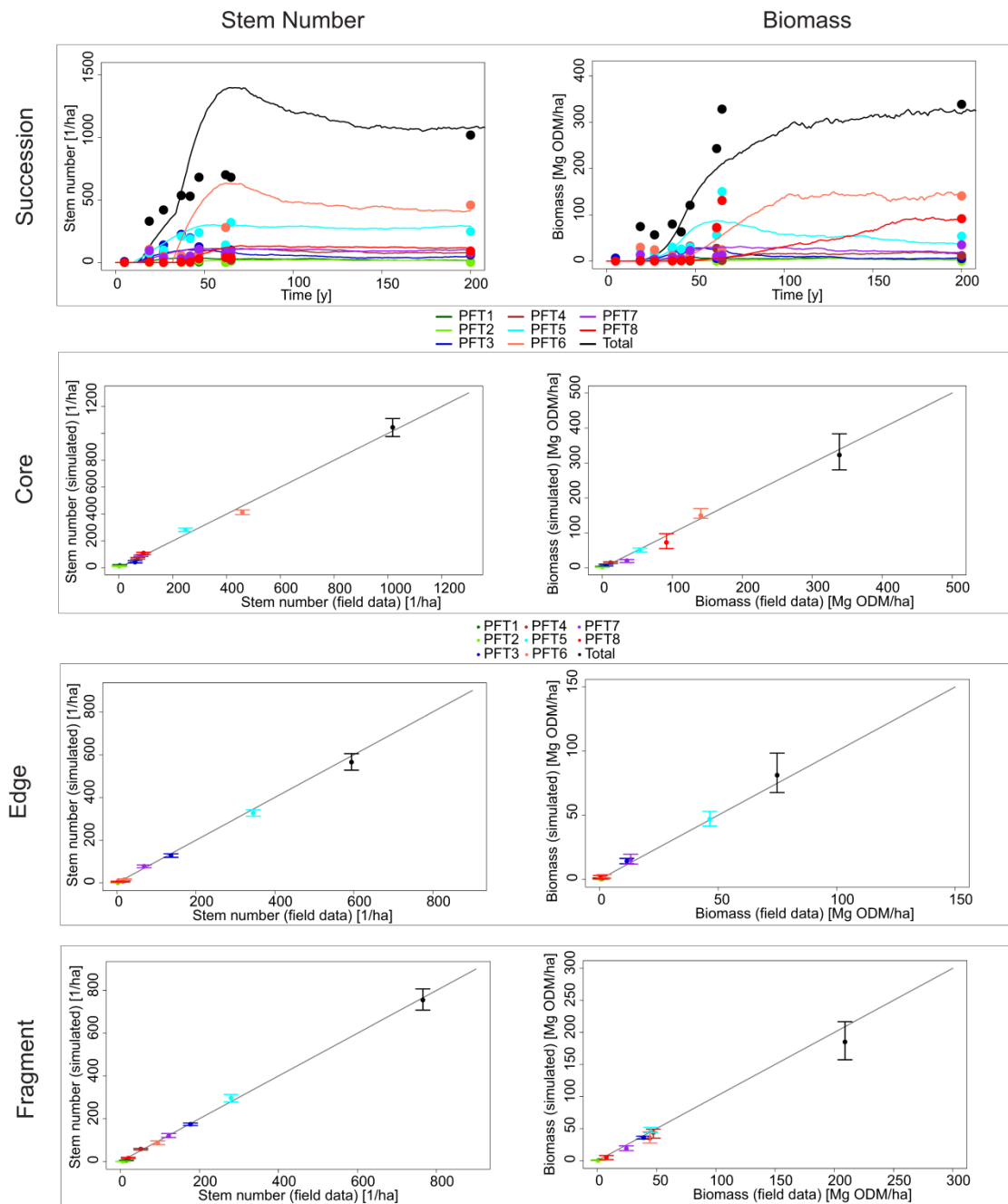
Figure 7. Forest succession simulation (core of large fragment parameterization, lines show simulation results) using the secondary forest plot data (points below 100 years) and core of large fragment field data (points at 500 years). The plant functional types (PFTs) are defined by maximum height as: understory, >19 meters (PFTs 1 & 2); canopy, >27 meters (PFTs 3 & 4); and emergent, >40 meters (PFTs 5, 6, 7 & 8). Shade-intolerant species are odd PFT numbers, and shade-tolerant are even PFT numbers. PFT 7 and 8 are very large trees with maximum diameter up to 250 cm. Cross plots show comparisons to field data after 200 years simulation, with vertical bars showing maximum and minimum values for the 10 simulation runs. Biomass is represented as Organic Dry Matter (ODM). More information on parameterization is available in the appendix.

Table 3. Mortality and seedling input parameterizations for core of large fragment, edge of large fragment and small fragment areas. The change represents a comparison with the core of large fragment area.

	PFT	Core	Edge	Change	Small Fragment	Change
Mortality (% death of individuals per year)	1	3	7	133.3%	6	100.0%
	2	3	6	100.0%	6	100.0%
	3	4.5	11.5	155.6%	6	33.3%
	4	3	7	133.3%	1	-66.7%
	5	0.2	7	3400.0%	4	1900.0%
	6	2.5	8	220.0%	4	60.0%
	7	0.2	6	2900.0%	4	1900.0%
	8	1.1	6	445.5%	4	263.6%
Seedling input (no. of sprouted seedlings/ha/y)	1	5	2	-60.0%	2	-60.0%
	2	20	5	-75.0%	5	-75.0%
	3	22	200	809.1%	80	263.6%
	4	100	60	-40.0%	20	-80.0%
	5	15	130	766.7%	60	300.0%
	6	500	200	-60.0%	180	-64.0%
	7	7	30	328.6%	30	328.6%
	8	66	66	0.0%	66	0.0%

The simulation results of the transitions between the three habitats can be seen in Figure 8, for biomass per hectare in each PFT. For the core-edge degradation scenario we can perceive the change from a high biomass PFT6 (shade-tolerant emergent) dominated forest to a lower biomass PFT5 (shade-intolerant emergent) dominated forest, as well as a sharp loss in the large shade-tolerant emergent (PFT8) tree group during the first years. Total biomass values stabilize at about 80 years, but the tree community only seems to acquire its definitive assemblage after around 100 years, when the stable point for the PFT5 is reached. For the recovery scenario the transition seems more complex, as higher seed input and lower mortality levels first allow the PFT5 to grow in relative dominance, and then be substituted by the PFT6. This time the stabilization process takes much longer (145 years for total biomass values), with most PFTs reaching their stable point later.

Since small fragment conditions are slightly different from edge of large fragment conditions, stabilization times also changed, especially in PFTs 3,4,5 and 6, which also dominate the habitat's biomass (see appendix Figure A 5). For the degradation transition, we can also see PFT6 and 8 losing a large quantity of their previous biomass values, with the latter experiencing the same sharp first-year mortality as seen in edges (Table 4). There are a number of additional variables that can be shown from the FORMIND equations, but these are too numerous to be cited here. We have included the transition results for leaf area index (LAI) and gross primary production (GPP) in the appendix because many researchers may find these measurements important for their work (Figure A 7).
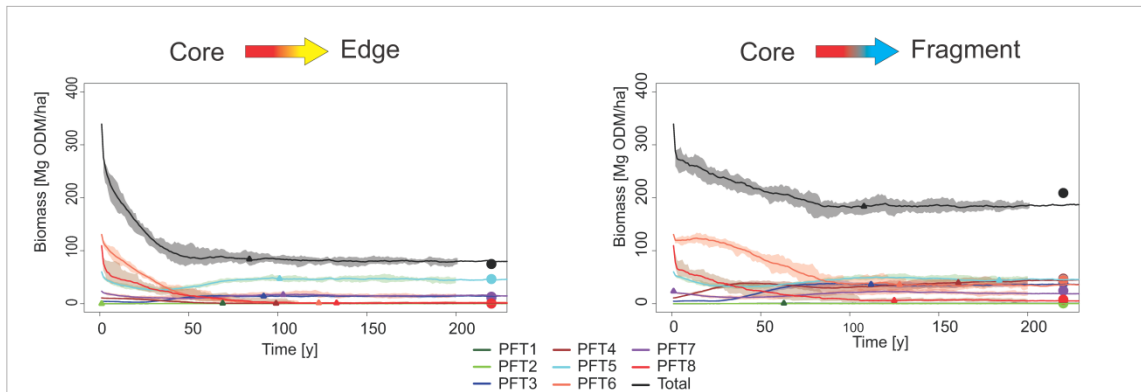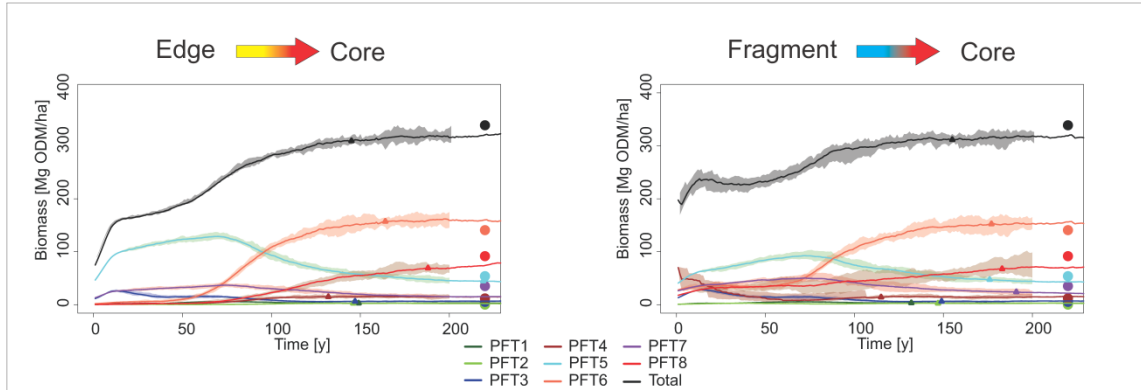
Figure 8. Results for the transition simulations (10 runs with a 4-hectare area) for biomass. Points represent field data, and triangles times where PFTs reached the stability criteria.

Table 4. Time in years after which a stable state in relation to the last 50 years of simulation is reached, for each PFT and transition. CLF: Core of Large Fragment; ELF: Edge of Large Fragment; SF: Small Fragments.

BIOMASS	Total	PFT1	PFT2	PFT3	PFT4	PFT5	PFT6	PFT7	PFT8
Succession	160	128	96	133	120	206	164	170	210
CLF->ELF	84	69	1	92	99	101	123	103	133
CLF->SF	108	63	375	112	161	184	128	1	125
ELF->CLF	145	149	146	147	132	219	164	299	188
SF->CLF	155	132	147	149	115	176	177	191	183

STEM NUMBER	Total	PFT1	PFT2	PFT3	PFT4	PFT5	PFT6	PFT7	PFT8
Succession	175	130	98	134	151	90	205	81	106
CLF->ELF	87	66	1	81	72	87	75	87	79
CLF->SF	99	73	53	86	115	93	97	93	104
ELF->CLF	211	135	103	156	118	164	141	149	122
SF->CLF	163	127	116	135	100	140	119	146	125

The results for the modeling of forest hydrology and aboveground carbon are shown in Figure 9. Forest succession from an empty plot shows a spike in carbon sequestration during the first 50 years, with a following period of fluctuating net positive sequestration values which lasts until approximately 160 years. For the degradation transitions, we observed a sharp spike in emissions during the first 5 years, where yearly values for aboveground carbon loss are above 5 Mg C ha^{-1} y^{-1}. This time period corresponds to the initial phase of fragmentation, when a large pulse in tree mortality is expected (Laurance et al. 1998). The recovery scenarios show that for edge of large fragment-core of large fragment and small fragment-core of large fragment (as shown in the appendix Figure A 6) transitions, total carbon sequestration consists of two main pulses, in contrast with the succession scenario, which has only one. This can be explained by the sudden reduction in mortality (indirectly simulating the improvement in microclimatic conditions), which initially benefits the current dominating shade-intolerant PFTs, but gradually permits development into a shade-tolerant dominated community. This process results into two distinct peaks in carbon sequestration that could be important to take into account in activities that focus on carbon management in fragmented landscapes.

The forest hydrology results, in addition to time transition values, show quantitative data which was not acquired in the field. The results also show that the three habitats differ significantly from one another ($F_{(2,1527)}$ = 45135; $p < 0.001$). Core of large fragment areas in their stable state have, on average, yearly per hectare values of 925.01 mm (± 12.30 SD) and 1237.13 mm (± 10.75 SD) of

total runoff and evapotranspiration respectively. As expected, edge of large fragment areas show significantly higher values for runoff (1456.49 mm ± 40.38 SD) and lower values for evapotranspiration (705.59 mm ±26.52 SD). Standard deviations for both runoff and evapotranspiration are higher in the edge of large fragment than in the core of large fragment habitats. This suggests that runoff and evapotranspiration are more stable in core of large fragment than in edge of large fragment-affected habitats. Forest degradation simulations show that typical edge of large fragment runoff and evapotranspiration values appear around 100 years after fragmentation, and that core of large fragment values are reached sooner (after approx. 70 years) during the recovery transitions.
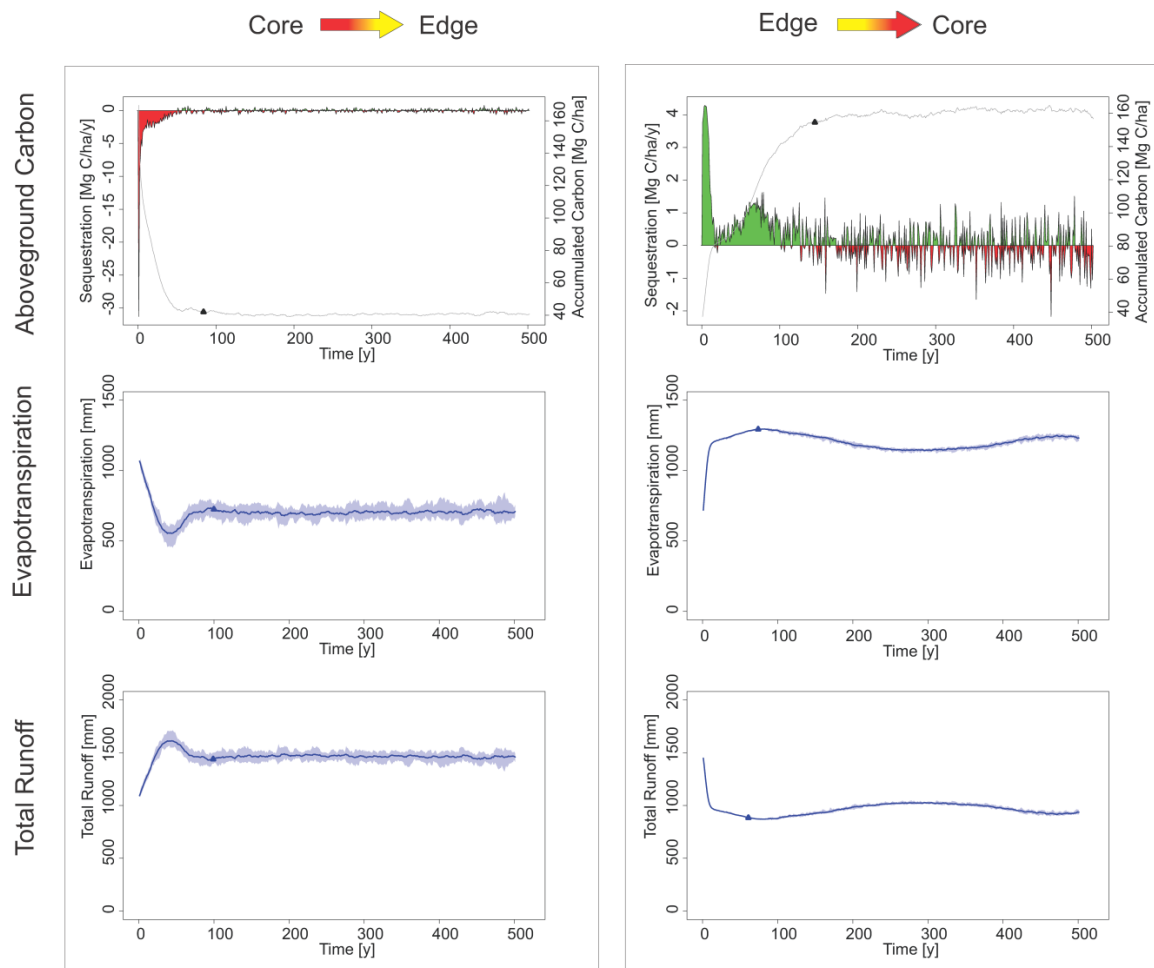
Figure 9. Forest hydrology (total runoff and evapotranspiration) and yearly aboveground carbon change. Green values indicate carbon sequestration, red values indicate carbon emissions. The gray line represents accumulated carbon values. Triangles indicate stabilization points in relation to the stability criteria.

2.4. DISCUSSION

This study is the first attempt to use final-state fragmentation field plots to explain in detail both the degradation and recovery of tropical forests in fragmented landscapes in relation to changes in the tree community and ecological processes. Empirical and process-based models have a natural and promising complementary nature that can help answer many questions in ecology. Although riddled with simplifications, our forest model succeeded in painting a picture which is in line with several field-based empirical studies, and was able to present predictions that can be tested in the

field. The FORMIND model is limited by its simplifications, but it can nevertheless be useful in exploring the consequences of land use in fragmented landscapes. The reliability of its projections is based on a well-tested and continuously updated individual-based model, and well-designed field plots. Furthermore, it can provide new insights which can subsequently be tested in the field.

2.4.1. INSIGHTS FROM THE PARAMETERIZATION PROCESS

Even before the start of the simulations, the definition of mortality and seed input parameters for the core of large fragment, edge of large fragment and small fragment areas provided us with new insights into the drivers of tree community change. Although in comparison with core of large fragment areas mortality rates from edge of large fragments and small fragments were higher for nearly all groups, the rates changed less for shade-tolerant groups than for shade-intolerant groups. As for seed input, there was a marked change in relative PFT composition towards a higher proportion of shade-intolerant and a lower proportion of shade-tolerant species in edge-dominated habitats. There are two possible explanations for this: 1. Shade-tolerant tree species are more sensitive to small rises in mortality, and are quickly outcompeted by the faster growing shade-intolerant species even when the former are subjected to a higher mortality; 2. The collapse of large, shade-tolerant trees in the edge is caused by recruitment failure due to lower dispersal rates (Melo et al. 2006, Oliveira et al. 2008). In the literature, a greater focus has been placed on mortality as the major cause of changes in tree community composition and structure in forest edges (Köhler et al. 2003, Groeneveld et al. 2009, Laurance et al. 2011), but we were unable to reproduce edge dynamics (stem number and biomass values) simply by raising mortality in core of large fragment parameterizations – changes in seed input were also needed. Indeed, empirical studies show that edges have lower proportions of larger-seeded and vertebrate-dispersed trees, and higher proportions of small-seeded tree species in relation to preserved core of large fragment areas (Melo et al. 2006). This pattern is also retained into the seedling stage (Santo-Silva et al. 2012). Most large-seeded trees are also shade tolerant, which explains why the seed input was lower for PFTs of this category, and higher for shade-intolerant tree groups. Our edge of large fragment parameterization showed this clearly, and it appears to be an important driver in long-term fragmented areas.

2.4.2. TEMPORAL BEHAVIOR OF THE TREE COMMUNITY

Understanding the temporal response and final states of forests following human interventions is central to identifying the conservation value in human modified landscapes (Melo et al. 2013a). Our modeling results can provide actors in the field of forest management with a better understanding of forest dynamics and thus help to prevent reckless deforestation. They can also be used to illustrate the impacts of deforestation on ecosystem processes vital to human economic activities, and to identify the time scale of natural regeneration of fragmented landscapes.

That said, we can derive 2 main implications from the obtained simulation results. First, the transitions last between 40 and 100 years on the forest level, depending on the type of value measured (stem number or biomass) habitat and direction of transition. It would be also particularly interesting to know if species richness stabilizes at similar time values. The simulation results for total biomass stabilization in the transitions agree with existing empirical (Laurance et al. 2002) and forest model (Groeneveld et al. 2009) studies. Although extremely detailed and thorough, the large-scale Biological Dynamics of Forest Fragments Project (BDFFP), a major reference for fragmentation and edge effect studies, covers only 36 years – still insufficient for many degradation processes to occur (Laurance et al. 2011). Therefore a discrepancy exists between total biomass losses on edge habitats from studies in the BDFFP (36%) and BNAF (63%) in relation to preserved core of large fragment forests. Even so, our results can be compared, and conclusions can be drawn especially in relation to the temporal behavior. Considering an initial aboveground biomass value of 339.05 Mg ha^{-1}, for the core of large fragment-edge of large fragment degradation scenario the simulation shows an average drop of 50.2% in the first 17 years – this is higher than the maximum 36% biomass loss (mean = 8.8%, SD = 10.2, n = 30) found by (Laurance 1997) for the same time period. The biomass loss rate we estimated (9.93 ± 0.61 Mg ha^{-1} year^{-1}) is also above that found by (Laurance 1997) 3.5 ± 4.1 Mg ha^{-1} year^{-1}. The simulation also shows the familiar transition from a shade-tolerant to a shade-intolerant dominated scenario, but this process takes longer than for total biomass values. The sharp loss of biomass experienced by the PFT8 during the first years of the degradation scenarios agrees with studies which show that the loss of large trees is characteristic for edge of large fragment habitats, and occurs during the first years of fragmentation (Dantas de Paula et al. 2011a, Laurance et al. 2011).

Second, we observed that plant functional types recover or degrade at different rates, and that attributes for the whole forest are reached much sooner than for individual PFTs. This seems to indicate that some ecosystem functions recover much sooner, and can be supplied by different community arrangements. It nevertheless suggests that some plant functional groups take a longer time to reach pre-deforestation stem number and biomass levels. A study comparing long-term forest data from Belgium and England (Vellend et al. 2006) showed that forest plants with slow rates of population extinction and colonization (a category that has similarities with the tolerant

plant functional type) were overrepresented in the Belgian landscape, which had its forest cover reduced to under 10% more recently (from 1850 onwards) than the English landscape (over the last 1000 years). This indicates that complete biotic homogenization of a region under low forest cover takes time, and typically most tropical regions are composed of a mixture of landscapes altered in different periods, a fact which could mask some small fragments with a representative biota, but which simply had not yet had time to degrade. In view of this, (Melo et al. 2013a) suggested a framework to evaluate the potential of tropical landscapes to conservation, where transitions from natural landscapes, to a conservation landscape, and from there to two possible paths, either degraded or functional landscapes, depending on the nature of the human impact. Our findings may thus provide a glimpse of the time of these transitions, for focal plant functional types, and in future analysis, consider different types of human intervention.

The dynamic nature of species-rich environments shows that even in the best case scenario (non-isolated, totally colonizable areas with a full input from the regional species pool) forests can take a long time to recover their original species composition, remaining dominated by altered communities that can, on the other hand, reach total biomass values in less time. These conclusions are invaluable, since many fragmented forest landscapes are expected to be targeted for ecological restoration efforts, and long-term studies with empirical methods are impractical. A next step would be to further analyze forest restoration with computer models, simulating different seedling planting arrangements, and observing how mature forest recovers from the different initial land cover conditions found in fragmented landscapes.

2.4.3. IMPACTS ON ECOSYSTEM PROCESSES

Modeling carbon balance in disturbed forests is of major interest, especially given the need to obtain precise measurements for REDD+ (Reducing Emissions from Deforestation and Degradation) schemes (Asner 2009, 2011). Carbon balance is but one of several ecosystem services provided by tropical forests, and this analysis also shows the potential of individual-based forest models in evaluating long-term and detailed changes to forest functions. Recent articles also explore the net emission of fragments after their isolation (Nascimento and Laurance 2004, Houghton 2005, Berenguer et al. 2014, Pütz et al. 2014). Our results can, in addition, suggest and detail the time frame of this emission and provide end states based on the field data from a long-term fragmented forest. The time until the balance reaches zero is of particular importance, since at this point no more carbon credits can be accounted for. The shape of the transitions show almost constant emissions for the degradations, but a more complex picture for the recovery: The second peak in carbon sequestration can be related to the growth of shade-tolerant trees, which is not

observed in a succession from an empty area. The observed double peak pattern in carbon sequestration for recovering degraded diverse forests is clear when we consider the initial growth of shade-intolerants and then of shade-tolerants, but may come as a surprise to managers of carbon projects such as REDD (Reducing Emissions from Deforestation and Degradation), especially in the long term.

In relation to forest hydrology, we observed a reduction in total evapotranspiration of 43%, and an increase of 57% in total runoff. Our model suggests that the BNAF is in a much altered state in relation to its pre-deforestation hydrology conditions, since 92% of the forest area is located within 300 meters of the forest edge. Lower evapotranspiration and higher surface runoff means that climatic patterns and river dynamics must have been very different 200 years ago, and historical accounts attest to this fact, especially regarding the volume and water quality of rivers in the region (Sobrinho 1971). Recent collapses in the Brazilian water management system have also been linked to deforestation, especially in the Amazon, and can impact both water and energy supply (Nobre 2014). The BNAF's precipitation patterns originate from the Atlantic Polar Front, which moves from the ocean westward in the direction of the semi-arid interior. It is possible that observed lower precipitation patterns on the transition area between semi-arid and Atlantic forests (Oliveira et al. 2006) have been driven by lower recharge of the air mass, passing over the BNAF, and contributing to the on-going desertification of the semi-arid area. Therefore, forest restoration efforts can be also vital to the recovery of other regions. Finally, water environmental services schemes are becoming increasingly popular, and several arrangements exist where forest owners are paid to protect areas which contribute to water flow and/or quality (Kosoy et al. 2007, Ojeda et al. 2008, Pagiola 2008). Forest models such as FORMIND could be an invaluable reference for rapidly and impartially determining the importance of a particular area for the provision of water services.

2.4.4. CONCLUDING REMARKS

As tropical deforestation rages on at around 2.101 km² per year between 2000 and 2012 (Hansen et al. 2013) - despite local reductions in Brazil and recent commitments to halve it by 2020 and end it by 2030 (UNFCC 2014) - fragmented landscapes will play an increasingly important role as representatives of original pristine forests. Since most changes are fairly recent, it is crucial that policy makers get an idea of the possible future impacts on ecosystem and ecological processes so that they can make informed decisions. Additionally, the quantification of selected environmental variables plays an important role in payment for environmental services (PES) schemes involving

cash transfers. herefore, a simple, fast and inexpensive method is needed. Forest models such as FORMIND have much to offer, especially in a field where time is running out.

2.5. ACKNOWLEDGEMENTS

The extent of edge effects in fragmented landscapes: Insights from satellite measurements of tree cover

Authors: Dantas de Paula, M[1,a], Groeneveld, J[1], Huth, A[1,2,3]

3.1. INTRODUCTION

In tropical fragmented forests, a rich amount of research has focused on the ecological process changes that occur in the edges of forest fragments (Wade et al. 2003, Laurance et al. 2006, Laurance et al. 2011, Ibáñez et al. 2014, Haddad et al. 2015). Due to microclimatic changes such as higher light incidence, reduced humidity and higher temperatures (Camargo and Kapos 1995), the forest structure in edges is remarkably different from interior forest (Oliveira et al. 2008). Edge tree communities are more similar to early successional stages, with larger abundance of pioneer species, and low recruitment of large-seeded shade tolerant groups (Tabarelli and Lopes 2008). Trees in these areas suffer from increased mortality, especially in the emergent stratum (Oliveira et al. 2008), resulting in lower aboveground carbon stocks in edges (Dantas de Paula et al. 2011a). The continuing degradation of edges in recently fragmented forests presents a challenge for the control of carbon emissions (Pütz et al. 2014, Chaplin-Kramer et al. 2015). Even though global forest emissions have decreased by over 25% between the period 2001-2010 and 2011-2015 due to decline in deforestation rates, emissions due to forest degradation have more than doubled, and now represent one-quarter of total forest emissions (FAO 2015), persisting especially in poor tropical countries (Sloan and Sayer 2015). This means strategies to monitor forest degradation will become more relevant as deforestation rates decrease.

The spatial scale in which edge effects occurs vary from 10 meters, in case of reduced density of fungus fruiting bodies, to more than 1000 meters in the case of changes in plant phenology, increased fire frequency and weed invasion, although most changes happen up to the 200 meter distance range (Laurance et al. 2002, Broadbent et al. 2008). The temporal scale has also been observed, and the transition from an interior into an edge community at least 5 years (Laurance et al. 2002), although simulations suggests changes in stem number and biomass content can take up to 100 years (Dantas de Paula et al. 2015). The temporal dimension of fragmentation is important to note, because changes can take several years to manifest (Ibáñez et al. 2014). Therefore, three "debts" of recently fragmented forests have been identified (Haddad et al. 2015): the "extinction debt", where loss of forest species takes more than 10 years to reach 50% of previous pristine areas; the "immigration lag", where fewer species arrive in remote areas; and "ecosystem function debt", described as delayed changes in nutrient cycling and to plant and consumer biomass.
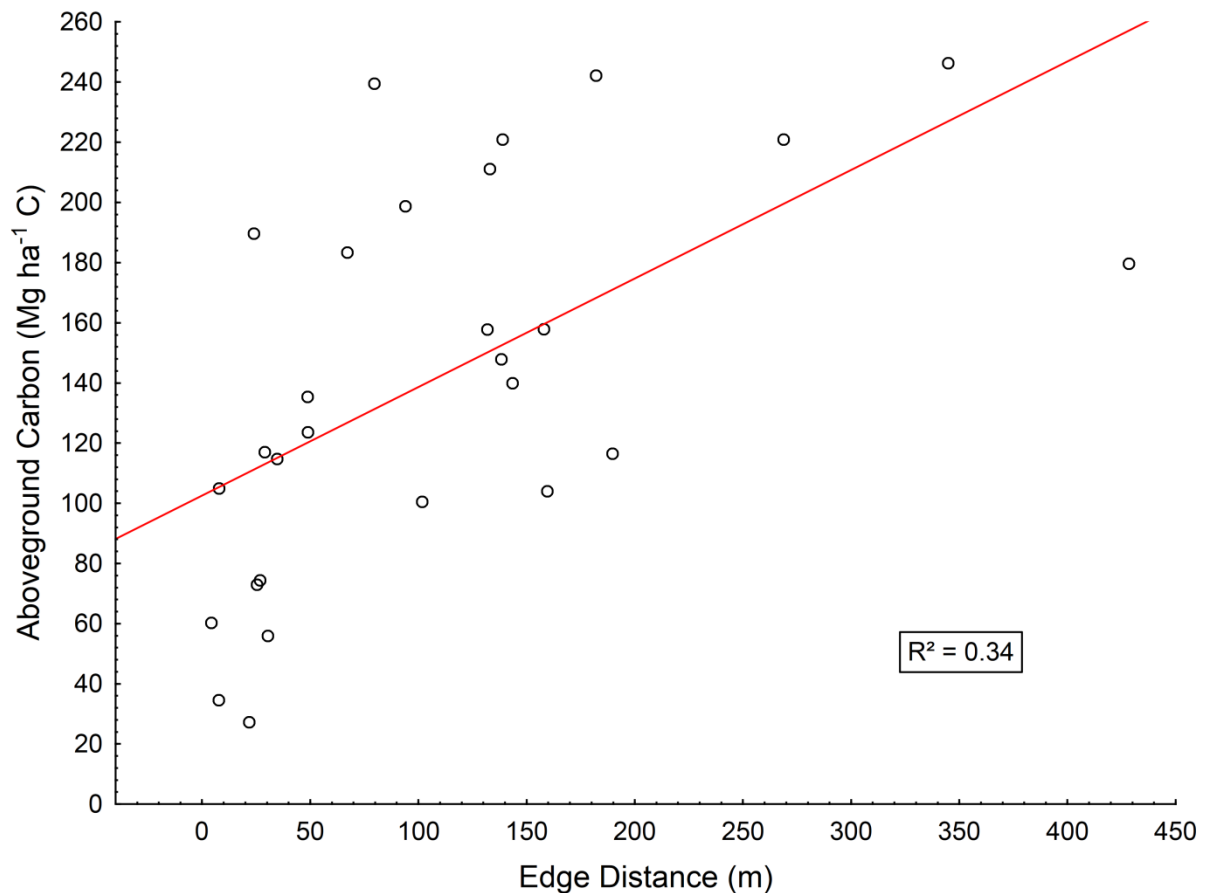
Figure 10. Above ground carbon tree content from 0.1 hectare (upscaled to 1 ha) samples measured in the Northeastern Atlantic Forest of Brazil (adapted from (Dantas de Paula et al. 2011a)) in relation to sample edge distance.

However, these debts still predict that edges will become degraded in relation to core areas. Therefore, specific observations have been reported for several biotic and abiotic variables – for example, edges have up to 36% less biomass than interior forests (Laurance 1997). In spite of this, when samples, not average values are considered, some forest edge areas measurements show great variation and retain in some cases core area conditions (Pinto et al. 2010, Ibáñez et al. 2014), as can be seen with aboveground carbon content in Figure 10.

Recent advances in remote sensing have been particularly useful for conservation biology, providing access to large amounts of data in short time, and permitting researchers to work in large scale with detail (Kerr and Ostrovsky 2003). A particularly interesting dataset is the LANDSAT tree cover, a global 30 meter resolution rescaling of the MODIS (Moderate Resolution Imaging Spectroradiometer) vegetation continuous fields (VCF) product (Sexton et al. 2013). The original MODIS VCF, with 250 meter resolution, is a classification of annual global tree cover (each pixel having a value of 0 – 100%), and now is in its 5th version with yearly data from 2000 to 2010. It was

developed in order to substitute conventional methods of categorical land classifications, which suffer from the imposition of arbitrary thresholds between classes (DeFries et al. 1995). The resulting tree cover pixel values, represent light penetration to the ground, as opposed to simple "crown" cover (Townshend et al. 2011). Several global and regional studies exist evaluating vegetation patterns of the MODIS VCF product (Hansen et al. 2005, Montesano et al. 2009, Ranson et al. 2011), its advantages and limitations (Hansen et al. 2005), and applicability in monitoring using ground validation data (Hansen et al. 2008a, Hansen et al. 2008b). Higher errors for MODIS VCF estimation of tree cover can be expected for values of tree cover lower than 20% (Jeganathan et al. 2009) The 30 meter LANDSAT VCF dataset is a further improvement of the original MODIS product, and was created using 2000 -2005 LANDSAT images and MODIS' own Cropland Layer in order to increase the accuracy of agricultural areas. Also, validation with high resolution LIDAR data was used, having a post-calibration RMSE of 9.4% compared to 13.5% in MODIS VCF estimates. (Sexton et al. 2013).

Tree cover is considered to be an important forest descriptor - it is has been used for calculations of absorbed photosynthetically active radiation (FPAR), albedo, canopy conductance, roughness, photosynthesis and transpiration, net primary production, and carbon and nutrient dynamics (DeFries et al. 1995). Furthermore, tree cover affects patterns of animal diversity (Harvey et al. 2006), large predator habitat preference (Conde et al. 2010), bird foraging dynamics (Trainor et al. 2013), and soil water balance (Joffre and Rambal 1993). Also, tree cover influences human property value (Sander et al. 2010), and may help to indicate areas rich in the offer of environmental services (Huang et al. 2009). Finally, in regard to fragmented forests, tree cover has been identified as one of the most significant variables driving the microclimatic patterns of forest edges (Pinto et al. 2010).

One of additional goals of having large-scale information on the environment in fragmented forests is identification of areas for conservation (Poiani et al. 2000, Groves et al. 2002, Sanderson et al. 2002). Since the main focus for conservation biology is the preservation of endangered species, their occurrence, or of indicator species that signal preserved habitats, is the main pointer that an area should be protected. In the absence of those (or if indicator species are large area ranging carnivores), forest fragment size is used as criteria (Poiani et al. 2001), being larger fragments preferred. This makes sense because larger fragments have larger interior to edge ratios (less prone to edge effects) (Metzger and Décamps 1997), can meet more species requirements in terms of area and heterogeneity(Martensen et al. 2012) and have more area isolated from human disturbances (Veríssimo et al. 1995, Tabarelli et al. 2004). However, several studies have pointed out the importance of very small (<100 ha) fragments in large-scale conservation schemes, due to their role in the increase of connectivity, use as stepping stones, and simply because in many cases a very large part of the remaining forest area is contained in the small fragment category (Ribeiro et

al. 2009, Hernandez-Ruedas et al. 2014). Most approaches to conservation areas identification however, are limited due to the fact that no information on habitat quality within forest patches is included. In those cases fragment delimitations can include secondary and degraded forests, or patches occurring in poor soil types which are of suboptimal conservation value (Ribeiro et al. 2009).

In this work, we aim to observe how tree cover fraction changes in relation to forest edge distance, a measurement that is crucial to understand the ability of fragmented landscapes to retain biodiversity and ecosystem services. We use as an indicator of forest conditions LANDSAT Tree Cover (LTC) (Sexton et al. 2013), which although is indirect, can provide much more data and in a larger scale than field measurements of biotic variables. For this we analyzed 11 LTC images from different fragmented forest regions around the world in order to answer the question: How does LTC vary in relation to edge distance? It is crucial to use for this analysis the highest resolution sensors available, since edge effects are known to occur in the 100 meter range (Laurance et al. 2002), and many sensors used for large scale studies have 300, 500 or 1,000 meter resolution (Loveland et al. 2010, Saatchi et al. 2011, Pérez-Hoyos et al. 2012, Chaplin-Kramer et al. 2015). Also, since many studies on edge effects (e.g. carbon loss in fragments) define a fixed distance for forest edges e.g. (Pütz et al. 2014), it is important to investigate the distance threshold beyond which edge effects do not affect our measured variable.

3.2. MATERIALS AND METHODS

3.2.1. ANALYSIS OF EDGE EFFECTS ON LANDSAT TREE COVER

We selected 11 complete LANDSAT tree cover (LTC) scenes (each 170 x 185 km, with 30 meter resolution) from several fragmented forests around the world (Figure 11) using the Global Land Cover Facility (http://glcf.umd.edu/data/) website, for the year 2000. The 11 scenes are home to 3 different forest types: Closed broadleaved deciduous forest, Closed to open broadleaved evergreen or semi-deciduous forest, Closed to open mixed broadleaved and needle leaved forest, as categorized by the GLOBCOVER 2009 v2.3 map (http://due.esrin.esa.int/page_globcover.php). We calculated statistical information for each fragmented landscape and present them in Table 5. This illustrates the diverse conditions of our selected scenes (Forest extent varying from 1.86% in scene 7 (Northeastern Brazil) to 56.89% in scene 11, Northern Brazil 2). As an example in Figure 12, LTC

values for two sites in Brazil are shown. In each selected scene, we defined forest fragments, using a > 30% LTC threshold criterion. Other thresholds (20%, 50% and 70%) were also tested for one of the scenes, and are available in the appendix (Figure A 9). In order to evaluate the gradient of tree cover in the images, we executed a focal neighborhood analysis calculating the mean and standard deviation of tree cover around each pixel, generating output maps of local mean and SD. These maps were then correlated with edge distance maps, where each pixel represents the distance to nearest edge. Since pixels on the border of a forest fragment can be potentially an average of forest-non forest areas, we consider only pixels with an edge distance larger than 60 meters (two pixel distance from edge). We tested different window sizes for the neighborhood analysis (Figure A 10), from 2 to 200 pixels and concluded that a window size of 4x4 (1.44 hectares, with approx. 60 meter radius) is adequate since we want to try and capture the tree cover variation within the 100 meter mark. This distance value is interesting because many processes are known to be affected at distances up to 100 meters (Laurance et al. 2002).
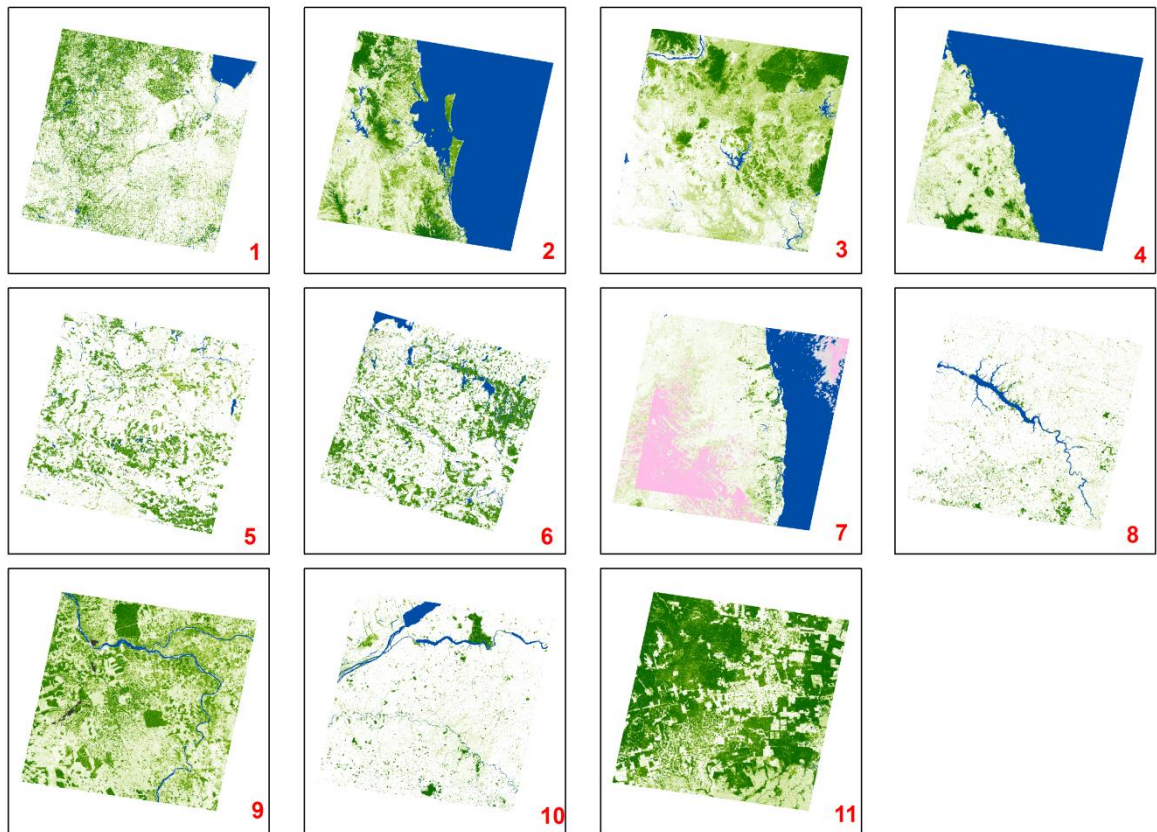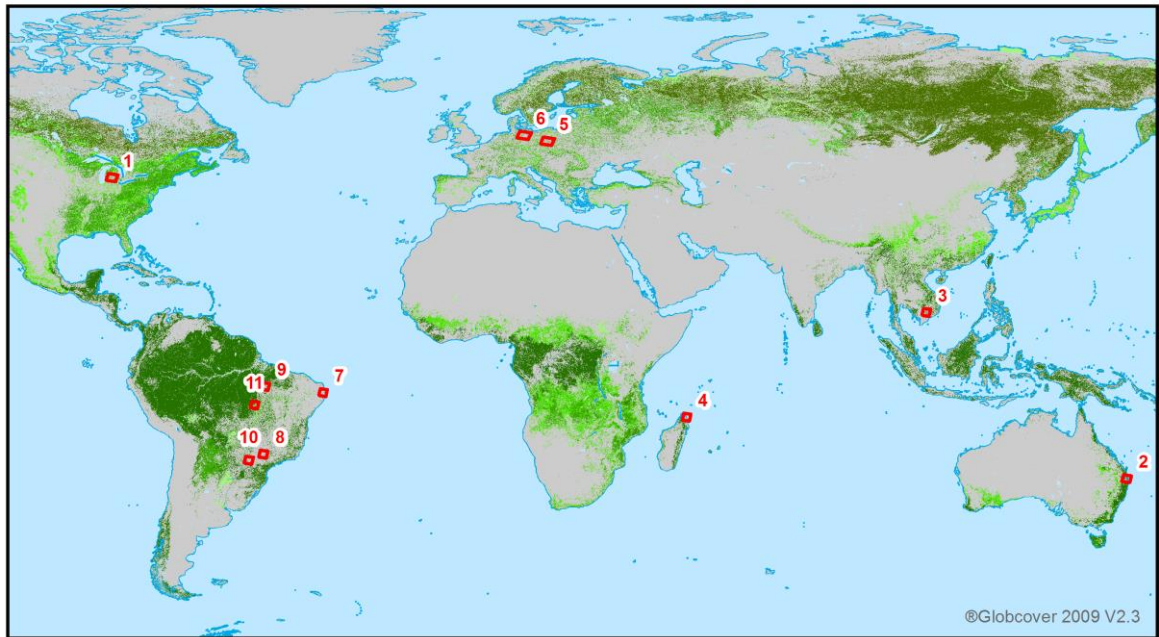
Figure 11. Selected LANDSAT tree cover scenes for image analysis. 1. Northern United States; 2. Eastern Australia; 3. Central Cambodia; 4. Northern Madagascar; 5. Central Poland; 6. Central Germany; 7. Northeastern Brazil, 8.

Southeast Brazil 1; 9. Northern Brazil 1; 10. Southeast Brazil 2; 11. Northern Brazil 2. The pink areas in scene 7 are cloud and shadow coverage.

Table 5. Landscape statistics for the selected LANDSAT scenes. Areas are in square kilometers (km^2). SD: Standard Deviation; VAR: Variance; NE – Northeast, SE – South East, N - North. Forest types were defined using the 2009 GLOBCOVER map. A: Closed broadleaved deciduous forest; B: Closed to open broadleaved evergreen or semi-deciduous forest; C: Closed to open mixed broadleaved and needle leaved forest.

Scene No.	1	2	3	4	5	6	7	8	9	10	11
Location	USA	Australia	Cambodia	Madagascar	Poland	Germany	NE Brazil	SE Brazil 1	N Brazil 1	SE Brazil 2	N Brazil 2
LANDSAT Scene Id.	p021r030	p089r079	p125r052	p159r069	p190r024	p194r023	p214r065	p221r075	p223r064	p223r076	p224r067
Forest Type	A	B	B	B	C	C	B	B	B	B	B
Land	32,085.04	16,477.43	30,167.23	11,967.91	33,246.92	32,254.04	18,626.09	32,725.96	32,037.44	32,563.95	32,820.26
Forest	6,768.00	4,506.81	7,341.42	1,168.58	4,834.22	7,063.02	347.79	716.17	9,554.90	1,192.28	18,670.19
Forest Extent (%)	21.09%	27.35%	24.34%	9.76%	14.54%	21.90%	1.87%	2.19%	29.82%	3.66%	56.89%
Largest Fragment	145.87	695.45	2,360.51	302.12	399.43	794.93	18.24	28.07	458.85	182.08	9,260.07
Non-Land	1,306.16	16,913.77	3,493.70	21,640.70	395.62	1,209.13	14,303.44	769.08	828.32	949.95	27.61
Average Fragment Size	0.77	2.17	3.32	1.80	1.73	2.01	0.69	0.55	2.06	0.98	10.75
Fragment Size VAR	14.83	809.34	3,053.04	181.16	98.02	262.34	2.73	2.43	173.99	52.11	67,335.21
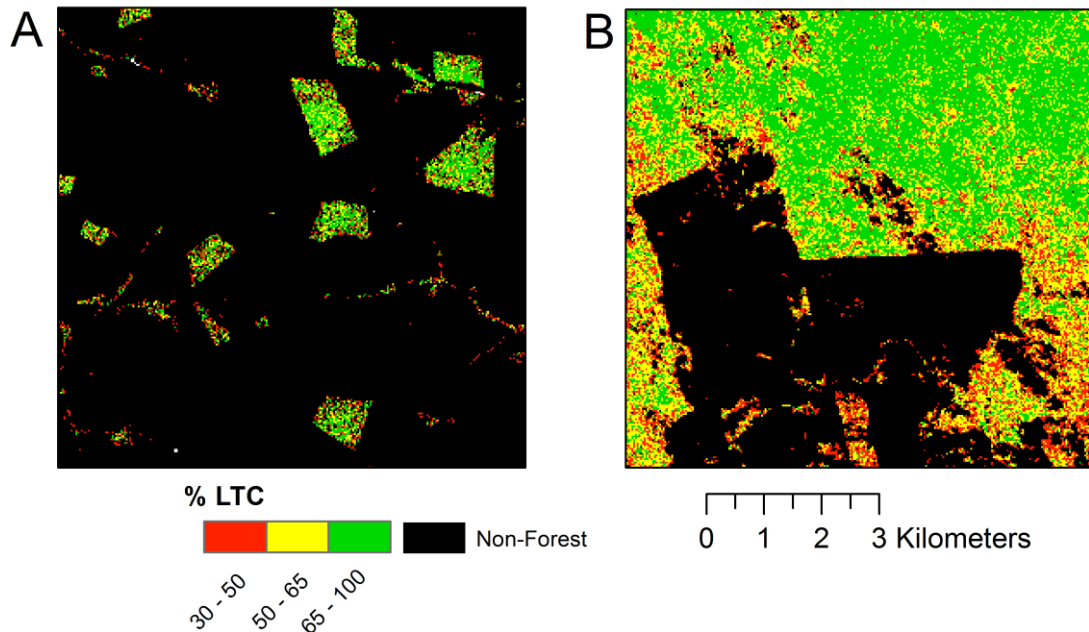
Figure 12. Detail of two scenes (A: Scene number 10. SEB2. B: Scene number 11. NORB2), showing typical LANDSAT Tree Cover (LTC) values grouped into 3 categories. Note that low LTC values (red pixels) occur often close to deforested areas (black), but also many medium (yellow) and high (green). The scale bar is valid for the two scenes, and water bodies are a separate class.

In order to better visualize the distance where the neighborhood standard deviation in edges stabilize (i.e. the distance where edge effects stop occurring, and the interior forest begins) we executed a local regression and plotted a LOESS (locally weighed scatterplot smoothing) curve through the data. We decided here not to develop a model yet explaining the reduction in tree cover variation in relation to edge distance, because of the potential complexity of the explanatory variables (land use history, forest type, topography, soils, etc.) and limitations of LTC.

3.2.2. TEMPORAL ANALYSIS

Finally, we selected one large fragment from the deforestation arc in Brazil, near the city of Araguaia, State of Pará, which is intact in the year 2000 scene, but becomes fragmented in the year 2005 scene. This area allows us the opportunity of observing possible tree cover changes over the period of 5 years or less caused by edge effects and their extent. This analysis was done in the same manner as the previous one, using a 4 pixel window neighborhood analysis to calculate mean LTC.

The edge distance map for 2005 (when the landscape became fragmented) was used for both images in order to evaluate edge influence before and after fragmentation.

3.3. RESULTS

The temporal analysis from the fragmentation images of Araguaia, in Northern Brazil (Figure 13) show the relevance of LANDSAT Tree Cover for fragmentation studies. According to the forest change data for the area from (Hansen et al. 2013), the main fragment has been systematically cut between 2000 and 2005, resulting in forest remnants with different edge ages. The scatterplots in Figure 13 show that the range of LTC values between 30 and 100 meters from the edge between 2000 and 2005 increased, with more lower LTC values in the 2005 image than in the 2000. If we consider the mean for this distance class, it is significantly lower in the 2005 image (T test, LTC mean 2000 = 60.55 ±7.489 SD; LTC mean 2005 = 49.63 ±11.975 SD; $p \ll 0.05$), and the variance increased from year 2000 (56.09) to year 2005 (143.4).
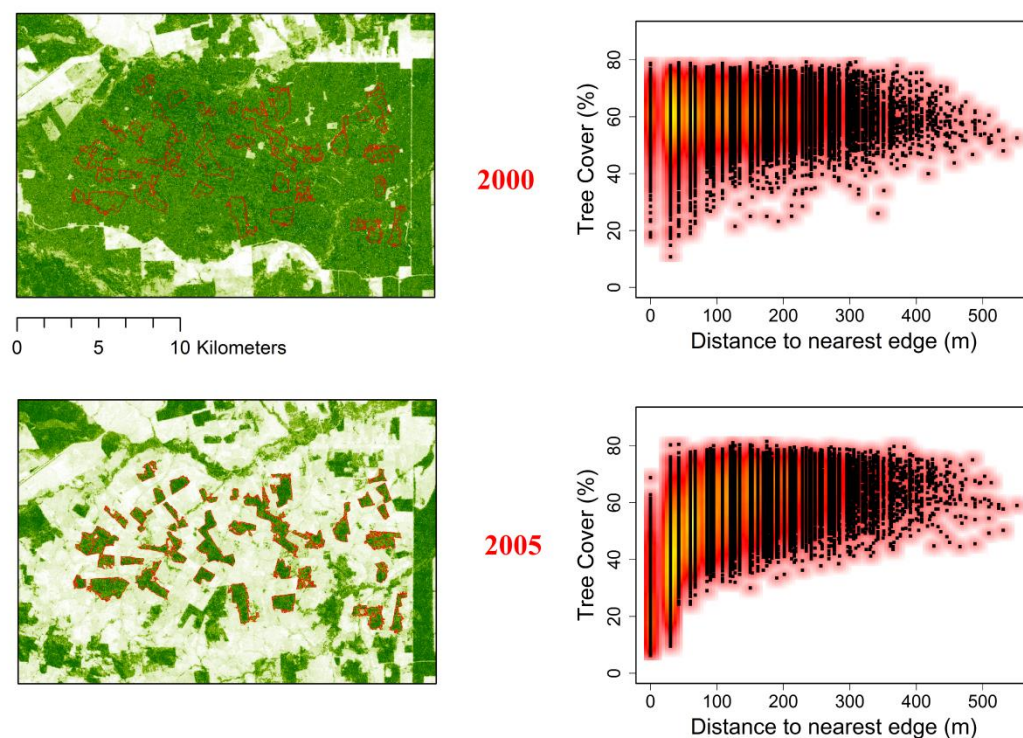
Figure 13. Analysis of the rapid breakup of a large fragment in the Araguaia region, Northern Brazil (part of LTC scene 11, N. Brazil 2). The scatterplots compare tree cover values before and after fragmentation. Colors indicate low (red) to high (yellow) point density, representing the amount of pixels which have a particular tree cover value

at this distance. It can be seen that there are more points with low LTC is in the 2005 scatterplot for the first 100 meters edge distance, pushing the mean LTC significantly lower than in the 2000 image for this distance class.

The graphics for the 11 LTC scenes (Figure 14) show an interesting similarity for the heterogeneity of tree cover in edges, even when including temperate regions. All 11 scenes have a significant trend on lower tree cover for edge habitats, but a more striking pattern is the great variability in sampled tree cover near edges. In this graph all scenes have reduced standard deviation of LTC as edge distance increases, although the steepness and leveling value of the curves differ for each scene. From the mean LTC values in Figure 5 it is also possible to observe higher values and less variation as we penetrate into the core, indicating that these areas can be considered "interior forest". These areas far from edges are of course only present in larger forest tracts. Tree cover therefore seems to exhibit a characteristic "fan shape" pattern in relation to edge, reducing variability as distance from the edge increases. This pattern shows similarity with the forest carbon-edge distance plot from Figure 10.
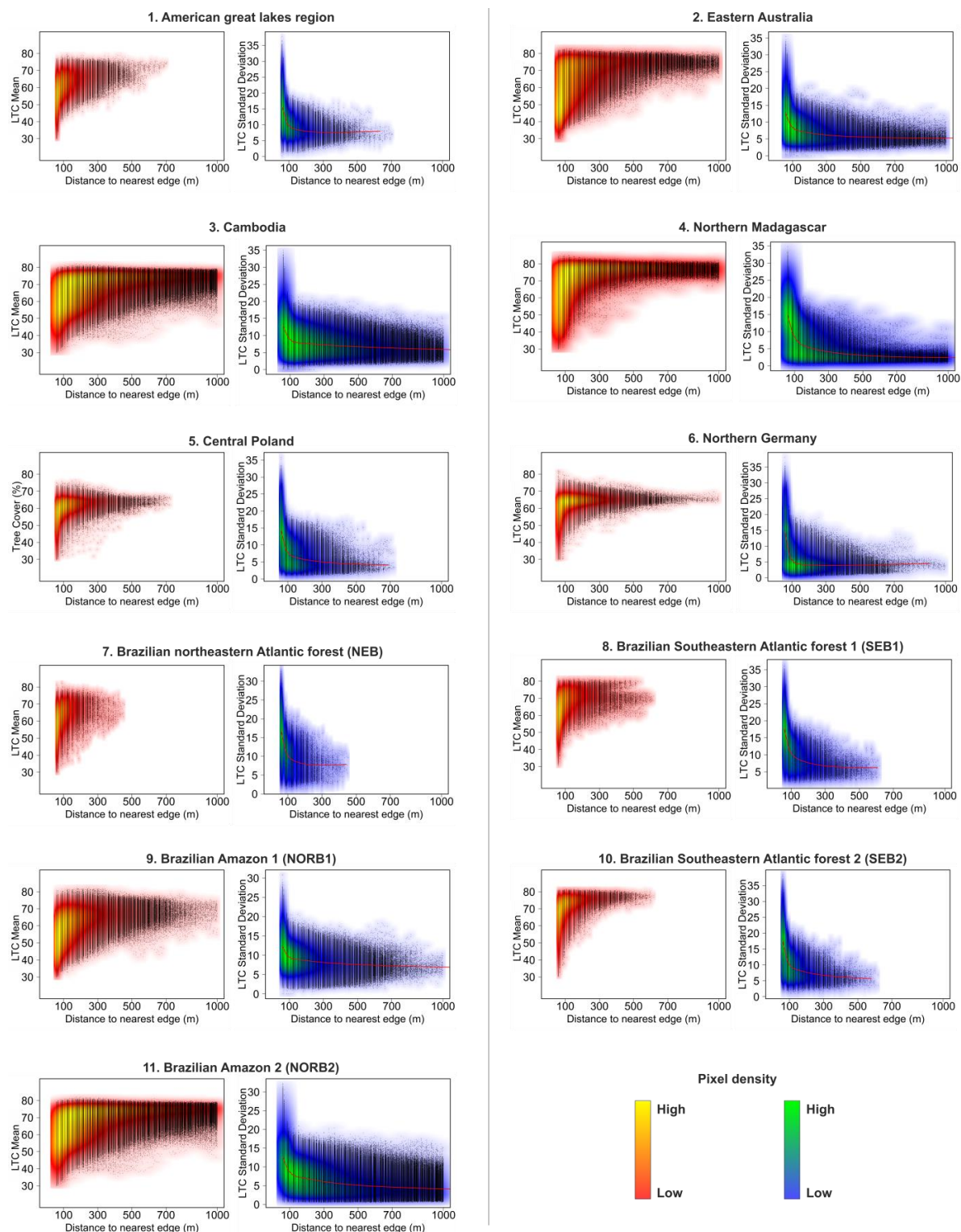
Figure 14. Graphs of neighborhood (4 pixel window) means and standard deviation of LANDSAT Tree Cover (LTC) pixel values in relation to edge distance for the 11 scenes. Colors indicate low (red or blue) to high (yellow or green) pixel density. In the standard deviation graphs, the red line represents the LOESS fitted curve, which suggests possible thresholds for the end of edge-affected habitats.

In order to better visualize the standard deviation curves and compare our 11 analysed regions, we plotted them into a single graph, and normalizing the SD values in relation to its maximum (**Figure 15**). Here we can observe the difference between the steepness of the LOESS curves, greater for some regions such as 6. Germany, and lower for 9. N. Brazil 1 and 12. N. Brazil 2.
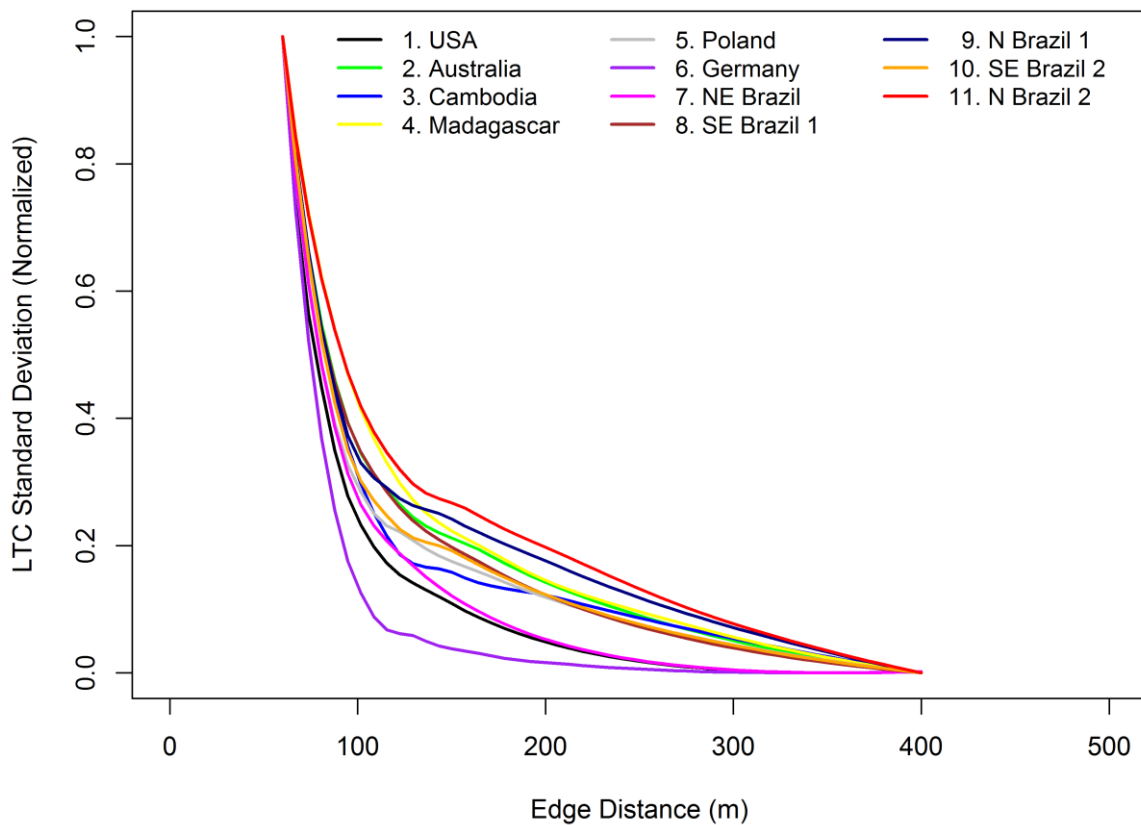
Figure 15. LTC Standard deviation LOESS (locally weighed scatterplot smoothing) curve in relation to edge distance for each region, normalized in relation to maximum and minimum values, within the first 400 meters.

3.4. DISCUSSION

In this study although we are considering only one environmental variable, LANDSAT Tree Cover (LTC), to quantify habitat quality using remote sensing, we have reason to believe that it can be an invaluable tool for assessments of edge effects in forested landscapes and fragment conditions. We decided to maintain our approach data driven and not specify a function to fit the patterns we observed. However, we believe the approach we have shown here can be a step up from defining

core areas through a fixed distance from the literature. We suggest that researchers in forest fragmentation to acquire freely LTC data from the global landcover facility (http://glcf.umd.edu/data/) for their study region and plot LTC variation in relation to edge distance in order to objectively define forest edge habitats.

For ecosystem and ecological processes that correlate to tree cover, we can expect their values to also vary with a fan pattern in relation to edge distance. Indeed, in a recent study using biomass maps, a fan pattern can be glimpsed from the biomass density/edge distance correlation, even though their map resolution was 1 km x 1km (Chaplin-Kramer et al. 2015). Our initial expectations in relation to the behavior of tree cover in relation to edge distance, was that it had lower average values, and that standard deviation remained constant. After observing our results, we can say that LTC values present a "fan shape" pattern in relation to forest edge distance, with high variance near the edge and lower variance towards the forest interior. The fan shape suggests the distance in which the variation significantly reduces (this can also be well observed in Figure 15). This has important implications for conservation, since fragments that have forest area beyond this point will probably retain undisturbed conditions. We can infer the extent of the penetration of edge effects by observing the LOESS curves in Figure 14 and its steepness in Figure 15, and while for some scenes the standard deviation curve steepness is larger and the values level off at around 100 meters (ex. 5, Poland; 6, Germany; 7, NE Brazil), for others the steepness of the curve is lower and it levels at around 500 meters (4, Madagascar) or not at all within the plotted 1000 meters (3, Camboja; 11, N. Brazil 2). This estimation is of course still at a subjective state, but we can nevertheless speculate on the possible mechanisms behind these patterns.

We suggest that this large variance in edges and "fan pattern" arises from three possible causes: Degradation debt, Hyperdynamism and Landscape Heterogeneity.

3.4.1. DEGRADATION DEBT

Here we define "degradation debt" as a broad term referring to the mentioned three debts identified for fragmented forests (extinction, immigration and ecosystem function debts). In any landscape undergoing forest change, we can expect to see simultaneously several stages of edge degradation at any particular time, as is the case of a satellite image "snapshot". This means that the observed fan pattern could arise from edges areas that still had no time to degrade. In landscapes with no or little deforestation, based on degradation debt we should see edge areas having low tree cover values.

If degradation debt is the main cause for high edge LTC variation, then the steepness of the standard deviation curve should be lower in landscapes undergoing recent change, and higher in landscapes without recent change (since in these the edges had time to degrade). We have not analyzed forest change data for our scenes, but in future work it would be interesting to combine our results with recent forest change maps, such as (Hansen et al. 2013). In Figure 15 we can observe that scenes 1 (USA), 5 (Poland), 6 (Germany), 7 (NE Brazil) and 8 (SE Brazil 1), areas where fragmentation has occurred furthest in time have the largest steepness of the SD curve. The scenes known to present higher and recent rates of forest change, such as N. Brazil (9 and 11), Australia (2) and Cambodia (3) have lower steepness in the LTC SD curves, which seems to confirm the role of degradation debt in generating the fan pattern. However, the LTC standard deviation – distance graphs from Figure 15 still show a large amount of edge variation for all scenes, highlighting the need for a more thorough study of how much deforestation patterns and rate influence the difference between edge and interior tree cover variation.

3.4.2. HYPERDYNAMISM

The observed fan pattern can be related to the hyperdynamism concept presented by (Laurance 2009), which states that population and community dynamics of forest edges will become unstable. Edge areas and small fragments are more prone to environmental stochasticity and are strongly affected by the human influenced areas that surround them. Field observations has been consistently showing a large variation in several abiotic and biotic measurements in edge habitats, even though average values are as a rule significantly different from interior fragment areas (Ibáñez, Katz et al. 2014; Haddad, Brudvig et al. 2015). For example, edges located at same distances from the forest border have been found to exhibit different microclimatic conditions (Camargo and Kapos 1995; Pinto, Mendes et al. 2010). This edge variance can also be noted clearly in our study. Since LTC is considered as an indicator of several processes, we should expect large variation in LTC in the vicinity of edges due to hyperdynamism.

One of the questions proposed during the formulation of the hyperdynamism concept is whether this process is chronic (edge areas will always be unstable) or not (will tend to an equilibrium after some time). Analyzing tree cover as a function of edge distance (Figure 14), we can observe that standard deviation in edges is always larger than in interior forests, even in what we consider to be older and more stable landscapes. This would seem to support the chronic nature of hyperdynamism in fragmented forests. Further studies therefore are necessary to elucidate the role of hyperdynamism in the edge variation of tree cover.

3.4.3. LANDSCAPE HETEROGENEITY

Since edges are considered altered habitat up to a certain distance for a given process, it is assumed that a distance "buffer" strip alongside a fragment's edge represents the region affected by degradation effects. It has been shown however that "edges" take complex shapes, and may be completely absent (i.e. they may retain interior forest conditions), as shown by (Camargo and Kapos 1995, Pinto et al. 2010). One of the reasons for this could be heterogeneity in the landscape: topography, soil conditions, prevalent wind conditions, proximity to water bodies, and any other factors that affect microclimatic and tree survival conditions in edge areas. We should definitely then expect large LTC variation due to varying conditions of the landscape in forest edges, since degradation intensity would be dependent on local conditions. This hypothesis could be tested in a fairly straightforward way, by crossing the LTC data with other landscape maps such as topography. Finally, it is possible that differences between interior forest SD values of each scene, as seen in Figure 14 are caused by different forest dynamics in each region, which lead to tree cover heterogeneity. It is natural to assume that different forest types would react differently to edge effects, but within the GLOBCOVER categorization forest types did not seem similar in relation to standard deviation of tree cover. This does not exclude the possibility of finding patterns of edge effect penetration in relation to forest types. Such a pattern if found would be very interesting, and should be explored in future studies.

3.4.4. IMPLICATIONS FOR CONSERVATION

Since in severely fragmented forests most remaining habitat is located in small fragments comprised entirely or in part of edge forests, we can expect that these forest remnants will exhibit the same variance observed for the sampled edges in our study. This means surprisingly, that some forest fragments completely consisting of edge areas can also retain high tree cover values. In these fragments, the mortality of large trees predicted for edge dominated habitats (Oliveira et al. 2008) has probably not taken place with the same intensity as in other remaining patches of forest. This still does not mean that these smaller fragments are a substitute for larger tracts of forest, due to their lower connectivity and higher vulnerability to human encroachment (Tabarelli et al. 2004). But it does seem possible that if protected, they will retain good habitat conditions and would be invaluable as stepping stones. Also, forest restoration efforts in such areas could be much facilitated in relation to known degraded edge areas (Rodrigues et al. 2011). Although much can and should be investigated correlating the varied edge tree cover data with other landscape characteristics

(soil, topography, distance to roads), the fact that such edge-effect resistant areas could exist and readily identified is already great news for the development of biodiversity-friendly landscapes, where human management can promote species coexistence (Melo et al. 2013a).

The concept that edge habitats are necessarily inferior to core areas has motivated the emergence of many conservation strategies. For example, fragment size and shape are used as proxies for high quality habitats, as well as fragment core area presence, according to typical edge effect distances (Villard et al. 2014). This approach is frequently complemented in landscape analysis categorizing fragment area into edge and interior forest, separating both by a distance buffer. Considering the extreme variation of edge habitats, of which small fragments mainly consist, we have shown that this approach is limited and can lead to imprecise large-scale estimations of any particular edge affected variable, as well as the neglect of important small forest remnants. On the other hand, in this study areas far from the edge have shown consistently high tree cover values, confirming the importance of large fragments that are able to exhibit these regions. In summary, fragment size can be considered as a measure of habitat quality (using as LTC environmental indicator of quality), but the high variability of smaller fragments and different distances where edge effects are detected for each region must be considered.

3.5. CONCLUSION

Based on our results on the 11 LANDSAT scenes, we conclude here that forest edges in fragmented landscapes have low average and high variation in tree cover values. As the distance from the forest edge increases, tree cover variation decreases and its average values becomes higher. The resulting tree cover-edge distance graph resembles a fan, which can be used to characterize edge effects. This variation of tree cover in relation to edge distance (fan shape) varies depending on the analyzed region, meaning that maximum edge effect penetration distance and intensity differs between landscapes.

A tool such as Landsat Tree Cover can be very useful for ecologists to analyze large scale habitat conditions in fragmented forests. Its use, along with maps of forest cover change which are now available, should be encouraging for research, since LTC can offer much information on the influence of fragmentation in the tree structure of forests. As degradation becomes a relevant process in relation to forest carbon emissions and threat to biodiversity, identifying its drivers and management options are increasingly important research topics. Although here we have not tested drivers for our pattern, we suggest that degradation debt, hyperdynamism and landscape

heterogeneity are the possible underlying causes for our observed fan shape pattern and high edge variability. Land use history will definitely also play a major role (Lambin et al. 2003), highlighting once more the importance of direct and indirect measurements of habitat quality for suitable assessments of human modified landscapes.

For conservation actions it is essential to accurately quantify habitats, and not simply consider fragments as homogeneous tracts of forest. Correctly identifying edge and core areas is essential in this aspect, and LTC can be used as an objective tool in order to point out thresholds between both habitats – however more studies are needed in order to construct an edge limit identifying framework which can be incorporated into standard methodologies. As new remote sensing products such as Landsat Tree Cover become available, landscape and regional scale studies can be greatly improved, helping to understand habitat change in the very dynamic landscapes of fragmented regions.

3.6. ACKNOWLEDGEMENTS

Dispersal collapse of large seeded tree species – a modelling experiment on its consequences to forest biomass retention.

Authors: Dantas de Paula, M.[1,a], Groeneveld, J.[1,5], Fischer, R[1]., Taubert, F[1]., Martins, V. F.[4], Huth, A[1,2,3]

4.1. INTRODUCTION

Forest patches after deforestation are considered to be fundamentally different from pristine ones in relation to tree community composition and structure (Laurance et al. 2011). Internally, forest fragments suffer from degradation caused by edge effects, *i.e.* the alteration of microclimatic conditions (Camargo and Kapos 1995, Pinto et al. 2010) (increased light and wind, and reduced humidity) due to the proximity to another land use type, generally agriculture. These microclimatic conditions result in higher turnover rates due to increased mortality and establishment, known as hyperdynamic conditions (Laurance 2009), favoring early successional species that dominate the community in the long term (Santos et al. 2008, Tabarelli and Lopes 2008). Early successional tree communities store less carbon due to their lower wood density, promote less water infiltration and may cause higher surface runoff rates than late-successional communities (Dantas de Paula et al. 2011a, Dantas de Paula et al. 2015).

In addition, in fragmented habitats the ecological processes of seed dispersal and seedling establishment are profoundly altered (Melo et al. 2006, Melo et al. 2007, Santo-Silva et al. 2012). First, direct alterations such as desiccation and seedling damage due to changes in the microclimate and increased competition with more ruderal pioneer tree species, lianas and vines. Second, more complex changes can also be observed, such as those caused by extirpation of the large bodied vertebrates (>1kg), causing an ecological release of herbivores and seed predators. Large animals require more space and resources per individual (Chiarello 1999, 2000). Carnivores use large home ranges and frugivores depend on a food source with a patchier spatial distribution than insects, leaves or herbs (Milton and May 1976). Since fragmentation also increases accessibility to humans, fragmented habitats are essentially defaunated of large-bodied vertebrates in relation to conserved areas – a fact which is also corroborated with the general extinction trend of the Anthropocene (Dirzo et al. 2014). Trees which depend on large animals to disperse their seeds are therefore more susceptible to local extinction – it is estimated that 33.9% of Atlantic Rainorest tree species will disappear if we consider seeds larger than 15 mm, which cannot be dispersed by birds with smaller beaks (Silva and Tabarelli 2000). The size and weight of seeds is one of the most significant traits for the prediction of vital rates in tree ecology (Visser et al. 2016), and has a high correlation with adult wood density (Bello et al. 2015). Additionally, forest fragments can be isolated in space, which has a strong effect on seed dispersal. The human changed matrix acts as a "filter", which only selected seed dispersers cross – therefore the arrival of seeds becomes limited in comparison to an otherwise connected landscape (McConkey et al. 2012).

These changes cause small forest fragments and forest edges to become impoverished in terms of large (>15 mm diameter) and very large seeds which display vertebrate seed dispersal, representing up to 27% of the total number of species in preserved forests but only 9% in forest edges (Melo et al. 2006). Therefore, it is not unexpected that the species assemblage of large seeded

seedlings also becomes altered in edge habitats, representing in some studies only around 2.5% of edge species, instead of around 14% of the interior forest tree species community (Santo-Silva et al. 2012). These findings lead us to expect that altered fragmented landscapes are or will become impoverished in large seeded and shade tolerant species, therefore classifying tree species according to seed size and shade tolerance is an efficient way of analyzing functional changes in the ecosystem properties. This evaluation is interesting because there is much intersection between seed ecology properties and other functions in tree groups, for example carbon retention. Small seeded species have significantly lower adult wood density than large seeded tree species, meaning that the impoverishment of the latter would also impact the carbon retention ability of remaining forests (Peres et al. 2016).

Human disruptions in animal communities can therefore have a disproportional effect also in future tree assemblages, affecting seed dispersal and seed predation (McConkey et al. 2012). Abundance in biological communities is self-regulated through trophic levels in bottom up (prey defenses controlling consumer numbers) and top-down (prey numbers becoming hyperabundant through absence of predators) (Dyer and Letourneau 1999). Predators of vertebrates living in small and medium forest remnants (up to 4 hectares in size) in fragmented landscapes could experience large changes in relation to larger forest areas, because of the absence of vertebrate predators in these areas (Terborgh et al. 2001). This means densities of rodents, leaf-cutter ants, iguanas and howler monkeys can have 10 to 100 times greater abundance than in larger areas, and cause higher herbivory pressure on seeds, and seedlings due to top down relaxation of their larger predators (Terborgh et al. 2001). Wright et al. (Wright et al. 2000) found that in areas where poaching of mammals occurs, only 3% to 40% of seeds were dispersed in relation to areas protected from poaching, and 30% to 50% more seeds were predated by beetles. Therefore human influences in changing forest landscapes or removal of specific biological groups can have a large indirect influence of tree community abundance and composition, which in turn can modify ecosystem processes (Silva and Tabarelli 2000).

In order to glimpse the consequences of forest fragmentation with many synergisms occurring (Tabarelli et al. 2004), individual based computer forest models are an interesting option. In such models the main processes creating forest communities are represented, such as light competition, seed dispersal, establishment, mortality and so on. In these models tree species are represented as plant functional types (PFTs) – since grouping species according to life history characteristics has gained traction as a way to understand patterns of biodiversity loss (Dirzo et al. 2014). One of these models, FORMIND has a 20 year long history of successful representation of forest dynamics, also under several disturbance scenarios such as logging (Huth and Ditzer 2001, Huth et al. 2004), climate change (Fischer et al. 2014, Hiltner et al. 2016), and landslides (Dislich and Huth 2012).

FORMIND has been used to study forest fragmentation, and found out that density dependence of seedlings is essential to simulate observed biomass distribution, long-term coexistence and a realistic speed of the forest succession (Groeneveld et al. 2009). Also, temporal dynamics of edge degradation after edge creation are in the order of 100 years in relation to biomass, stem number, evapotranspiration, runoff and leaf area index (Dantas de Paula et al. 2015). Finally, an analysis by (Pütz et al. 2011) showed that forest fragments below 25 ha suffer substantial structural changes, biomass and biodiversity loss in the long term. Two recent studies have related defaunation to the loss of biomass in fragmented forests, by removing large seeded trees and estimating carbon stocks (Bello et al. 2015, Peres et al. 2016). By using a forest model such as FORMIND However, it becomes possible to analyze directly seed loss and its effect on tree biomass, incorporating a much greater range of interacting ecological processes.

Here we simulated edge effects and several landscape scenarios using the individual based forest model FORMIND, parameterized with tree, seed and seedling field data from a fragmented tropical landscape in order to answer the question: How does reduced seed dispersal and increased or decreased seed predation of large seeded species affect the biomass of fragmented forests? We test this by parameterizing the FORMIND model using seed, seedling and adult tree field data from a fragmented landscape, and incorporating into the model a spatially explicit seed predation mechanism. By doing this we expect to see the synergistic effect of lower seed dispersal within a dynamic and diverse forest community, where competition for light and space, as well as seed number and density, play a major role. We run the following simulation experiments: 1. Simulation of unfragmented forests under higher seed predation caused by the loss of large animals; 2. Simulation runs using fragment sizes from 1 to 121 hectares starting from a mature forest, with varying predation pressures and varying the seed number; 3. Simulation runs in a 121 hectare sized landscape, with a constant total forest area divided into 1-7 fragments, in order to see the effects of varying predation and seed number in a meta-community context.

With these modelling experiments we aim to gain insights on long term consequences of forest fragmentation, loss of ecological groups in fragmented areas, the consequences of defaunation, as well as possible characteristics of these landscapes. We also aim to observe the importance of nearby seed sources to compensate the lower seed values, and shrinking fragment sizes.

4.2. MATERIALS AND METHODS

4.2.1. FOREST GROWTH, SEED PREDATION AND FRAGMENTATION MODELLING

FORMIND is an individual-based model that simulates the growth of a forest by modelling growth of individual trees based on simplified carbon balances. Since each tree belongs to species groups with distinct properties, environmental conditions such as light environment, stem density, temperature and disturbances influence individual survival. More information about processes implemented at FORMIND can be found in (Fischer et al. 2016) also www.formind.org.

One of FORMIND's important features is the ability to simulate directly from forest inventory stands (as well as empty forest areas). Trees are modelled from measured DBH values using allometric equations to estimate total height, crown size, total LAI, etc., and are placed in one of 20x20 m plots inside the simulation area. In order to simulate environmental conditions, each plot is assigned a "landscape code", which can represent any spatial parameter. In this framework, raster data of real or simulated environments with compatible 20x20 meter resolution can be used as an input, and their properties transferred into the FORMIND initialization file. In the present study, we assigned a landscape code of 0 to non-forest plots and integer landscape code values of 1 – N to forest plots, where N represents the distance (measured as number of plots) to the closest 0 plot (i.e. the edge), as can be seen in Figure 16.

The activation of "edge effects" in FORMIND causes the simulation to raise the base mortality of simulated trees (mortality without considering extra disturbances) in relation to the plot's distance to the edge. FORMIND defines distinct basic mortality parameters for the PFTs depending on diameter class – one base mortality value for individuals with DBH≥15 cm (our defined threshold for this study) and another for smaller plants for each PFT. In simulated edge effects, the mortality is calculated as: $Frag_{mort} = base_{mort} + base_{mort} *multiplier$, where the multiplier equals 1, if distance to edge is 0 – 20 meters; 0.5, if distance to edge is 20 – 40 meters; 0.25, if distance to edge is 40 – 60 meters; 0.125, if distance to edge is 60 – 80 meters; 0.0625, if distance to edge is 80 – 100 meters; and 0, if distance to edge is > 100 meters.

In addition, base mortality of trees with DBH≥60 cm are further multiplied by 2 in border areas (<100 meters) in order to simulate the specific loss of individuals in this size class due to unfavorable edge conditions (Oliveira et al. 2008).

Seed dispersal was simulated by FORMIND using seeds produced by living parent trees, which in our study had a dispersal kernel described by a negative exponential function. In this study we parameterized the simulation according to field seed rain data (Melo et al. 2006). In order to calculate seed dispersal distances, we used the dispeRsal R module developed by (Tamme et al. 2014). This method uses a cross-validation statistical approach to determine how well various plant traits predict dispersal distances, reaching a R^2 of up to 0.60 when using dispersal syndrome, growth form and terminal velocity (the maximum speed in m/s of a falling diaspore in still air) as traits in the model. We calculated maximum dispersal distance for each inventoried species using as traits dispersal syndrome and maximum seed release height (using the maximum heights from the field inventory). Then, we averaged maximum dispersal distance for each PFT in order to have values for each group. Since mean dispersal distances were needed, they were estimated from the maximum using the maximum-mean dispersal relationships provided by the table of (Thomson et al. 2011). The dispeRsal script produced maximum dispersal distances for all inventoried species, and when grouped per PFT produced the expected large variation from short dispersal distance in non-animal dispersed species (PFT4, max. dispersal 67 meters, mean dispersal 8 meters) to animal dispersed (PFT5, max. dispersal 1327 meters, mean dispersal 550 meters).

In relation to post-dispersal seed predation, we developed a model that depends on the density of seeds and parent trees in each individual plot, turning it into a spatial process. We included the density of parent trees, since seed predators are known to be attracted to the neighborhood of the food sources (Janzen 1970). On the other hand, relative seed predation is lower with high seed numbers, due to predator satiation. Typically, seed dispersal strategies are related to escape from predation – either through smaller numbers with high energy content to attract dispersers that can bring large dispersal distances (and therefore raise the chances of finding sites with lower number of conspecific parent trees), or producing vast amounts of seeds to satiate predators. These two strategies have multiple evolutionary causes, and represent a trade-off between quantity and quality (size) of seeds. In fragmented landscapes, the reduction of seed dispersers means that large seeded species cannot disperse as much seeds per year, and pre-dispersal predation will cause the mortality of non-dispersed seeds. In our simulations, we consider that undispersed seeds will not germinate due to predation at the source, therefore pre-dispersal predation is represented as a percentual reduction in seed dispersal. This seed loss may happen even though post-dispersal predation of large seeds may be lower, according to (Dirzo et al. 2007) in the absence of large animals which prey on large seeds, or because larger seeds can more often contain chemical defenses (Janzen 1969). Since we do not have information on seed chemical defenses for our species, we consider the same post-dispersal predation rates for all PFTs.

Total seed mortality for each plot is calculated using two terms (Equation 1): the seed mortality rate unrelated to post dispersal seed predation for each PFT (μ) and mortality caused by post dispersal seed predation (*P*).

Seed mortality equation in simulation plot i:

Eq1. $$Seed\ Mortality_{i,pft} = \mu_{pft} + P_{i,pft}$$

Eq2. $$P_{i,pft} = MTree_{i,pft} \cdot N_{pft} \cdot \Psi_{i,pft}$$

Where,

Eq3. $$N_{pft} = \frac{2 \cdot \beta_{pft}}{\pi \cdot q^2}$$

Eq4. $$\Psi_{i,pft} = \frac{a}{1 + a \cdot T_h \cdot SPool_{i,pft}}$$

Seed predation *P* is calculated for each plot *i*, per PFT, and depends on the local number of mother trees (M_{Tree}) for each PFT, the predator density N (using the predator intensity factor β and predator distance q. We maintain q constant at 10 m, because we consider predator attraction by parent trees to occur at this scale (Nathan and Casagrandi 2004), and inside the plots the tree positions are not explicit). We also consider the predator response factor Ψ calculated based on Holling's disc equation (Nathan and Casagrandi 2004), which accounts for predator satiation. In Ψ we have as parameters a (predator efficiency), T_h (handling time) and *SPool* (total seeds in the seed pool for a particular PFT and plot). This approach creates a "seed mortality map" with values between 0 and 1, which influences the establishment of each PFT.

When simulating a fragmented landscape, we consider that seeds falling in a non-forest plot (landscape code 0) do not germinate. Conversely, animal dispersed seeds that would fall into a non-forest plot or outside the simulation area (according to the dispersal algorithm) are automatically placed in the plot of its parent tree. This implementation aims to correct the seed distribution, since animals spend a relatively short time in the matrix (Gorchov et al. 1993). In fragmented forests, animals either disperse seeds in the local fragment or complete the journey to the next area.

Parameters not directly based on local field data, were the base mortality of adults and seedlings. In order to define the base mortality values, we executed calibration runs with 1 ha and adjusted the mortality (i.e. "inverse modelled") of adults and small trees so that the stem number and basal area, per PFT, reproduced measured tree stands of mature forests. For this reference simulation, we used a predation factor β of 1,000, which seemed to reproduce best the field inventory values. The complete parameter set is documented in the Appendix (Table A1).

1.1.1. REFERENCE FIELD DATA AND FUNCTIONAL GROUPING

We parameterized the FORMIND forest model using field data from a fragmented landscape in the Brazilian Northeastern Atlantic Forest (BNAF). This landscape is located in the Serra Grande sugar mill property, which comprises approximately 9,000 ha of forest fragments entirely surrounded by a uniform matrix of sugar-cane monoculture. The property is located in a low-altitude plateau (300–400m a.s.l.) covered by remnants of the lowland terra firme tropical forest. Some fragments are evergreen and some are semi-deciduous, containing altogether 219 species distributed among five main families: Leguminosae, Lauraceae, Sapotaceae, Chrysobalanaceae and Lecythidaceae. Serra Grande is also home to one of the best-preserved forest fragments of the BNAF, namely Coimbra forest. It has 3.500 ha and is frequently used as a control area representing undisturbed conditions (Silva and Tabarelli 2000, Melo et al. 2006, Melo et al. 2007, Oliveira et al. 2008, Santos et al. 2008, Pinto et al. 2010, Dantas de Paula et al. 2011a, Santo-Silva et al. 2012).

The field data consists of three datasets obtained in the interior of Coimbra forest, edge of Coimbra forest and other smaller fragments in the landscape (<100 ha): 1. Seed rain assessments during a 1 year period using 200 1m² seed traps (total sampling effort of 200 m²) (Melo et al. 2006, Costa et al. 2012); 2. Adult tree inventory consisting of 60 field plots (20 plots in mature forest located > 200 m from the edge of Coimbra forest, 10 plots located < 200 m from the edge and 30 plots in the center of other nearby fragments smaller than 100 ha) where all trees > 10 cm diameter at breast height (DBH) were measured for total height and DBH; the species were also identified to its lowest taxonomic level (Oliveira et al. 2008); 3. Secondary forest inventory in Coimbra forest, where 25 sampling areas with age between 5 and 65 years were used to compensate the absence of repeated inventories and to estimate growth rates for each species (Santos et al. 2008). In addition, data on total seedling values per hectare in mature Coimbra forest plots (seedlings defined as 10-50 cm in height) were also used to calibrate the model (Melo et al. 2007, Santo-Silva et al. 2012). This field dataset was used as a reference for the adjustment of adult and seedling mortality parameters, which are unknown. In our model we consider seedlings and small trees being of the same continuous category.

We grouped all inventoried species into 6 plant functional types (PFT). The PFTs were defined through two light tolerance classes (shade tolerant and shade intolerant) and three seed classes: non-animal dispersal, small seeds (<15 mm) and large seeds (>15 mm) dispersed by animals. These groups are the most affected (negatively or positively) by fragmentation, as shown by studies in Serra Grande (Silva and Tabarelli 2000, Melo et al. 2006, Melo et al. 2007, Oliveira et al. 2008, Santos et al. 2008, Tabarelli and Lopes 2008).

Table 6. Reference field data for mature forest plots of Brazilian Atlantic Forest in NE Brazil (Coimbra forest). Information from the field inventory data, with species grouped according to the 6 Plant Functional Types. Data represents trees larger than 0.1 m DBH. Values are averaged by hectare. Classifications for shade tolerance were taken from the literature; Non-Animal seed dispersal can be wind or ballistic, and the size threshold between small and large seeds is 15 mm; species richness, stem number and basal area were taken from (Oliveira et al. 2008); Seeds per year data were based on (Melo et al. 2006); Max. dispersal distance was calculated using the dispeRsal R module developed by (Tamme et al. 2014); Max increment of growth diameter was based on data from (Santos et al. 2008).

						Coimbra (Mature Forest)			
PFT	Shade Tolerance	Seed Dispersal Category	Species Richness	Number of Stems	Biomass (Mg/ha)	Basal Area (m²/ha)	Seeds per year/ha	Mean Max. Dispersal Distance (m)	Max. Increment of Stem Diameter per Year (mm)
1	Intolerant	Non-Animal	55	133.5	34.94	8.77	1,110,666	115.41	30.00
2	Intolerant	Small Seeds	103	155.5	47.99	8.48	2,926,997	1139.48	43.25
3	Intolerant	Large Seeds	23	102	10.66	3.46	12,333	1120.15	15.89
4	Tolerant	Non-Animal	16	78.5	12.65	2.12	55,222	67.31	19.79
5	Tolerant	Small Seeds	49	391	102.39	14.8	42,444	1327.87	16.84
6	Tolerant	Large Seeds	29	149.5	106.39	12.26	25,889	1142.61	19.21
Total	-	-	275	1010	315.02	49.89	4,173,551	-	-

1.1.2. LANDSCAPE ARRANGEMENTS FOR MODEL AND SIMULATIONS

With our parameterized model, we now run the simulations in order to investigate the effects of varying predation rates and shrinking seed dispersal of large seeded PFTs in ecosystem processes. First, we evaluate how unfragmented (core, i.e. FORMIND without activation of fragmentation effects) areas respond to these seed disturbances. Then, we activate the fragmentation module of FORMIND and run the various predation and dispersal conditions.

In our first analysis without activating fragmentation effects, we executed several 4 hectare 1,000 year simulations, activating the seed dispersal reduction (pre dispersal predation effect) and post dispersal predation effects after 350 years running in undisturbed conditions. This allows enough time for the model to transition between the forest inventory conditions (which only have trees larger than 0.10 m DBH) into our running model (with 0.002 m minimum tree DBH). These simulations have closed, continuous boundaries, therefore the simulation area functions as a torus - therefore seeds falling outside the simulation area come back on the other side. The extreme parameter values of 0% - 98% large seeded PFT seed dispersal reduction and post-dispersal predation intensity (β) by 1000, 3000, 5,000 and 10,000 were tested.

Finally we explored fragmented landscape conditions.

We executed two different fragmentation experiments:

1. Increasing post-dispersal predation and pre-dispersal predation for large seeded species (PFTs 3 and 6). We run FORMIND in isolated fragments of 1, 2, 4, 16, 25, 36, 49, 64, 81, 100 and 121 ha (sizes chosen due to computational limitations) for 1,000 years, considering 0%, 50% and 90% large seeded PFT seed dispersal reduction, and post-dispersal predation intensities (β) of 1000, 3000, 5,000 and 10,000. Then, the average aboveground biomass values from the last 100 years of simulation were compared.

2. The effect of multiple fragments in a landscape with varying fragment numbers. We maintain fixed a total forest area of 25 ha and run the simulations on 1 – 7 fragment scenarios (Figure 1A). The total landscape area is 121 ha, composed of forest and non-forest plots, and the same dispersal reduction and predation intensities are considered as the first experiment, as well as total simulation time and averaging interval.
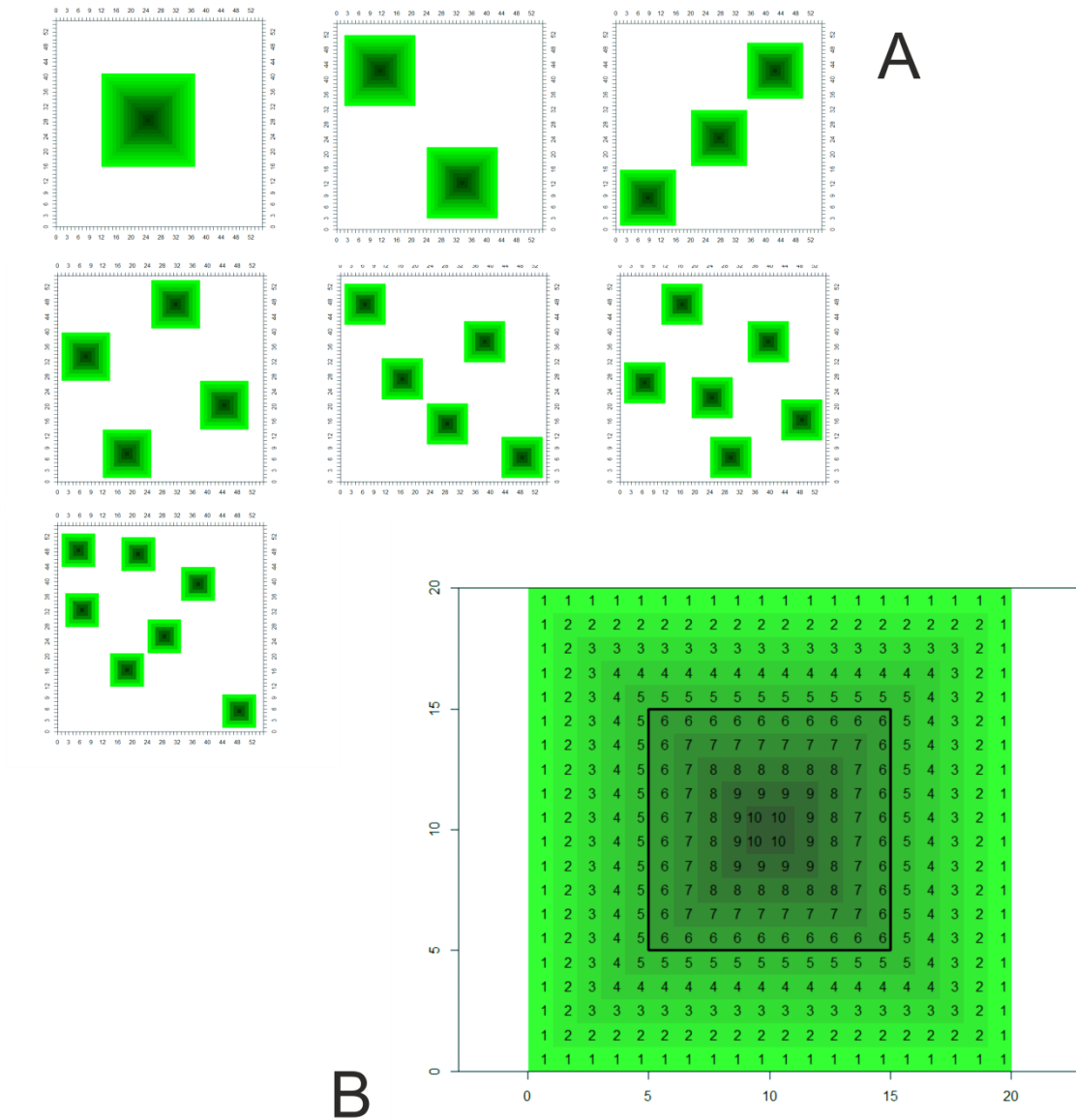
Figure 16. Representation of the simulation areas for FORMIND in this study. A. The seven fragmented forest scenarios of experiment 2, with a total of 25 ha of forest divided into different fragment numbers and simulated in a total of 121 ha. B. Simulation area of 16 ha showing patches affected by elevated edge mortality (outside of the black box, numbering 1 to 5).

4.3. RESULTS

4.3.1. ANALYZING THE FIELD DATA

Analyzing the field data (Table 6 and Table A 4), we found a general trend of less stems and lower basal area per hectare in small fragments (Stems: 765.57 ind/ha; Basal Area: 27.31 m²/ha) and forest edges (S: 594 ind/ha; BA: 18.81 m²/ha) in relation to forest core areas (S: 1010 ind/ha; BA: 49.89 m²/ha). It is especially notable the change in stem and basal area dominance of shade tolerant to shade intolerant species from core to edge conditions. In addition, in the line of other similar studies small seeded species have significantly smaller adult wood density values than large seeded species (ANOVA, $F(1,217) = 5.9933$, $p = 0.015$; Mean Small = 0.4977 g/cm³, SD Small = 0.1409, Mean Large = 0.5568 g/cm³, SD Large = 0.1515) as can be seen in Figure A 11).

4.3.2. DEFAUNATION OF CONTINUOUS FORESTS

The unfragmented forest simulations demonstrate the consequences of seed disperser loss, as well as predation pressure variation for biomass retention and community composition. In relation to no reduction (0%) of dispersed seeds due and post-predation intensity of 1,000, similar biomass values in relation to field measurements were observed (Figure 17). After activating a pre-dispersal predation of 95% for large seeded trees at the 350 year mark, we can note a delay in the effect on parent tree number and biomass change which is longer for some species than others, and affecting the total biomass after around 100 years. Next, the pre- and post-dispersal parameters were varied (Figure 18 and Table A 5) and the most significant changes in total biomass are noted after pre-dispersal predation of 80% and post-dispersal predation of 10,000 (although with low post-dispersal predation of 1,000 seed dispersal can be reduced up to 93% without major changes in total biomass). In the extreme cases however, total biomass will be reduced up to 29% due to the community shift caused by the loss of large seeded tree species.
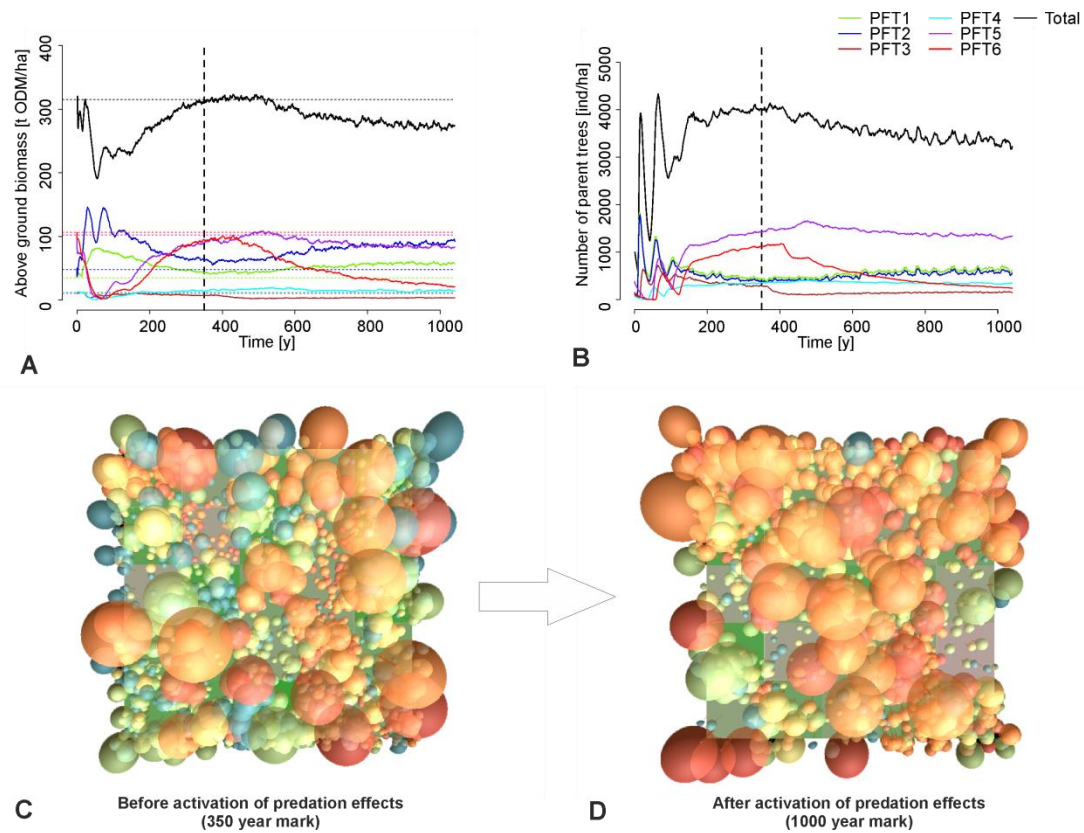
Figure 17. Reference simulations with results for (A) aboveground biomass and (B) number of parent trees considering post-dispersal predation of 1,000 and pre-dispersal predation of 95%, in an unfragmented and undisturbed forest of 4 hectares. The black vertical lines indicate the activation of pre-dispersal predation effects, at the 350 year mark. The horizontal dotted lines represent field measured values for the mature Coimbra Forest (Error! Reference source not found.**). Figures C and D indicate visualizations (1 ha) of the model from above, with balls representing tree crowns. Note the loss of the blue PFT6 from the pristine (C) to the defaunated (D) area.**
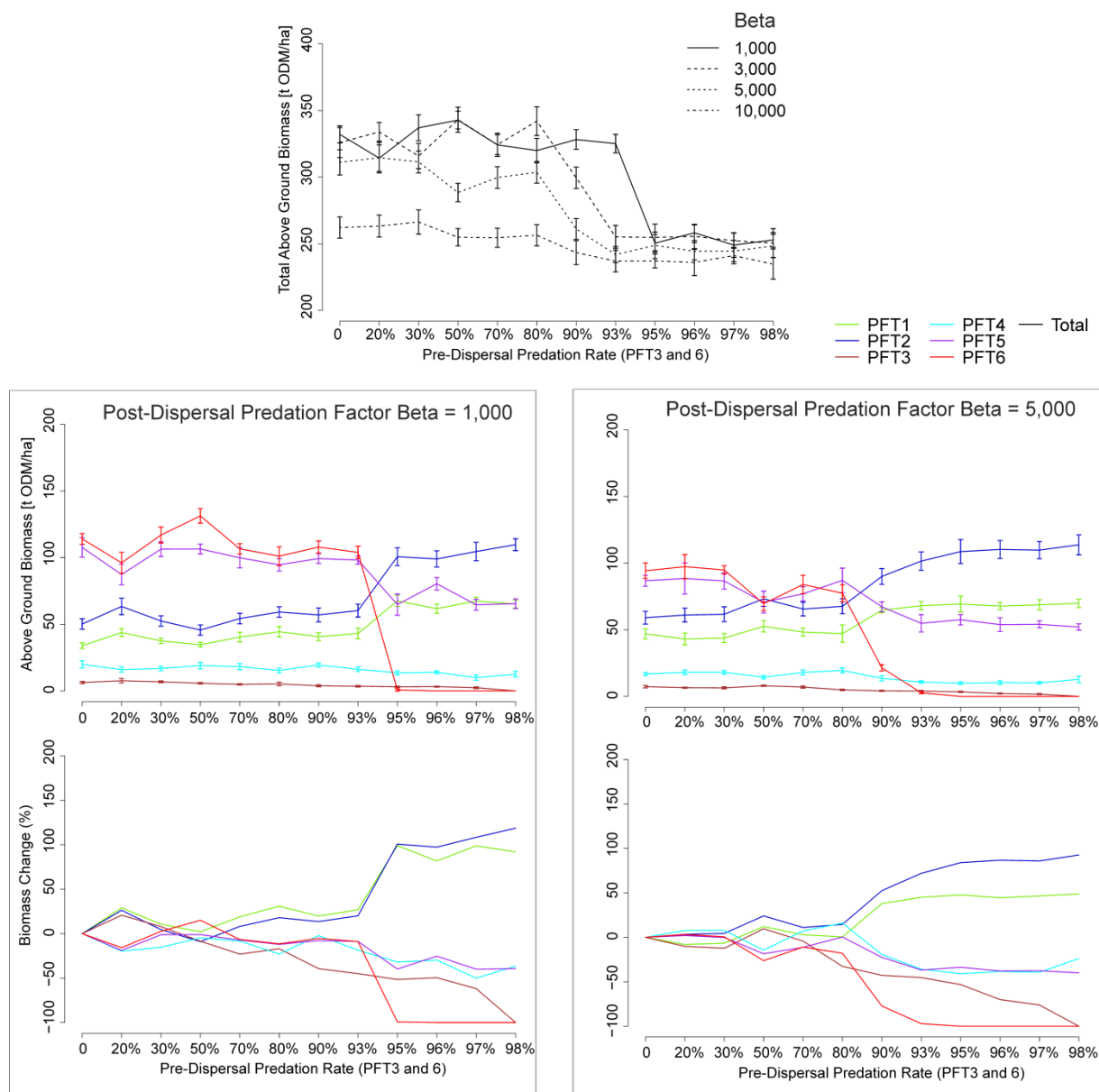
Figure 18. Above ground biomass results of 12 simulations with predation parameters parameter varying from 0% to 95% seed dispersal reduction for PFTs 3 and 6, and varying post-dispersal predation pressures. Values are averages of the last 100 years of a total 1,000 year run for each simulation. Biomass change graphs show percentual changes in relation to 0% pre-dispersal predation. Graphs for the other post-dispersal predation pressures can be found in Figure A2.

A stepwise reduction in dispersed seeds, using post-dispersal predation pressure variation of 1,000, 3,000, 5,000 and 10,000 results in significant changes to the simulated forest community only after an 80% reduction in dispersed seeds. This tipping point value was similar for all predation pressures (Figure 18)

4.3.3. SIMULATING DEFAUNATION AND FRAGMENTATION

With the activation of the fragmentation effects after 350 years of simulation, we observe no delay in biomass and parent tree number change, since fragmentation acts directly in adult tree mortality (Figure 19). When we observe the biomass change simulating fragments of different sizes, with a predation pressure β = 1,000 from an increasing size of 50 ha onwards the community composition becomes more similar to habitats unaffected by edge effects (Figure 20). Higher pre dispersal predation however, causes the largest fragments (121 ha) to retain 17% less average biomass in relation to undisturbed seed dispersal values. A similar effect is found with higher predation pressures, as a shift to a succession-arrested shade-intolerant community occurs, and larger fragments retain 15% less biomass (Table A 6).
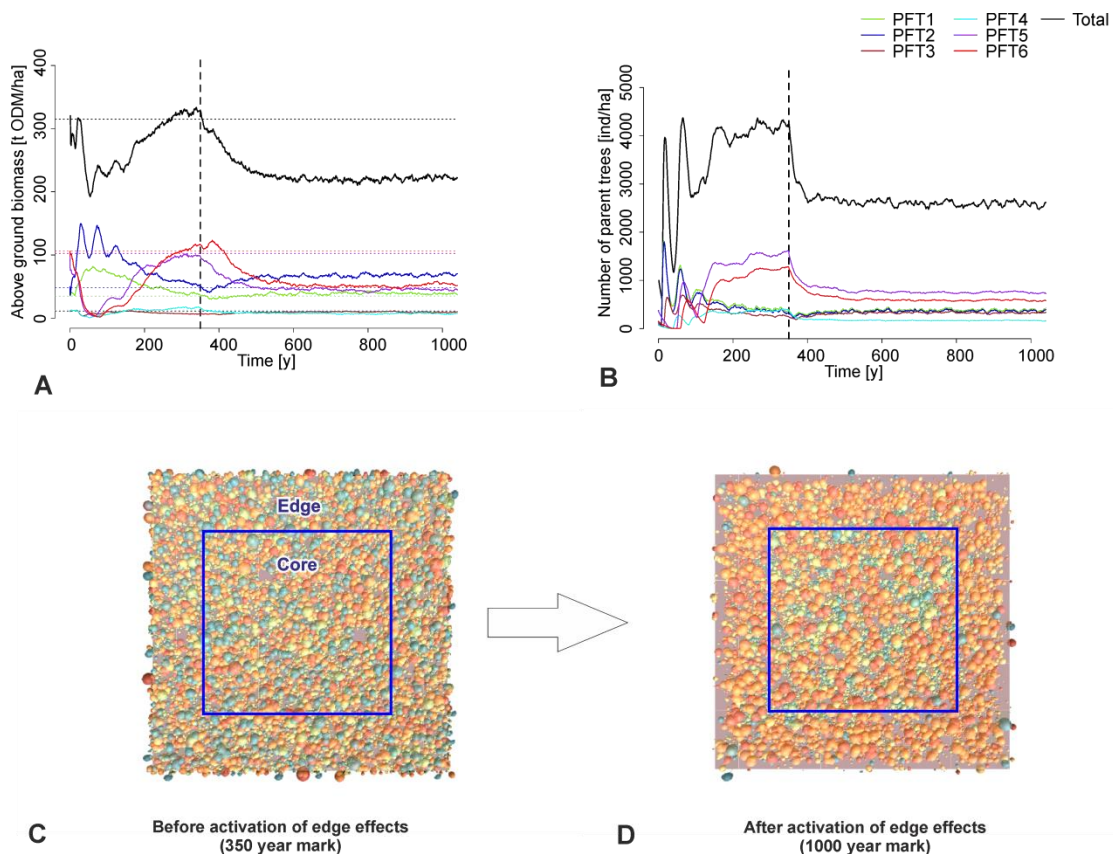
Figure 19. Fragmented landscape simulations with results for (A) aboveground biomass and (B) number of parent trees considering post-dispersal predation of 1,000 and pre-dispersal predation of 0%, in a fragmented forest of 4 hectares. The black vertical lines indicate the 350 year mark, the time of fragmentation effect activation. The

horizontal dotted lines represent the field measured values for the mature Coimbra Forest (Santos et al. 2008). Figures C and D visualize simulation results for 25 ha showing tree crowns. The blue square represents core areas which are unaffected by edge effects. Note the loss of the blue PFT6 from the pristine (C) to the fragmented (D) edge area.
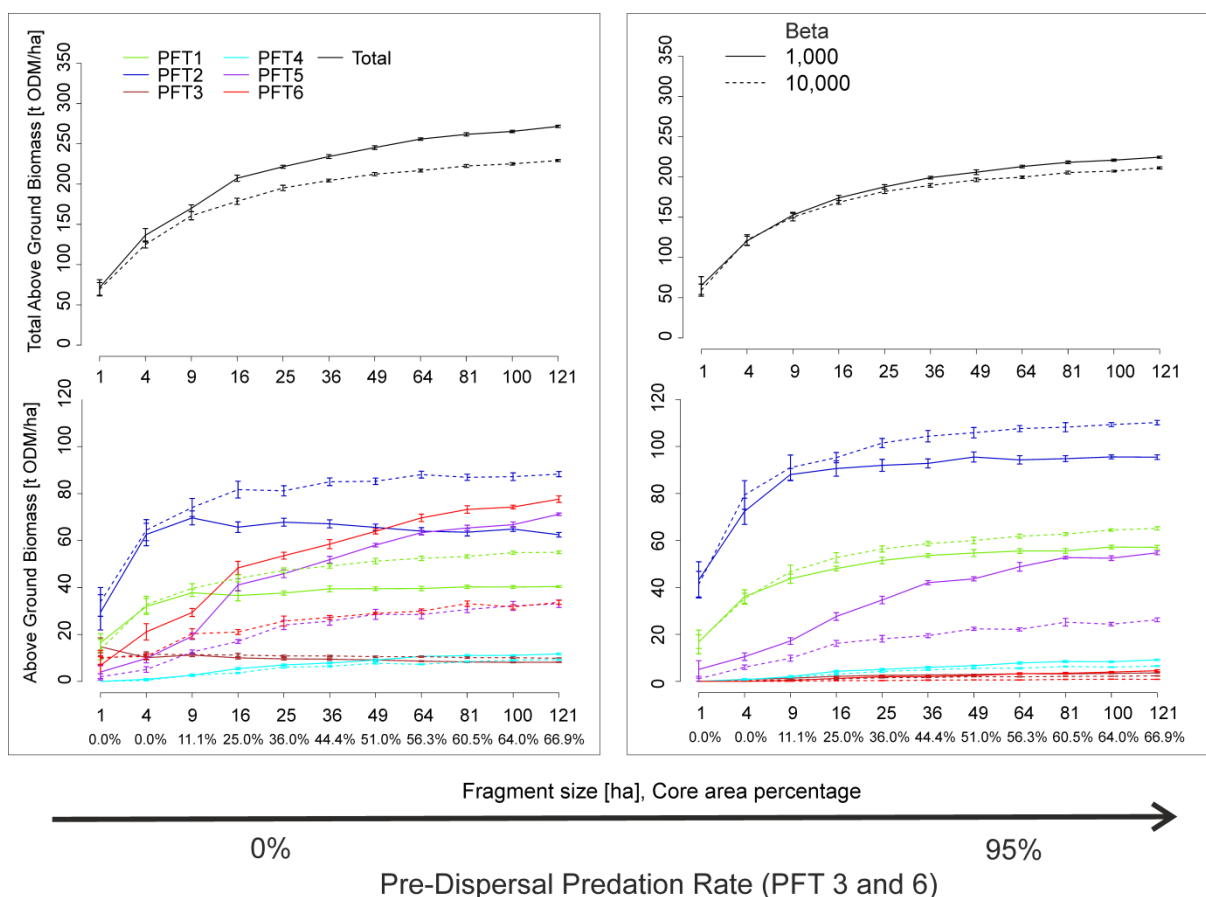
Figure 20. Above ground biomass results from varying fragment size and changing total community post dispersal predation pressure and reducing seed numbers for large seeded PFTs. Values are averages of the last 100 years of a total 1,000 year run for each simulation.

Varying the fragment size and number in a larger landscape (121 ha), we observe similar effects of diminishing large seed dispersal and higher predation (Figure 21). As reference, we analyze the 6 fragment number case, in which each fragment has approximately 4 ha. Comparing with the isolated 4 ha fragment from Figure 20, we can observe that sharing seeds among fragments provides a 4.8% increment in total biomass in relation to an isolated 4 ha-fragment. However, the trend of lower total average biomass values remains for reduced seed numbers (-11%) and higher predation pressures (-6.2%).
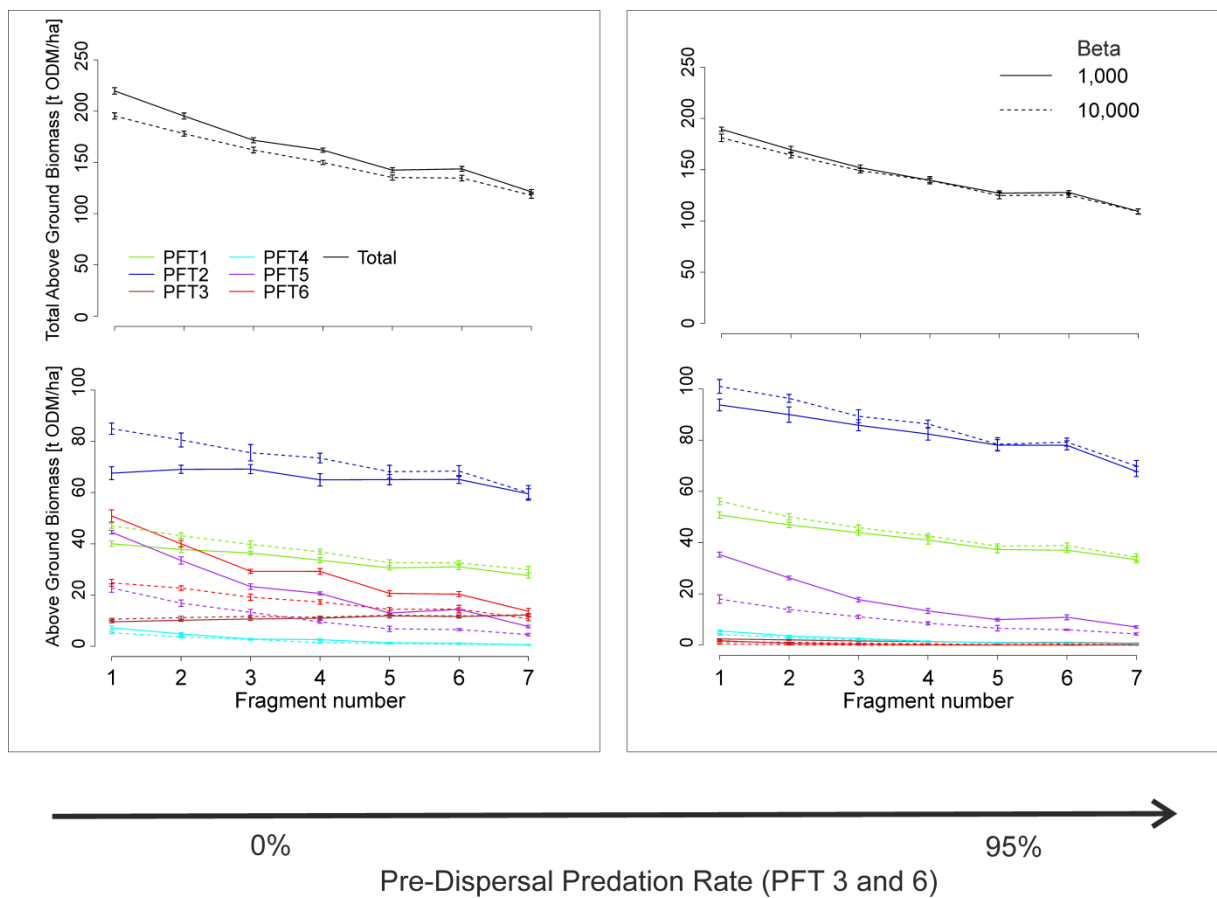
Figure 21. Above ground biomass results from varying fragment number in a constant 121 ha-landscape, with a total forest area of 25 ha, and changing total community post dispersal predation pressure and reducing seed numbers for large seeded PFTs. Values are averages of the last 100 years of a total 1,000 year run for each simulation.

4.4. DISCUSSION

Applying our three defaunated landscape conditions of 1. Higher general mortality at edges; 2. higher pre-dispersal seed predation rates of large-seeded PFTs; and 3. Higher general post-dispersal seed predation rates, had the consequences of transforming our initial old growth forest into an early successional, shade intolerant, small tree dominated landscape. By using the FORMIND forest model, we were able to quantify the direct effect of changes in seed dispersal and survival to consequences in forest biomass and community composition.

Our initial reference simulation showed an expected but nonetheless interesting delay in seed dispersal change and biomass changes, which was different for each plant functional type. This delay is related to the lifespan of the trees in each PFT, causing the tree community to take time to react due to the lack of seedlings (Melo et al. 2007), and to exhibit "living dead" communities (Janzen 1986). By varying pre-dispersal seed predation rates, we observed major changes in biomass after around 80%. If we consider that field studies found values of 60 – 97% dispersal reduction in areas of poaching (Wright et al. 2000), an 80% reduction scenario becomes plausible in real environments and is an important threshold to be further tested. In our model, predation intensity is linked to the number of parent trees and seeds in the seed pool for each PFT, therefore longer dispersal distances mean a higher chance of finding low-predation sites, and enhances survivorship. The high number of seeds produced by PFTs 1 and 2 means that they are able to be relatively unaffected even in the extreme scenario of a β = 10,000 predation pressure, due to predator satiation. Although the edge area size varies greatly between forest types and possibly landscape structure, it is clear that up to a certain distance from the edge tree community structural properties will become stable and reach higher average values than near forest edges.

Considering no defaunation, fragmented landscapes retain average undisturbed forest biomass distribution conditions with fragment areas larger than around 50 ha. Higher pre- and post-predation pressures due to defaunation sum up to edge effects, and increasingly larger areas are needed for preserved conditions, until in the extreme cases the community is shifted into an early successional state regardless to fragment size. These cases should become increasingly more frequent, as defaunation has in several regions reached very high levels. They also demonstrate the effect of community homogenization due to forest fragmentation, in which small and large fragments retain similar impoverished species pools (Lôbo et al. 2011). In the Brazilian Northeastern Atlantic forest, most of the remaining forest area (73.3%), which has a mean size of 2.8 ha, is home of only 19% of the total species pool for the region of large and medium mammal species (Mendes Pontes et al. 2016). This confirms also the pivotal role of large forest fragments in

retaining biodiversity and ecosystem services, since these areas are more likely to contain significant core areas where large mammals thrive.

4.4.1. ECOLOGICAL CONSEQUENCES

The loss of large and medium sized mammals, which predate mostly on large seeds to hunting or due to habitat size constraints, causes a reduction in the predation rates of large seeds, leaving only small mammals (mostly rodents, not preferred for hunting) that prefer smaller seeds (Dirzo et al. 2007). Therefore heavily defaunated landscapes would also present a lower number of large seed seedlings in relation to non-hunted areas (Wright et al. 2007). On the other hand insect predation, especially bruchid beetles, is thought to be higher in larger seeds (Janzen 1969), and since larger seeds are produced in smaller numbers additional predation can have a larger effect than in the small seed group (Foster 1986). This would depend of course on the appearance or not of chemical defenses in the evolutionary pathway, cases which are more common in the large seed group (Janzen 1969). Successful establishment of larger seeds is also heavily constrained in fragmented landscapes, due to edge effects, which reduces their abundance in border areas (Melo et al. 2006), an effect which was also found in seedlings (Santo-Silva et al. 2012). In conclusion, complexity and conflicting field results make it hard to disentangle whether large seeds are more or less affected by predation in defaunated and fragmented landscapes. Greater agreement of results is found on seed dispersal, where the stronger impact on the large seeded group is more accepted (Silva and Tabarelli 2000).

Considering seed size strategies, our predation model has correctly predicted that higher predation rates will benefit smaller seeds, shifting the community into a small-seed dominated environment. This is one potential effect of the loss of large animals, which predate on small seed predators or ovipositors (bruchids). However, it is surprising that considerable effects on biomass are only notable at pre-dispersal predation rates of over 80% and post-dispersal predation rates of over 10 times our initial conditions. Considering that we have used real seed rain data, we can speculate that even large seeded trees produce more seeds than needed for the maintenance of their abundance. This hints at a high resilience of tropical tree species for our study region within the context of the seed production/predation race. Indeed, such a high seed production buffer would be invaluable in the occurrence of years of lower productivity due to harsh climate for both the trees and the dispersers. Unfortunately, due to the high mortality of the seed sources (parent trees) in fragmented landscapes such resilience mechanisms do not seem to be buffering tree communities against a shift into early successional communities, as can be seen in field results for edge effects in seeds (Melo et al. 2006, Costa et al. 2012), seedlings (Melo et al. 2007, Santo-Silva et al. 2012), and

trees (Broadbent et al. 2008, Oliveira et al. 2008, Santos et al. 2008, Dantas de Paula et al. 2011a). This is an example of complementing field and model results, providing exciting new research questions of just how resilient are tree communities to human land use.

Seed dispersal determines the spatial pattern of tree populations as well as the community composition (Janzen 1969; Howe and Smallwood 1982; Seidler and Plotkin 2006; Wiegand, Martinez et al. 2009; McConkey, Prasad et al. 2012; Augspurger, Franson et al. 2016). Dispersal vectors such as wind or animals are believed to be evolutionary responses, and are related to energy and environmental constraint trade-offs (Foster 1986). Tree establishment is therefore directly linked to animal groups through the processes of seed predation and seed dispersal. Since seed predators are attracted to seed sources, and can also be satiated by large seed numbers, strategies to disperse long distances or to produce large amounts of seeds are thought to be evolutionary responses (Janzen 1969; Howe and Smallwood 1982).

The loss of vertebrate dispersers has some interesting implications for seed dispersal, predation and seedling establishment The predator parameters (i.e. number, distance, search efficiency and handling time) will therefore determine which dispersal strategy (short or long distance) is more favorable in terms of establishment values, as envisioned by Janzen-Connell model. Vertebrate-dispersed species usually disperse long distances because short distance dispersal would render the seeds more vulnerable to predation and thus reduce seed establishment. Also, larger seeds are more vulnerable to predation (Janzen 1969). In a fragmented landscape scenario, this means that the loss of a disperser has not only the consequence of isolating populations (Silva and Tabarelli 2000, Melo et al. 2006), but also of leaving the functional group further prone to seed predation, reducing its establishment numbers. It is clear however that some large seeded species from the field inventory are able to thrive in fragmented landscapes – especially *Tapirira guianensis* and *Thrysodium spruceanum*, both from PFT3. It seems clear however that the fact that small-seeded species have adults with lower wood density than large-seeded species is behind the cause of lower total biomass retention in our large-seed extirpated simulations.

4.4.2. CHANGES TO ECOSYSTEM PROCESSES

Considering our seed loss simulations, we conclude that niche liberation for the growth of small seeded trees is unable to compensate the loss of large seeded plants in fragmented forests, even in large fragments not influenced by edge effects. These experiments thus show a possible direct link between defaunation and collapse of ecosystem processes. The results here present a reduction of 17% biomass for our extreme seed loss and predation pressure cases. This effect is dependent on

our analyzed community, and of our PFT grouping, which means that the results may vary greatly depending on the undisturbed conditions of large seeded tree species for each tropical forest domain. Indeed, in the recent study by (Peres et al. 2016) considering the whole of the Amazon, a large variation in possible biomass loss of 2.5% to 37% was found, and in another study by (Bello et al. 2015) conducted in the Atlantic Forest, a loss of up to 3.7 Mg/ha of Carbon (which should translate to a maximum 2% loss) was estimated. Therefore, while on empirical-based models a linear relationship of defaunation and biomass was observed, in our study we were able to observe a significant effect only after more than 50% large seed number loss. It seems also quite clear that understanding just how much biomass is lost due to large-seed species dispersal collapse depends on simulation of local tree community and understanding the threats to the local fauna.

Our observed results in this paper allow us also to glimpse a long-standing perception of long term fragmentation field studies: the loss of ecosystem function in fragmented landscapes can extend farther than the expected only through edge effects, but bring the tree community into early successional states by alterations in ecological processes. Both lower seed dispersal of threatened species due to defaunation and higher general predation rates due to relaxed top-down effects have the potential to cause this shift in plant communities, with consequences to biomass retention. In such a scenario, we cannot expect fragment size (or better, core area percentage) to be an adequate descriptor of conservation value in absolute terms (considering total functional richness), since the functional group loss would cause altered ecosystem processes in relation to preserved conditions. In relative terms however, larger fragments can benefit from less edge influence.

4.4.3. USING FOREST MODELS IN PLANT COMMUNITY SHIFTS

Using individual-based models allows us to expand on empirical information, using well-known processes and predict unseen consequences. This approach shows the possible interplay between models and empirical data, bringing forth questions that can be tested in the field in order to improve the model. Since we did not parameterize mortality from field data and had to estimate it, loss of adults and seedlings due to unmodeled processes has been likely incorporated into the mortality values. This of course does not mean that all uncertainty in the predictions are caused by unknown mortality values – there are many other processes and conditions that have not been included in our simulations, such as polinization, herbivory, soil and topographic conditions, not to mention human disturbances. Nevertheless, we want to observe with our given idealistic conditions which patterns can already be replicated.

Real landscapes are heterogeneous, and can contain different tree communities. It is important to simulate entire heterogeneous landscapes with different levels of boundary contrast, because tree communities which establish in each condition interact with one another and this transition is often complex, becoming a particular community on its own. Although we have explored here only simple landscapes, it is possible to include values from any grid based maps into FORMIND, and observing how a particular tree community would react using all functionalities from the model such as climate, fire, landslide, etc. This simulation can then be validated against measured field or satellite data, providing a feedback to parametrization.

4.4.4. CONSERVATION IMPLICATIONS

The functioning and planning of landscapes with less impact on biodiversity has been addressed in a large number of empirical and theoretical studies (Hansson and Angelstam 1991, Forman 1995, Menon and Bawa 1997, Metzger and Décamps 1997, Foster et al. 1999, Poiani et al. 2000, Sanderson et al. 2002, Ibáñez et al. 2014, Arroyo-Rodriguez et al. 2015, Dantas de Paula et al. 2015, Gagné et al. 2015). Some questions, such as the SLOSS debate (Single Large Or Several Small forest fragments), provide arguments for the size or number of forested areas in human modified landscapes (Ovaskainen 2002), while concepts such as forest corridors for the connection of existing areas are analyzed for their benefits in preserving ecosystem function (Pascual-Hortal and Saura 2006). Even with an ever swelling body of knowledge, the science of conservation biology lacks straight answers for some of its basic questions (e.g. minimal area or percentage requirements for ecosystem functioning). This in part is related to the complexity of the study subject, but also due to the natural limitations of the research methods (Wright et al. 2000, Chave 2013, Shugart et al. 2015). Although deeply driven by data and statistics, the reduced temporal, spatial and community scale of traditional field ecology reduces its efficiency for a line of research that is naturally highly complex. This is why their findings have much to gain from new paradigms such as individual based ecology, and its analytical tool, the individual based computer models (Grimm and Railsback 2005).

We believe that individual based forest models have a large potential in integrating empirical biological data and producing consistent predictions of the effects of biological and environmental change in large temporal and spatial scales. Results such as we have presented carry a great sense of urgency especially in the context of human induced species loss and are of great value for the field of conservation biology. Conventional empirical studied have faced great difficulties in providing compelling arguments for species conservation, offering at most qualitative predictions of species loss consequences. Therefore, even considering the limitations of forest models, their

mechanistic nature and production of quantitative data provide at the very least concrete values with which policy makers can use to better plan conservation landscapes. The preservation of large tracts of forest are commendable actions for species protection and to maintain the environmental services they provide, but as other studies suggested (Silva and Tabarelli 2000), may not be enough. We have here also reached this conclusion, further suggesting seed loss tipping points and demonstrating the effects of higher predation rates. Therefore, due to defaunation causing the loss of seed dispersers and ultimately the tree species, in order to preserve ecosystem functioning more direct interventions are needed, such as high diversity reforestation (Rodrigues et al. 2009, Rodrigues et al. 2011), for severe fragmented landscapes. Initiatives which implement these techniques in the regional scale which introduce directly seedlings from threatened functional groups, such as the Atlantic Forest Restoration Pact (Melo et al. 2013b, Pinto et al. 2014), are thus paramount for reverting seed dispersal and community biomass collapse in severely fragmented landscapes.

4.5. ACKNOWLEDGEMENTS

5. CONCLUSION

In order to better understand the dynamics of forests, in their pristine and disturbed conditions, a temporal and spatial scale much larger than conventionally used by field ecology is needed (Chave 2013). Although field ecology uses very sound and accepted inquiry methods, time, space and ultimately financial constraints render the field approach limited for forest ecosystems (Schmolke et al. 2010). Therefore, to advance in understanding the multiple challenges of forest ecology research, new methods must be implemented that can embrace larger scales (Huston et al. 1988). However, the integration of modelling and remote sensing represents a potential turning point for the field, helping us to improve predictions of ecosystem processes. Through the three chapters presented in this thesis, I have used forest modelling and remote sensing in order to investigate the temporal and spatial consequences of forest fragmentation to tropical tree communities.

Remote sensing provides huge amounts of spatial data that can be analyzed in search for patterns. In our second chapter, we were able to observe long suspected patterns of tree cover in fragmented landscapes (i.e. higher variation of forest structural conditions), which were unremarkable when observed solely by field measurements. The high variation of tree cover near edges, which decreases as distances to human modified landscapes increase, as well the differences between landscapes in relation to edge tree cover are important indicators of forest conditions. Since temporal dynamics of forests are extremely difficult to investigate with field measurements, predictions by forest models such as FORMIND allow us to better investigate the time scale of forests facing disturbance regimes.

Additionally, the modular nature of FORMIND permits a stepwise increment in complexity that ultimately is able to generate predictions of indirect effects and cascades. Such process interdependence (e.g. animal influences in future tree community composition) is characteristic of species rich tropical landscapes, but using empirical models these effects seem impossible to disentangle. We have demonstrated however in an interesting example the power of forest models in generating predictions, by evaluating in the first chapter the impact of fragmentation in the forest hydrology processes, and in the third the effect of reduced seed dispersal and ultimately the impacts of dispersing animal loss for forest biomass retention.

5.1. PARAMETRIZATION AND CALIBRATION

In ecological modelling, the step of identifying reliable parameter values is central to producing results which can be trusted and used as reference. The Serra Grande Landscape, where the tree

field data was collected had only 5 ha total inventoried area and only in one point in time. However, many additional studies have been conducted in the area, considering all of tree life stages (seeds and seedlings) as well as other biological groups, giving the study site a remarkable sampling diversity and quality (Pôrto et al. 2006). Furthermore, this region is unique on the human influenced context, in the sense that land use was kept the same for a long time, and the fragments are very old, therefore long term effects of fragmentation are observable. For both my chapters which were focused on FORMIND, I observed that functional grouping characteristics must reflect the objectives of the study. In the first, functional groups were defined according to maximum height and response to light – classical definitions when analyzing forest dynamics. In the third, since I was interested in seed dispersal and its failure in fragmented landscapes, groups were defined based on light response, seed size and seed dispersal type. In the first study, I focused on different environmental conditions (edge, fragment and core areas). This means that mortality and seed input parameters were different, in order to reproduce forest dynamics in these different areas using the field samples on each habitat as reference. These estimated parameters become thus a result in itself. On the third chapter, I included field measured seed production and seedling data on the model, and modified the seed dispersal from global seed rain to one produced by individual trees. This also means that the seed number parameters for the field were fixed, and calibration was done by adjusting only the mortality values.

The available field data does not, unfortunately allow for a complete localized parameterization approach, therefore calibration is necessary. Calibration refers to the process of adjusting parameter values in order for the model to reproduce observed values (van Oijen et al. 2013). It is a time consuming process when the model is complex, and when calibration is done manually. Several techniques however have been evaluated in order to estimate parameter values from experimental results, known collectively as "inverse modelling". This has been attempted for dynamic vegetation models using for example, non-linear regression models (Lehmann and Huth 2015). In FORMIND inverse modelling for parameter estimation was attempted using approximate Bayesian inference (Hartig et al. 2014), which resulted in adequate estimations of parameters for a species rich Ecuadorian rainforest, although with considerable computational effort and only calibrating the mortality and growth parameters. An inverse modelling tool is available for parameter estimation in FORMIND (MOOP, Lehmann et al. unpublished), however the computational power for its many trial runs is still quite limited, especially when activating the seed dispersal by individual trees. Therefore manual calibration was chosen for this study.

Several key parameters such as photosynthesis rates and crown diameters were not measured, based on other measurements taken from literature and calibrated within a specific range determined. This was the case with adult tree mortality, which typically lies between 1 and 3% per

year, and was estimated in order to reproduce field basal area, biomass and stem numbers. The parameterization process is a good example of linking models and empirical work, where forest models suggest new variables to be measured in the field, or propose estimated parameter variables and hypothesis which can be measured in the study site.

5.2. SIMULATION RESULTS

The results of FORMIND's simulations are always specific for a parameterization defined in a study area. However, the ecological processes defined in the model should be the same for any forest type (as long as parameters are adjusted accordingly), and conclusions for one area can be considered for other similar forest types. FORMIND's strengths are in revealing hard-to-measure properties in forest dynamics and landscape structure, also when facing disturbances. Although field data could reveal in a straightforward way community shifts after fragmentation in forest edges and isolated fragments (Santos et al. 2008), FORMIND was able in the first chapter to estimate the time scale involved in these community shifts, laying around 100 years until mature forests suffering from the effects of deforestation reach a new stable state. During these shifts, details of carbon balance could also be seen, such as a double surge in carbon sequestration due to growth and death of fast growing species and then the forest's change into a new slow-growing species dominated state. By introducing climate and soil data information on forest water balance of the forest was calculated, showing that edge affected habitats will evaporate 43% less and lose 57% more water due to runoffs in relation to unaffected forests.

By adding seed rain data in the third chapter, I was able to observe how changes in seed survival affect latter stages in the forest life cycle, in special the delay between seed predation change and changes in the forest's properties, and the intensities needed to shift the tree community into new functional states. Tree communities proved to be resistant to changes in seed number, needing a loss of around 80% before major changes in the dominance of species groups was modified.

5.3. REMOTE SENSING RESULTS

The second chapter conducts an analysis which estimates internal fragment conditions at a much higher spatial resolution than previous studies (30 m LANDSAT Tree Cover (Sexton et al. 2013)), allowing for the observation of changes in tree cover due to edge effects. It was observed that a huge variation of tree cover occurs in the vicinity of edges (i.e. "fan shape"), suggesting that tree dynamics around this area are profoundly different. The maximum penetration of this effect varies

greatly according to different regions (100 – 500 meters), which could reflect in part the sealing dynamics of edges in time (undergrowth due to increased light in time blocks microclimatic changes to deeper parts of the forest), local landscape conditions (e.g. topography, soil) or different responses by the local tree community. In any case the study suggests that the tree cover of any particular landscape should be analyzed (using this freely available data) before classifying forest fragments internally as "edge" or "core" for research or management purposes. This tree cover evaluation allows also to detect individual forest fragments which are in a good or bad conservation state, when using tree cover as habitat quality proxy.

Although the concept of analyzing forest structure through remote sensing data in order to evaluate its conservation state is not new (DeFries et al. 1995), applying it to study forest degradation in relation to edge effects is novel, although one recent study has attempted to estimate carbon retention in edges using remote sensing (Chaplin-Kramer et al. 2015). This previous study however used satellite images with a spatial resolution (500 meters) which were in my opinion unsuited to study edge effects. Nevertheless, our 30 meter data showed a similar pattern to the Chaplin-Kramer study, that edges exhibit huge variation in tree cover (and probably in relation to other ecosystem properties), becoming lower as edge distance increases. I also observed by comparing several individual landscapes, that this high variation penetrates further in some areas than in others. This means that for example in some landscapes, small fragments may be enough to retain core area conditions, while in others a much larger size is needed depending on the landscape context (e.g. topography).

5.4. LINKING VEGETATION MODELS AND REMOTE SENSING

Integrating forest modelling and remote sensing provide exciting possibilities for tropical ecology, planning and management of biological conservation. Although field-data based empirical ecology remains the yardstick for ecological body-of-knowledge construction, and represent generally still most high confidence information, the tools used in this Thesis offer a chance to overcome its conventional limitations.

Over the last years, there has been a growing recognition that both above described fields, remote sensing and vegetation modelling are mutually beneficial (Plummer 2000). Remote sensing has been acknowledged as a valuable source of comprehensive spatial and repeatable temporal information. Similarly, models are able to integrate ecological knowledge and using equations predict future states or other ecosystem properties (Hurtt et al. 2010). The coupling of both fields

allow for some interesting research possibilities, which are illustrated in Figure 22. Three major directions for integrating remote sensing and models are shown below:

- Initialization of models through remote sensing (Figure 22a):

The most common interface between models and remote sensing is using remotely sensed data for input of vegetation models, establishing the starting point of model simulations. This is important because vegetation models are highly dependent on initial states in order to predict future properties of forests for example. Remote sensing is able therefore, to assist when having adequate spatial resolution, in providing large scale data for vegetation model input (Shugart et al. 2015). Sensors in remote sensing platforms measure radiation reflected or emitted by the Earth surface. In order for this radiation to be used by vegetation models, it must be translated into a variable compatible with the vegetation model input. Some remotely sensed data however, can be directly linked to models, such as canopy height (Neumann and Reigber 2010). Already some studies have been made using remote sensing as input data of vegetation models, such as radar measurements to initialize model biomass (Ranson et al. 1997), or LIDAR measurements of vertical height profiles to parameterize a canopy photosynthesis model (Lefsky et al. 1999).

- Comparing results from remote sensing and forest models in the temporal (Figure 22b) and spatial (Figure 22d) dimensions:

A relevant use of remotely sensed data in connection with ecological process models is to test whether they are able to produce reasonable results. In this approach, results from both remote sensing and vegetation models are correlated to one another (e.g. LAI measured from forest model in relation to NDVI calculated from a satellite image (Hunt et al. 1996)). This is especially useful in order to calibrate the vegetation model for the correct representation of current and of future ecological processes. Vegetation model output that can be correlated to spectral data can be a direct ecological variable such as biomass, or by coupling a radiation model to ecological models (Plummer 2000). In this case, radiation models simulate spectral signatures which can be compared to remote sensing spectral measurements (Friend et al. 1993).

- Producing maps of ecological variables not measured directly by remote sensing platforms (Figure 22c):

In this case, although remote sensing data are also used as input, the focus is on the production of a map by the ecological model. Here, the model must be able to produce a spatially explicit output of a variable which was or could not be measured directly by remote sensing. Attempts have been made to produce maps using simple statistical models, for example GPP estimates produced by satellite-derived NDVI (Xiao 2004), maps of aboveground biomass (Avitabile et al. 2016) or calculate the global number of trees (Crowther et al. 2015). However, more complex process based ecological systems are potentially able to produce maps of many other ecological properties such as forest evapotranspiration, by integrating soil and hydrological models, as well as improve previous mapping of biomass.
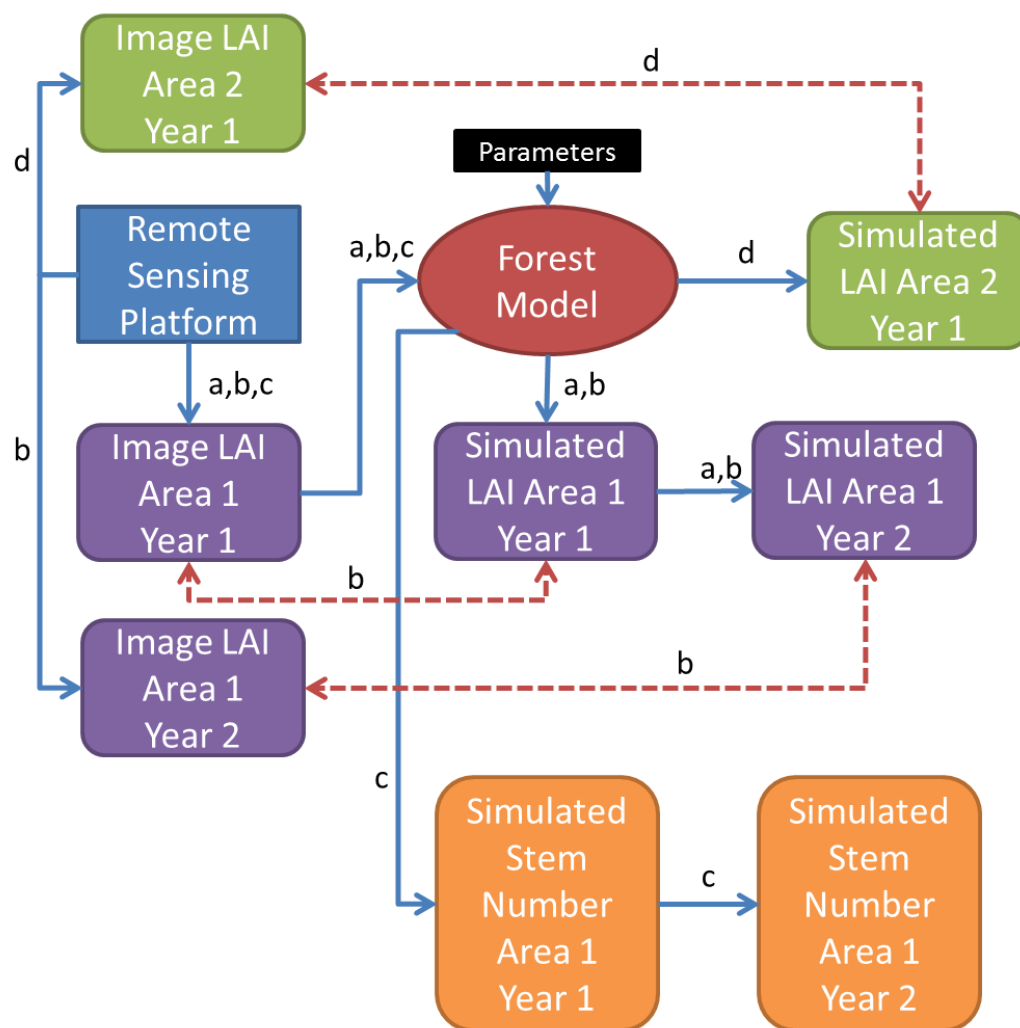
Figure 22. Conceptual diagram of possible interactions between remote sensing and forest models. The blue (remote sensing) and red (forest model) concepts interact through a. future predictions of LAI for Area 1 (purple); b. Comparisons of LAI between images and simulations of different years (purple); c. Production of stem number map for Area 1 (orange) using the forest model; and d. Comparisons of LAI between images and simulations of

different areas (green). The black (parameters) box represent data necessary for the model which could not be estimated from remote sensing. Blue lines are data inputs and red lines are comparisons.

The integration of remote sensing and vegetation models promises to improve our prediction of ecological responses to global change of forests over continental scales, due to factors such as deforestation, climate change and shifts in species distributions (Hurtt et al. 2010, Shugart et al. 2015). The chapters presented in this thesis can be gathered within the context of this integration process between the two fields in order to better understand the impacts of forest fragmentation. For two main reasons this represents a challenge in relation to previous work in remote sensing/vegetation model integration. First, the scale in which the main impacts of fragmentation are observed lie in the 100 meter range, due to the edge effects. This restricts the available remote sensing data in extent and temporal availability, and computer processing power, which must be considerable. Second, tropical forest dynamics are dependent on many ecological processes, such as seed dispersal, which must be considered in forest models in order to reproduce major ecosystem patterns such as biomass. Efforts to improve the representation of tropical ecological processes in forest models such as FORMIND and the identification of relevant remote sensing products should be encouraged. This is necessary in order to allow for the integration of models and remote sensing in a spatial and temporal scale which is compatible with the ecological processes which occur in tropical forests.

5.5. FUTURE STUDIES

These thesis' chapter results lay the groundwork for studies providing a more mechanistic understanding of forest fragmentation using remote sensing and forest models. The major goal of this approach is to be able to predict future changes in ecological and ecosystems processes in a recently fragmented tropical forest. Such an important tool for studying, planning and managing anthropogenically altered tropical forest landscapes can be developed through the integration of FORMIND and remote sensing products. This approach has also the power to help understand classic theoretical questions in ecology. I will discuss now a sample of possible future directions in the development of models and remote sensing.

5.5.1. FOREST MODELS AS ECOLOGICAL LABORATORIES

Considering its development history within the concepts of individual based modelling, modular approach and local scale, forest models have great potential to become highly relevant for studying tropical ecology. I have demonstrated in the third chapter how an ecological process which is commonly ignored or very simplified on some models (seed dispersal) can have a disproportional effect on matter fluxes (e.g. carbon). In order for the forest model FORMIND to construct its role as a virtual experiment environment in ecology, two major improvements are suggested.

First, an open and permanent research exchange with field ecology must be established. Field work measuring key abiotic and biotic variables plays an important role in the support of both remote sensing and forest modelling. Field based information is used primarily for the parametrization and calibration of forest models and is very important for the production of robust results. Although a wealth of field data has been collected, there are important knowledge gaps for the model parametrization which can be measured by field ecologists and improve considerably the robustness of models. This demand is an important call for project partnerships. The most important un- or poorly known field parameters in FORMIND are the ones related to photosynthetic production, such as maximum production rates, slope of light response curve and light extinction coefficient of leaves. These photosynthesis variables should preferably be determined for individual species (in order to allow for different functional type groupings) and under varying microclimatic and edaphic limiting conditions. Such project could be done in part or totally in greenhouse conditions with extensive use of commercially available light and gas exchange sensors for vegetation. This can be a huge task, but one which would inevitably increase greatly our knowledge of vegetation growth and allow for very robust simulations. Also related to light are the germination parameters of seeds, which although known for functional groups (Kitajima 1994), could still be improved at the species level. Additionally, repeated census of trees should be expanded and encouraged, in order to provide the important diameter growth and mortality parameters. This work should be done preferably on permanent, large scale plots (>50 ha) in order to obtain extensive and repeated field information.

Second, new ecological processes relevant to tropical dynamics must be introduced in FORMIND. Focus must be primarily on processes influencing the life cycle of tree species and functional groups, considering especially seed production, dispersal, germination, growth and mortality, and the ecological processes which influence them. Because these processes can change completely the tree community composition for a determined area, and different tree communities have other influences on matter cycles, they must be considered especially in the face of human induced changes. These processes which regulate the life cycle of trees are mostly dependent on other biological forms, and provide exciting research possibilities. Seed production is determined by

pollination, in tropical forest carried out especially by invertebrates such as bees (Bawa et al. 1985), whether seed dispersal is primarily conducted by vertebrates (Janzen 1969). Seed predation, as described in this thesis is fundamental for determining germination, but herbivory by ants can potentially alter tree community composition and impact long term forest dynamics (Wirth et al. 2008). This means that incorporating animal ecology into FORMIND could improve greatly the representation of tree life cycle dynamics. A good starting point for this challenge is to represent the animal groups which have the most influence in pollination (e.g. bees), seed dispersal and predation (e.g. birds and rodents) and herbivory (e.g. ants), as a separate model or as a module to FORMIND. A very important argument in favor of adding yet more layers of complexity into FORMIND is to better understand impacts of animal diversity on forest structure and functioning, and consequently major ecosystem services. Finally, other processes such as belowground ecosystem dynamics regarding tree root competition for water and nutrients, as well as interactions with fungi can also become relevant (Putz and Canham 1992).

In addition, the fragmentation module must be improved, being at the moment driven by increasing mortality directly in relation to distance. Microclimate conditions (Camargo and Kapos 1995, Didham and Lawton 2001, Pinto et al. 2010) and increased wind disturbance (Saunders et al. 1991, Laurance and Curran 2008) in edges are the ultimate drivers of the changes that happen in fragmented landscapes. Detailed field measurements of microclimate and wind speed in relation to canopy height and edge distance, as well as in time would allow to improve the representation of the edge effects in FORMIND. A better modelling of edge effects could greatly improve our knowledge of edge penetration distances, and to understand why and how edges become "sealed" a few years after fragmentation. Also, the forest fragmentation degradation of other ecosystem properties (e.g. evapotranspiration) can be better understood and upscaled to regions, allowing for a better estimation of the effect deforestation has on precipitation change (Aragão 2012, Spracklen et al. 2012).

Finally, forests exist in a heterogeneous landscape, with variations in topography, land use or soil properties. Simulating forests in FORMIND on an area where patches are different has been implemented on the third manuscript, when considering several fragments on a forest-non forest area. This is in reality a particular case of the implemented landscape code for patches, which allow for each 20x20 patch to be associated to a number representing a certain spatial property. The model's response to this property can reflect anything from elevation, to water content, or proximity to edges. Also any georeferenced (e.g. satellite derived) map can be used as an input and simulated through FORMIND, when using a resolution similar to the patch size of the simulation area (20x20 meters). This represents an important step towards model-remote sensing integration, since FORMIND is now able to input and output data which is compatible with remote sensing.

5.5.2. ADVANCES IN REMOTE SENSING

FORMIND is able to receive as input for the initial state of its simulations a forest inventory table containing the diameter at breast height (DBH) of each individual as well as the identity of its plant functional type (PFT). One of the main interests of models in remote sensing is for the latter being able to acquire field data without human intervention and for larger scales. In order satellite or aerial data to be able to initialize FORMIND, remote sensing measurements must relate to DBH and PFT identity. In the case of DBH, since in FORMIND tree height is derived from diameter using alometric equations, DBH can be estimated from tree height which in turn can be measured with precision using LIDAR or SAR sensors. The LIDAR and SAR available data is expected to increase greatly in the next years due to the increase of aerial campaigns and missions such as Sentinel, Tandem-X, ALOS and BIOMASS (Table 1). To identify the tree to which the signal returns belong, a topographic algorithm can be analysed, considering that tree crowns have roughly a concave shape. Although this is being attempted to with aerial LIDAR (Knapp et al. unpublished), satellite based SAR must have similar resolutions in order to identify the number of trees at a particular height. In the case of PFTs identification, expectations lie on the development of high resolution multi and hyperspectral sensors which are able classify the LIDAR or SAR measured tree crowns into desired PFTs. In relation to shade tolerance, this could be done potentially by identifying properties in leaves such as nitrogen content. However, hyperspectral missions (HYPERION and ENMAP) have sensors with a resolution unsuitable for this (30 meters), while it remains to be seen whether current multispectral (WorldView-3, 16 bands; Sentinel-2, 13 bands) or future hyperspectral missions have sufficient spectral and spatial resolutions in order to identify PFTs.

Regarding spatial output, FORMIND can produce yearly results of several forest properties such as basal area, tree number, surface runoff, number of seeds, etc. for each plot, resulting in a map of the simulation area with 20x20 meter resolution. Comparing these results for validation or calibration indirectly (e.g. LAI vs NDVI) is already possible with any compatible remote sensing platform. Comparing results directly however requires a radiation model which can simulate canopy reflectance and relate it to a remote sensing product – an interesting research opportunity. This has been attempted with LIDAR, with good results, by simulating the returning laser radiation on top of the canopies and comparing to real LIDAR measurements (Shugart et al. 2015). This is being developed at the moment for FORMIND, through a new module (SIDAR, Knapp et al. unpublished).

Finally the production of maps of forest properties which were not directly mapped by remote sensing using FORMIND is generally straightforward, considering the grid based plot output. However, special validation must be carried out in these maps to improve robustness. One recent

work by Rödig et al. (unpublished) uses FORMIND to improve biomass estimations of the Amazon basin, using simulations with several field datasets from the region. In relation to forest fragmentation, (Pütz et al. 2014) used FORMIND and remote sensing to estimate that degradation of carbon stocks in forest fragments due to edge effects can represent 9-24% of total forest carbon emissions. Studies producing carbon and biomass maps do not however explore the full power of forest models, since these properties can be estimated from simple alometric equations in field data. A true test for forest models is the calculation of complex multivariate, structural and species-dependent properties such as the effect of forest fragmentation on large-scale evapotranspiration patterns. FORMIND's advanced climate module allows for daily inputs of temperature, precipitation, potential evapotranspiration and radiation based on local climate data, as well as soil properties (depth, permanent wilting point, porosity, conductivity, etc.). This allows for calculation of canopy transpiration and surface runoff, which are dependent on forest structure. By including mortality changes due to edge effects, it is possible to estimate transpiration and runoff average values in relation to fragment size and core area proportion. This in turn can permit estimates of local and regional changes in fragmented forest hydrologic influence (Aragão 2012, Spracklen et al. 2012), by creating maps of evapotranspiration rates, and estimating their influence on rain-producing air masses. Accounting for the influence of vegetation has always been a great challenge in climatic and weather models (Foley et al. 1998), and forest models have the potential to produce a more realistic feedback of water transfer from the soil to the atmosphere. Such studies have great potential in producing maps which represent hard to measure variables such as evapotranspiration in a larger scale.

5.5.3. FORMIND AS A PLANNING AND MANAGEMENT TOOL

Evaluation of forest structural properties from space with remote sensing and reproducing their behavior in time are both important for environmental planning and management. They represent a broader need which is understanding the exact state of forests in large regions for a specific region, and being able to predict the future state of these forests of this area after a certain time (Didham and Ewers 2012, Spracklen et al. 2012, Chave 2013, Newbold et al. 2015, Visser et al. 2016).

Understanding resistance (ability to respond with little or no change in the face of a disturbance event) and resilience (ability to recover rapidly from a disturbance) of forest communities in the face of disturbances is an important theoretical question (Walker et al. 1999), but also of great value in forest management. The recent economic development of many tropical countries has pressured local environmental agencies into an arduous decision-making process in which species

and environmental services loss are weighed against land use change, and generally losing to the latter due to weak argumentation (Lamarque et al. 2011). Conventional empirical ecology is not well suited to answer questions such as "how much disturbance intensity can an ecological system endure?" However, urgent answers for these questions are needed, and continuing research with ecological modelling of forests can provide strong arguments for the limitations of our natural capital.

Besides land use change, which has been addressed in this thesis, climate change, quantification of environmental services and forest restoration are important topics in which FORMIND could play a major role for conservation biology as a whole.

With regards to climate change research, forest models allow for shifting the focus of current studies in quantifying carbon emissions to testing possible feedbacks in atmospheric carbon fertilization, direct temperature effects for tree survivorship, and the influence of mass forest evapotranspiration in local and regional precipitation patterns. Such complex questions could be potentially addressed using the climate and soil modules of FORMIND presented in this thesis.

In the case of environmental services, their quantification seems an interesting possibility using forest models, also regarding its response under disturbances. In this thesis I have shown for example how estimations of surface run-off can be made using FORMIND, and the change in this variable due to disturbances. Total surface run-off is an important component of many water-related services computation, influencing water quality and river recharge (Kosoy et al. 2007). Since in payment for environmental services schemes (PES) practical, fast and concise measures of ecosystem properties are important, the construction of a framework using FORMIND would be an interesting possibility. In such a framework estimations of water or carbon services could be generated for a large amount of service providers by entering local forest, soil and climate conditions.

In many tropical regions such as the Brazilian Atlantic forest studied in this thesis, the reduction of forest extent has reached a level which requires active human input for its recovery. The potential evaluation of these forest restoration actions is also a ripe field for forest modelling studies. Understanding the best actions in order to recover biodiverse forest areas in the fastest and with fewer amounts of resources, is an important future application of forest models.

Finally, in the light of the increasing number of aerial and space acquired information on vegetation and increasing computational power for processing this data, there is strong reason to believe that the individual based ecology concept, through its main tool the individual based computer model, will be able to provide both answers to long sought questions in theoretical ecology and support for management decisions.

6. ACKNOWLEDGEMENTS

7. APPENDIX

7.1. GENERAL DESCRIPTION OF FORMIND'S MAIN MODULES

Here I describe the main equations of the forest model FORMIND considering the main modules which they are located. The FORMIND's C++ software code, from which its binary executable is built, is divided into several files which contain commands organized in relation to the ecological processes or supporting functions they are related. Since the model is constantly updated, the specific details on function names or order may vary. Here I describe FORMIND version 3.0 used in this thesis (as of September 2016). Details on the current version, as well as other functions for describing ecological and ecosystem processes can be found in the FORMIND handbook available in www.forming.org.

The principal code file, *main.cpp* calls the well-known C++ *main* function, which executes the most important functions of FORMIND. They are the initialization *ReadCommandLineParams()* (reads the PAR file) and *Start()* (reads the PIN file and prepares the initial forest state and spatial structure of the model); the execution *Run()* (forest simulation); and the output *WriteResults()* (result output) functions of FORMIND Figure A 1. All these main functions can be found in the *formind.cpp* file. I define here the main modules of FORMIND as the functions responsible for running the simulation, and the submodules the functions influencing specific main modules, optionally activated. The description of the submodules used in this thesis can be found in the methods section of each chapter (e.g. climate module in chapter 1, or fragmentation and seed predation modules in chapter 3).
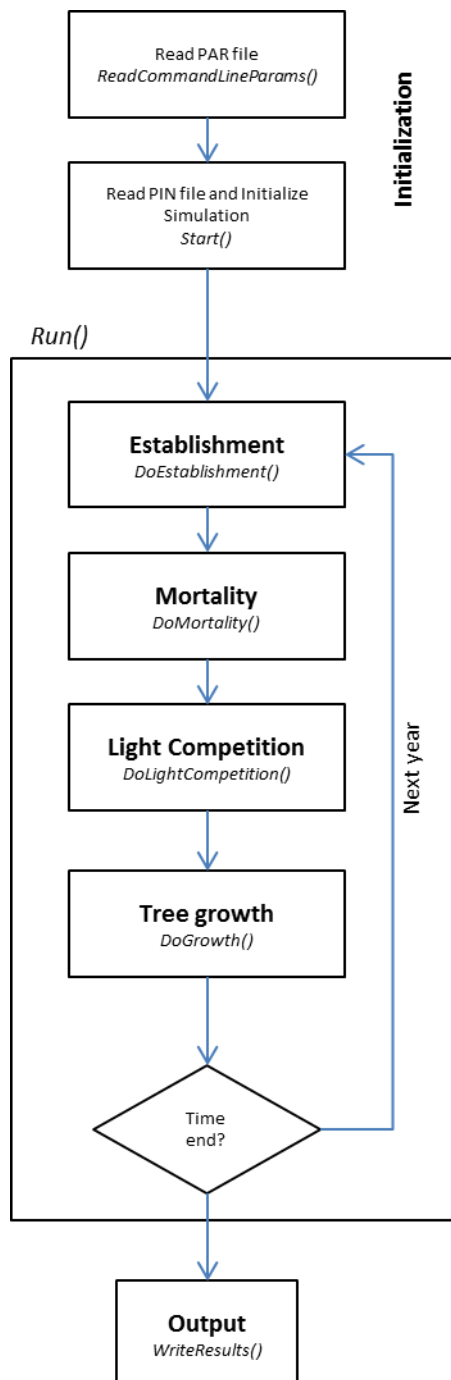
Figure A 1. Main modules (in bold) and functions (in italic) of the forest model FORMIND. PAR is the parameter file, and PIN is the forest inventory initialization file.

The main modules of FORMIND are **initialization, establishment, mortality, light competition, tree growth** and **output**.

7.1.1. INITIALIZATION

In order to run the FORMIND model, a parameter file (PAR) and an initial state file (PIN) are needed. The PAR contains all information related to the simulation conditions (e.g. duration, time step, simulated area, number of plant functional types, activation of submodules), result files which should be output (e.g. basal area, biomass, stem number, carbon balance, LAI) and ecological parameters (e.g. seed dispersal, establishment, mortality, geometry, production, climate, soil) described for the chapter 1 in Table A 1 and for chapter 3 in Table A 3. The PIN file contains field data (Diameter measurements of individual trees and their species plant functional type classification) related to the first year of simulation, i.e. whether it starts from an empty area or from a measured tree inventory, as well as the conditions of each 20x20 meter plot (i.e. edge distance or forest-non forest state) which are fixed for the entire duration of the simulation.

Geometric tree representation

By using the input inventory data, an initial forest is reconstructed from individual trees diameter at breast height measurements and geometric parameters from the PAR file for each PFT. This is done by the use of allometric equations, which correlate the size and shape of the tree's features such as height or crown diameter to the trunk's diameter. The allometric equations from FORMIND used in this study were:

Height (H): Calculated using a power law approach from the trunk diameter at breast height (D, in meters) using the parameters h_0 and h_1 (estimated using field measurements of tree heights):

$$H = h_0 \cdot D^{h_1}$$

Crown diameter (C_D): Calculated from the trunk diameter at breast height (D[m]) using a polynomial approach with the parameters C_{d0} and C_{d1}:

$$C_D = C_{d0} \cdot D + C_{d1} \cdot D^2$$

Crown area (C_A): Calculated from the crown trunk diameter at breast height C_D as:

$$C_A = \frac{\pi}{4} \cdot C_D^2$$

Form Factor (f): Change in trunk's conical shape according to height, calculated according to the parameters f_0 and f_1:

$$f = f_0 \cdot D^{f_1}$$

Leaf area index (LAI): Calculated using a power law approach from the trunk diameter at breast height (D) using the parameters l_0 and l_1:

$$LAI = l_0 \cdot D^{l_1}$$

Biomass (B, in Mg Organic Dry Mass, ODM): Calculated using the measured trunk diameter at breast height (D), modelled tree height (H), modelled form factor (f), literature-based average wood density (ρ), and fraction of stem wood biomass to total tree biomass (σ).

$$B = \frac{\pi}{4} \cdot D^2 \cdot H \cdot f \cdot \frac{\rho}{\sigma}$$

After the parameters are read, the initial state and spatial structure of the model is set, the *Run()* function executes the simulation for the whole defined period.

7.1.2. ESTABLISHMENT

This module is executed through the *DoEstablishment()* function found in the *for_seed.cpp* file.

Seed dispersal

I have used here two different types of seed dispersal, global (chapter 1) and parent tree (chapter 3). Global seed dispersal is a constant input of seeds per hectare and per year, determined by the parameter N_{seed} for each plant functional type. All plots receive the same number of seeds if possible; remaining seeds are distributed at random.

In the parent tree dispersal mode, all trees with diameter d > 5 cm threw a fixed number of seeds per year at a distance X_s, according to a negative exponential function, considering a mean dispersal distance *mdd* (Table 6), and a random number 0 < *rand* ≤ 1. Dispersal direction is also randomized from 0 to 360 degrees:

$$X_s = -mdd \cdot \log(rand)$$

The function *DetermineFallLoc()* then determines which plot the seeds has fallen into, and stores them in the transient soil seed bank *NewSeeds*. They are subjected to optionally activated predation mortality according to the equation 2 presented in chapter 3. Seeds which are defined as animal dispersed are re-thrown to the parent tree's plot if the target plot is outside of the simulating area or if it is a non-forest plot (see methods in chapter 3 for more details).

Seed germination

If the irradiance ratio between light falling into the forest ground floor I_{floor} attenuated by the crowns of the covering trees (see following item *light competition*) and light on top of the canopy I_0 equals or exceeds the value defined by I_{seed} (Minimum light intensity for germination) for a particular PFT, all its seeds in the transient soil seed bank germinate in the plot (Groeneveld et al. 2009). The germinated seedlings have an initial stem diameter of 1 cm (chapter 1) and 2 mm (chapter 3).

Seed pool mortality

Seeds which have not become seedlings die with specific mortality rate m_{seeds}, and are included in the persistent seed bank *SeedPool* for each plot.

7.1.3. MORTALITY

This module is executed through the function *DoMortality()* from the *for_dead.cpp* file.

Basic mortality

Each year individual trees die according to a general probability *m*, which is a sum of basic mortality m_b defined fixed for each PFT, and diameter dependent mortality m_{dia}, which corrects for a greater mortality of smaller trees.

$$m = m_b + m_{dia}$$

Where,

$$m_{dia} = \begin{cases} m_{d0} - {m_{d0} \cdot D}/{m_{d1}} & , for\ D \leq m_{d1} \\ 0 & , else \end{cases}$$

With m_{d0} being the maximum mortality rate for the smallest diameter D, and m_{d1} the maximum diameter where m_{dia} is applied. Another mortality factor aggregates further to m, the diameter increment based mortality m_{dinc}, but was not used in this study. If activated, the fragmentation mortality factor is multiplied directly to m_b, according to the forest edge distance (see methods in chapter 3).

Additional mortality

After the basic mortality probability m is applied to all trees in the plot, additional mortality may take place to the surviving trees.

The mode of tree death is also another important factor in FORMIND. The parameter p_{fall} (defined as 0.4 for both chapters 1 and 3) determines the probability of a tree to die and fall (it dies standing otherwise). In this case, falling trees may damage a randomly selected nearby plot (eight possibilities), and all trees with height lower than the falling tree are subjected to a mortality probability m_{fall}:

$$m_{fall} = \frac{C_A}{A_{patch}}$$

Where C_A is the crown area of the falling tree and A_{patch} is the patch area (400 m², 20m x 20m in the case of this study).

Another additional mortality factor calculated post general mortality is the self-thinning. When the sum of all tree crown areas in a given height layer exceeds the patch area, trees are randomly removed until the crowns of all trees "fit" into the patch (Groeneveld et al. 2009).

Other factors such landslide mortality and logging mortality where not considered in this study.

7.1.4. LIGHT COMPETITION

This module is executed through the *DoLightCompetition()* function contained in the *for_comp.cpp* file. In it, each tree receives its available light irradiation for each year dependent on the total solar

irradiation and the presence of other trees. Each tree has a leaf area index value for its crown calculated allometrically from its stem diameter. on top of an individual tree is I_{ind} in [µmol photons /m².s], where I_0 is the radiation above canopy, L_i is the total leaf area index of the height layer number i, L_{max} is the layer number where the top of the individual tree is located, and k is the light extinction coefficient. For a graphic representation, please see Figure 3B:

$$I_{ind} = I_0 \cdot exp\left(-k \cdot \sum_{i>L_{max}} L_i\right)$$

The available light for each tree will determine how much it can photosynthesize and grow in the next step.

7.1.5. TREE GROWTH

The final main module is the tree growth, determined by the function *DoGrowth()* from the file *for_growth.cpp*. It determines the total diameter gain for each tree using net biomass gain from photosynthesis and respiration, and converting additional biomass into diameter growth.

Gross primary production

Considering the total radiation available for the tree I_{ind} calculated in the last module, the mean yearly incoming Photosynthetic production during the day length P_{ind} in of an individual tree with total leaf area index *LAI* per year can be calculated as:

$$P_{ind} = \frac{P_{max}}{k} \cdot \ln\frac{\alpha \cdot k \cdot I_{ind} + P_{max} \cdot (1 - M)}{\alpha \cdot k \cdot I_{ind} \cdot e^{-k \cdot LAI} + P_{max} \cdot (1 - M)}$$

Where P_{max} is the maximum photosynthesis rate in [µmolCO$_2$/m².s], α initial slope of the light response curve, k light extinction coefficient, *LAI* total individual's leaf area index, and *M* light transmission coefficient of leaves, defined for each PFT.

To transform P_{ind} from [µmolCO$_2$/m².s] to [t$_{ODM}$/y] (tonnes of organic dry mass per year) the following calculation is applied:

$$P_{ind} \cdot C_A \cdot 3600 \cdot I_{day} \cdot \varphi_{act} \cdot \varphi_{ODM}$$

Where C_A is the crown area in m^2, 3600 is the conversion from seconds to hours (60 x 60), I_{day} the day length in hours, ϕ_{act} the vegetation period in hours and $\phi_{ODM} = 0.63 \cdot 44 \cdot 10^{-12}$, the conversion factor including the molar mass of CO_2, the conversion of grams to tonnes (Mg) and CO_2 to organic dry mass.

Having P_{ind} [Mg$_{ODM}$/y], the gross primary production (*GPP*) can be calculated as:

$$GPP = P_{ind} \cdot \varphi_T \cdot \varphi_W$$

Where ϕ_T is the limitation factor for temperature conditions and ϕ_W the limitation factor for soil water conditions (activated in the chapter 1 study).

Biomass increment

Now, the biomass increment *ΔB* in Mg ODM of a tree can be calculated by considering the photosynthetic production loss to growth respiration r_g and the loss to maintenance respiration r_m:

$$\Delta B = (1 - r_g) \cdot (GPP - r_m)$$

Growth respiration is assumed to be a fixed fraction of net biomass production, and is a parameter, while maintenance respiration is dependent on the current biomass of the tree *B* and diameter *D*, diameter growth rate function *g(D)*, and fraction of primary production r_g attributed to growth respiration:

$$r_m = \frac{1}{B \cdot \kappa_T} \cdot \left(P_{ind} \cdot \varphi_T \cdot \varphi_W - \frac{B(D + g(D)) - B}{(1 - r_g)} \right)$$

In this equation, $P_{ind} \cdot \varphi_T \cdot \varphi_W$ represents the GPP under the temperature φT and the water φW photosynthesis limitation factors. Here, P_{ind} is already converted to [Mg$_{ODM}$/y]. *B* is the biomass calculated from stem diameter, and κ_T is the respiration limitation factor due to air temperature (not activated in this study, equal to 1).

The diameter growth *g(D)* equation chosen for this thesis is the polynomial approach, and is calculated as a function of the tree's current diameter *D*, maximum growth rate g_{max}, growth rate of smallest trees, $g_{smallest}$ as a percentage of maximum growth rate, growth rate of largest tree $g_{largest}$ as a percentage of maximum growth rate, diameter where maximum growth rate is reached $D_{maxgrowth}$ as a percentage of maximum growth rate, maximum diameter D_{max}, and minimum diameter D_{min}.

$$g(D) = a_0 + a_1 \cdot D + a_2 \cdot D^2 + a_3 \cdot D^3$$

Where,

$$a_3 = \frac{x_0 \cdot x_1 + (g_{smallest} - g_{largest}) \cdot g_{max} \cdot x_2}{x_3 \cdot x_4 \cdot x_5 \cdot x_6 \cdot x_7}$$

$$a_2 = \frac{x_0 - a_3 \cdot x_8}{2 \cdot D_{min} \cdot (D_{\max growth} \cdot g_{largest}) - (D_{\max growth} - g_{largest})^2 - D^2{}_{min}}$$

$$a_1 = -3 \cdot a_3 \cdot (D_{\max growth} \cdot D_{max})^2 - 2 \cdot a_2 \cdot (D_{\max growth} \cdot D_{max})$$

$$a_0 = g_{smallest} \cdot g_{max} - a_3 \cdot D^3{}_{min} - a_2 \cdot D^2{}_{min} - a_1 \cdot D_{min}$$

Equation factors x_1 – x_8 are all dependent on g_{max}, $g_{smallest}$, $g_{largest}$, $D_{maxgrowth}$, D_{max}, and D_{min}, and their equations can be found in the FORMIND handbook in www.formind.org.

Finally, the new biomass of the tree for the next year y+1 ($B_{y+1} = B_y + \Delta B$) is converted to stem diameter D_{y+1}:

$$D_{y+1} = \frac{B_{y+1} \cdot \sigma}{\frac{\pi}{4} \cdot h_0 \cdot f_0 \cdot \rho}^{2+h_1+f_1}$$

Where h_0 and h_1 are the height-diameter parameters, f_0 and f_1 are the form factor-diameter parameters, ρ is the wood density and σ is the fraction of stem wood biomass to total tree biomass. This equation is used in order to calculate the new geometric properties of the tree for the next time step, according to the equations described in the initialization.

7.1.6. OUTPUT

At the end of the pre-defined simulation time, the program writes the selected result files from the parameter file, averaging forest properties such as biomass, basal area and stem number per hectare, or outputting them per plot position, allowing to observe the spatial distribution of forest properties.

Figure A 2. Sensitivity analysis for the defined core area parametrization. Morp1 = Mortality of trees with diameter smaller than Morp2. Mort = Mortality rate of the Plant Functional Type; Plant = Seed input rate for the Plant Functional Type; SN = Stem Number; AGB = Aboveground Biomass; BA = Basal Area.
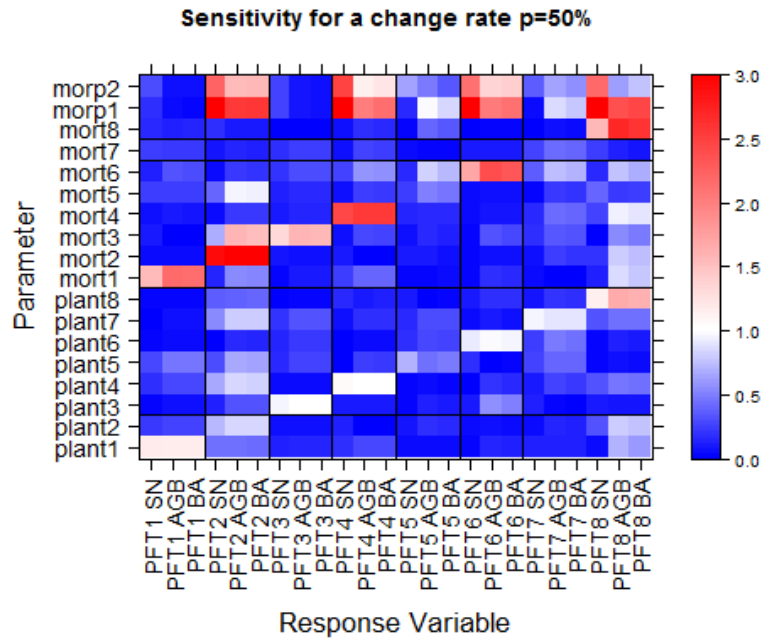
Figure A 3. Monthly average (1961-1990) Precipitation (P) and Potential Evapotranspiration (PET) of Maceió, aprox. 50 km from the study site.
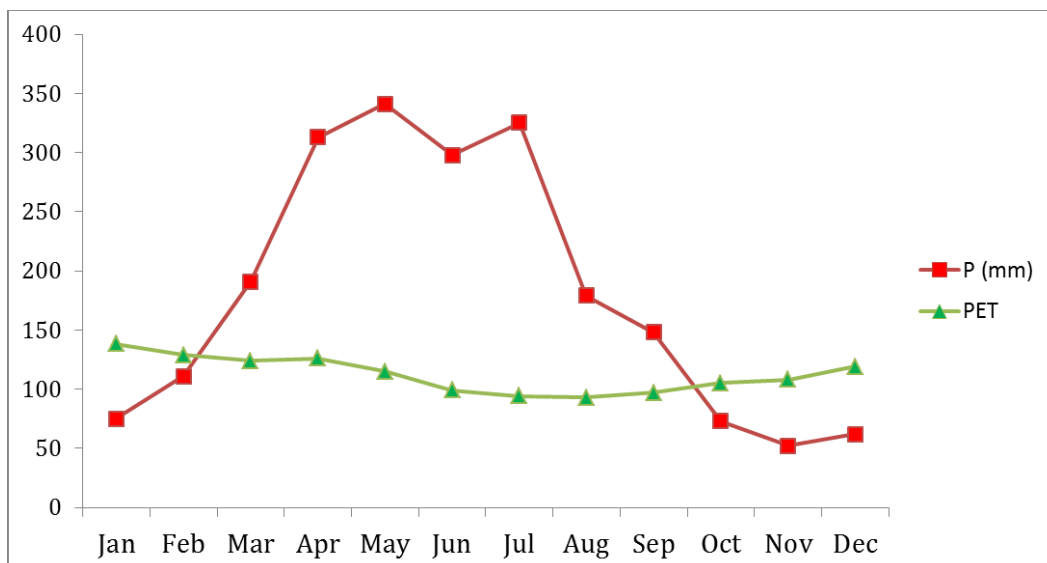
Figure A 4. Boxplot from the comparison analysis for the biomass in the field plots (size 0.1 hectares). Bands inside boxes show the median, top and bottom show first and third quartiles, and whiskers show highest and lowest data within 1.5 of the Interquantile range. Points show the actual data.
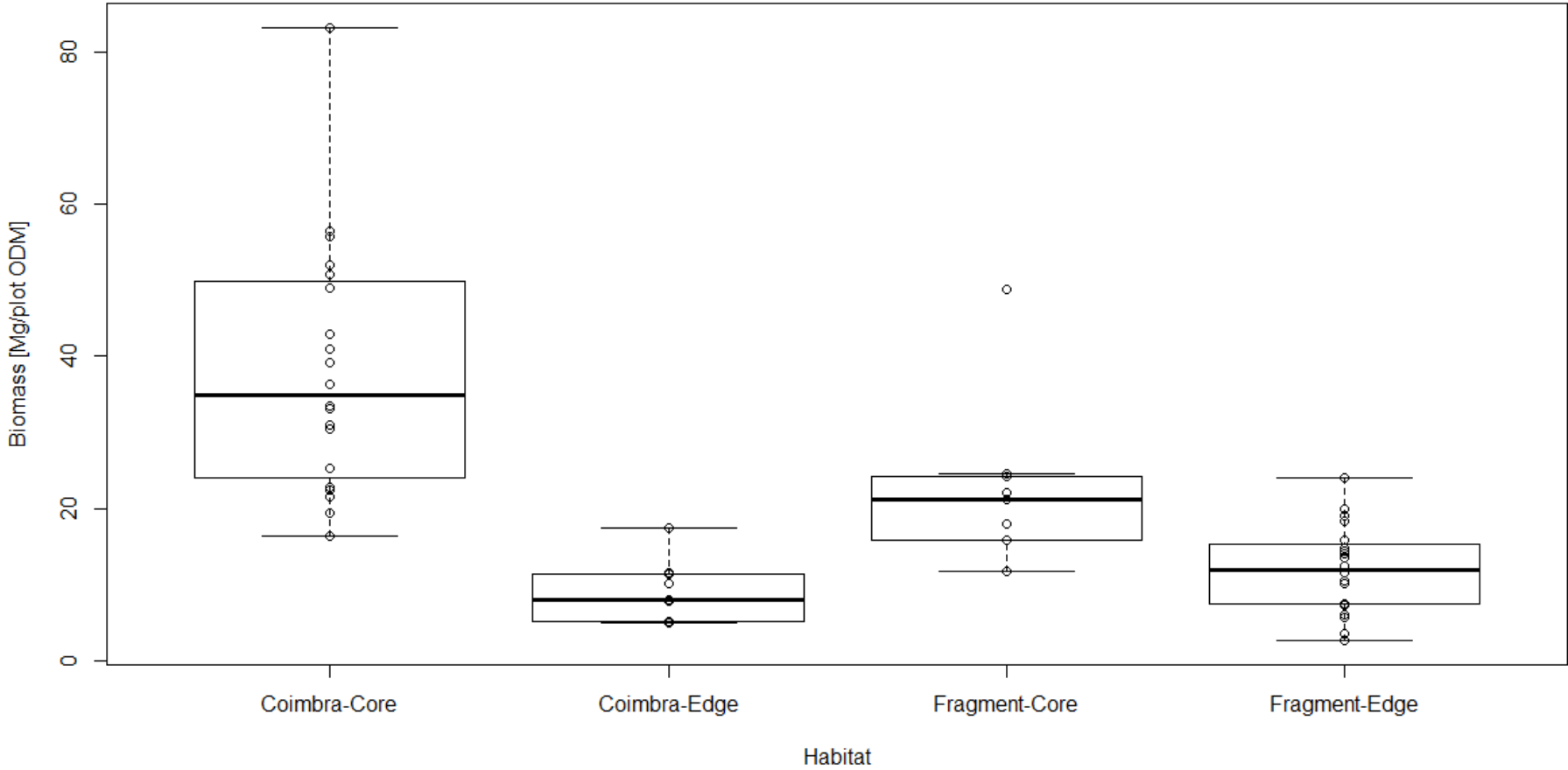
Table A 1. Parameters used in the FORMIND model. A complete overview of the Equations used in the model can be found in the FORMIND Handbook, available at http://formind.org/wpfor/wp-content/uploads/2014/12/FORMIND_Handbook.pdf. More details in (Dislich et al. 2009), and for the advanced climate in (Fischer et al. 2014).

Parameter	Description	Unit	PFT1	PFT2	PFT3	PFT4	PFT5	PFT6	PFT7	PFT8	Reference
k	Light extinction coefficient	m^2 ground m^{-2} leaf				0.6					
I_0	Average irradiance above canopy	$\mu mol(photons)$ m^{-2} s^{-1}				700					(Bendix et al. 2008)
I_{seed}	Minimum light intensity (relative to full light above canopy) required for establishment	% of I_0	10	5	10	5	10	5	10	5	(Rüger et al. 2008)

Parameter	Description	Unit	PFT1	PFT2	PFT3	PFT4	PFT5	PFT6	PFT7	PFT8	Reference
	of seeds										
M_{d0}	Mortality rate of individuals with less than 0.04 m (M_{d1}) DBH	y^{-1}				0.1					(Rüger et al. 2007)
H_{max}	Maximum size (height) of a tree	meters	19	19	27	27	40	40	40	40	Derived from inventory data
h_0	Diameter-Height relationship	-	6.66845	6.70534	7.00584	5.8819	5.26548	5.8314	7.24096	7.51551	Derived from inventory data
h_1			0.25632	0.24355	0.30550	0.35314	0.38614	0.38106	0.31534]	0.32424	Derived from inventory data

Parameter	Description	Unit	PFT1	PFT2	PFT3	PFT4	PFT5	PFT6	PFT7	PFT8	Reference
C_{d0}	Crown diameter as function of diameter-curves	-	0,2								Estimated, based on (Goodman et al. 2014)
C_{d1}			-0.0004								
C_{d2}			0.5								
f_0	Form factor-Stem diameter-Relationship	-	0.77								(Dislich et al. 2009)
f_1			-0.18								
l_0	Parameter of Leaf Area Index-Stem diameter function of a single tree	-	1.0	1.0	1.0	1.0	1.0	1.0	1.0	1.0	estimated
l_1			0.1	0.1	0.2	0.2	0.3	0.3	0.3	0.3	

Parameter	Description	Unit	PFT1	PFT2	PFT3	PFT4	PFT5	PFT6	PFT7	PFT8	Reference
P_{max}	Maximum rate of photosynthesis	$\mu mol(CO2)\ m^{-2}\ s^{-1}$	7	3.5	7	3.5	7	3.5	7	3.5	Calibrated
α	Slope of light response curve	mikromol(CO_2)/mikromol(photons)	0.6	0.8	0.6	0.8	0.6	0.8	0.6	0.8	Calibrated
ρ	Wood density	$t\ m^{-3}$	0.4	0.7	0.4	0.7	0.4	0.7	0.4	0.7	(Chave et al. 2006)
σ	Ratio of total aboveground biomass to stem biomass	-	0.7								(Stocks et al. 1996)
ΔD_{max}	Maximum yearly	mm/y	19	14	19	14	19	14	19	14	Calibrated

Parameter	Description	Unit	PFT1	PFT2	PFT3	PFT4	PFT5	PFT6	PFT7	PFT8	Reference
	increment of stem diameter										
Core											
N_{seed}	Number of seeds reaching a hectare from outside (global ingrowth rate)	ha^{-1} y^{-1}	5	20	22	100	15	500	7	66	Calibrated
M_b	Background mortality rate	y^{-1}	0.03	0.03	0.045	0.03	0.002	0.025	0.002	0.011	Calibrated, (Kornig and Balslev 1994)
Edge											
N_{seed}	Number of seeds reaching	ha^{-1} y^{-1}	2	5	200	60	130	200	30	66	Calibrated

Parameter	Description	Unit	PFT1	PFT2	PFT3	PFT4	PFT5	PFT6	PFT7	PFT8	Reference
	a hectare from outside										
M_b	Background mortality rate	y^{-1}	0.07	0.06	0.115	0.07	0.07	0.08	0.06	0.06	Calibrated, (Kornig and Balslev 1994)
Fragment											
N_{seed}	Number of seeds reaching a hectare from outside	ha^{-1} y^{-1}	2	5	80	20	60	180	30	66	Calibrated
M_b	Background mortality rate	y^{-1}	0.06	0.06	0.06	0.01	0.04	0.04	0.04	0.04	Calibrated, (Kornig and Balslev 1994)
Advanced Climate Parameters											

Parameter	Description	Unit	PFT1	PFT2	PFT3	PFT4	PFT5	PFT6	PFT7	PFT8	Reference
WUE	Water use efficiency	g (odm)/kg				6					(Maidment 1993)
ϑ_{PWP}	Permanent wilting point	Vol%				25					(Saxton and Rawls 2006)
K_L	Interception constant	mm/day				0.2					(Maidment 1993)
POR	Porosity of the soil	Vol%				46.3					(Lima et al. 2008)
K_s	Fully saturated conductivity	m/s				0.00000366					(Maidment 1993)
λ	Pore size distribution index	-				0.242					(Maidment 1993)

Parameter	Description	Unit	PFT1	PFT2	PFT3	PFT4	PFT5	PFT6	PFT7	PFT8	Reference
θ_r	Residual soil water content	Vol%				7.5					(Maidment 1993)
ϑ_{FC}	Field capacity	Vol%				28.2					(Saxton and Rawls 2006)
SD	Soil depth	m				2					(Lima et al. 2008)

Table A 2. Plant Functional Type (PFT) definitions for the species classifications. The maximum heights are the limits for the simulation, and the diameters are the maximum values from the field data.

PFT	Maximum Height (m)	Maximum Diameter (cm)	Example Species
1	19	27.8	*Centrolobium microchaete*
2	19	24.6	*Cytharexyllum myrianthum*
3	27	56.5	*Guapira opposita*
4	27	56.5	*Pouteria grandiflora*
5	40	138	*Plathymenia foliolosa*
6	40	106	*Couepia rufa*
7	40	220	*Ficus guarathynica*
8	40	200	*Sloanea obtusifolia*

Figure A 5. Results for the transition simulations (10 runs with a 4 hectare area). The table shows years (transitions with a stable state year larger than 400 are considered not to have reached stability). Black lines represent total values; Solid lines are averages, bands are min-max values, points represent field data, and triangles times where PFTs reached the stability criteria.
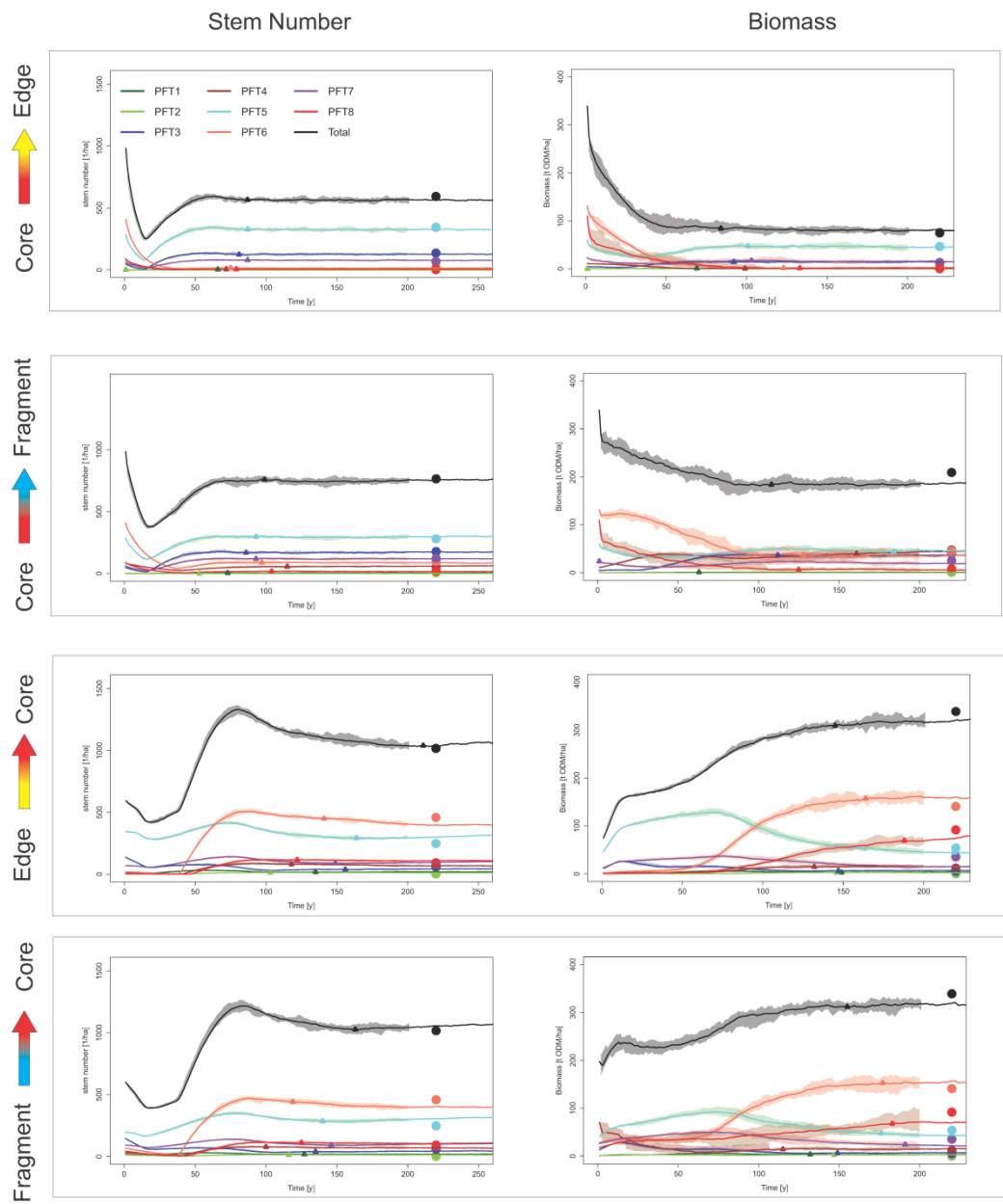
Figure A 6. Forest hydrology (total runoff and evapotranspiration) and yearly aboveground carbon change for all transitions. Green values indicate carbon sequestration, red values indicate carbon emissions. The grey line represents accumulated carbon values. Solid lines are averages, bands are min-max values, and triangles times where PFTs reached the stability criteria.
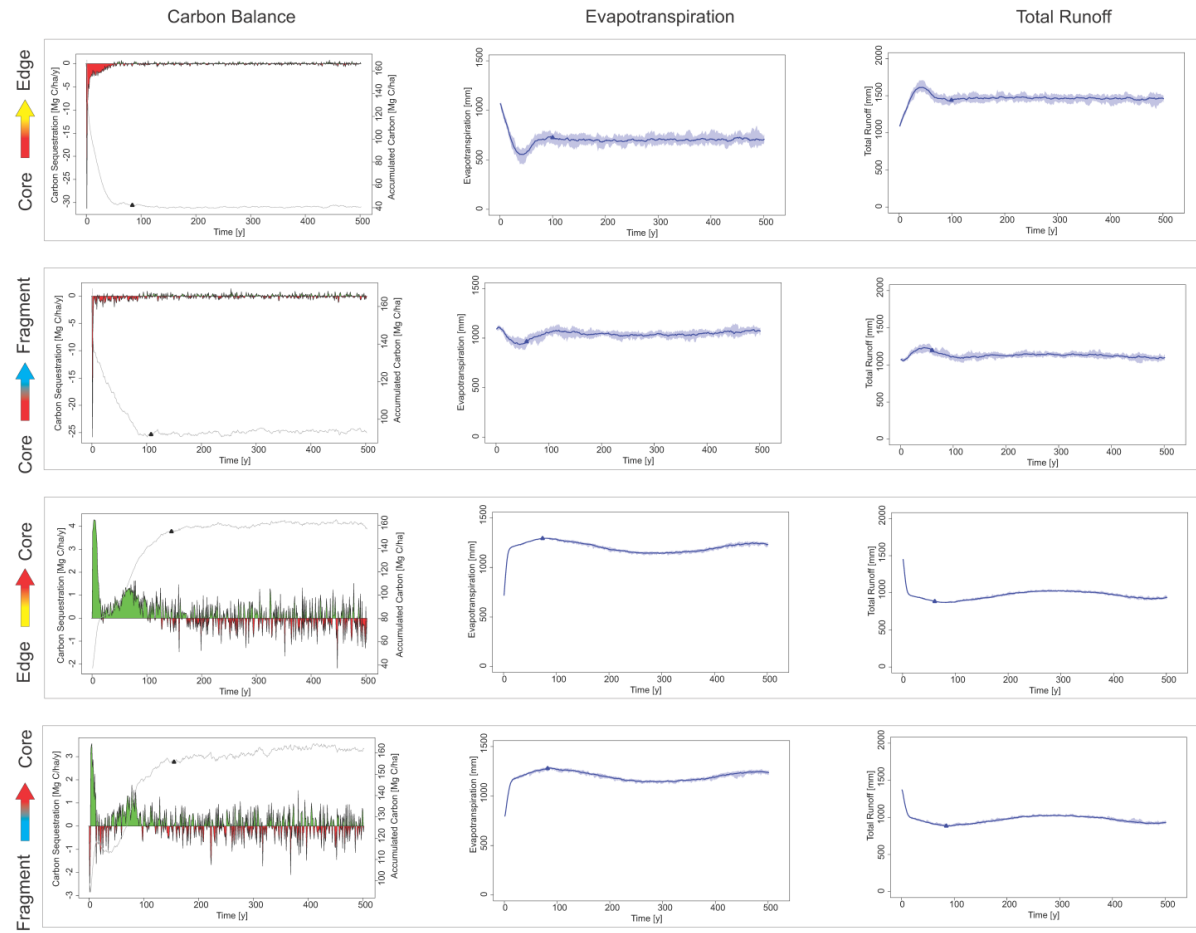
Figure A 7. Transition results for Succession, Core-Edge and Edge-Core simulations regarding Leaf Area Index (LAI) and Gross Primary Production (GPP). Solid lines are averages, bands are min-max values, and triangles times where PFTs reached the stability criteria.
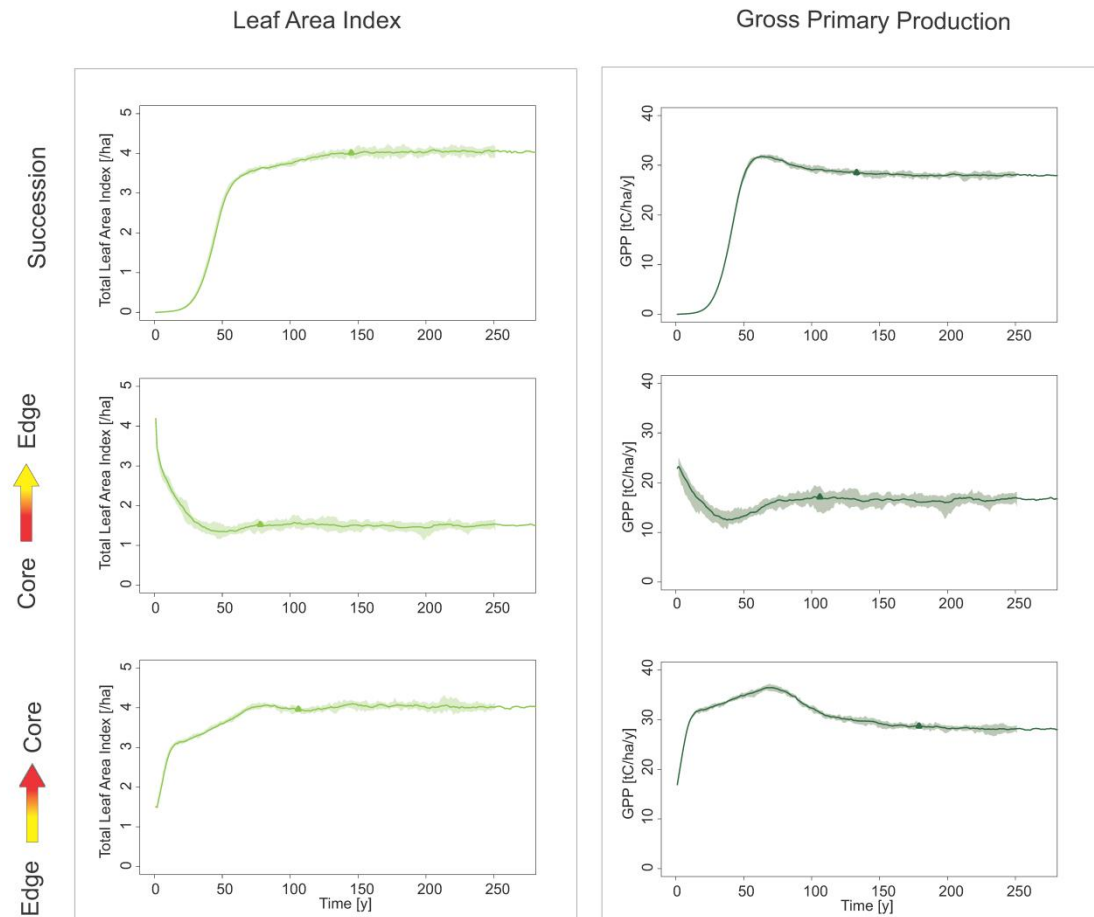
Figure A 8. Behaviour of selected parameters according to growth in DBH for the 8 plant functional types.

PFT1

PFT2
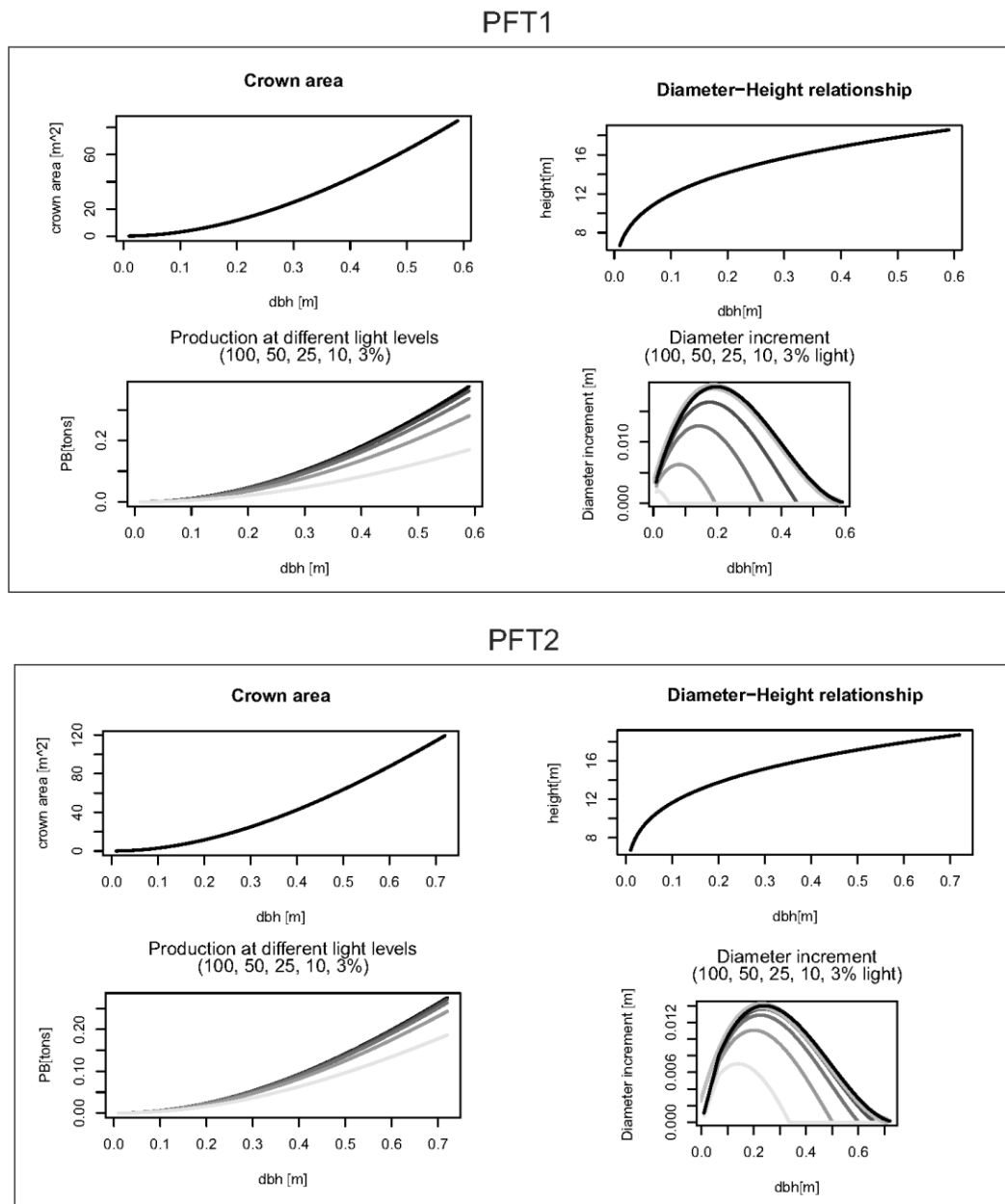
PFT3
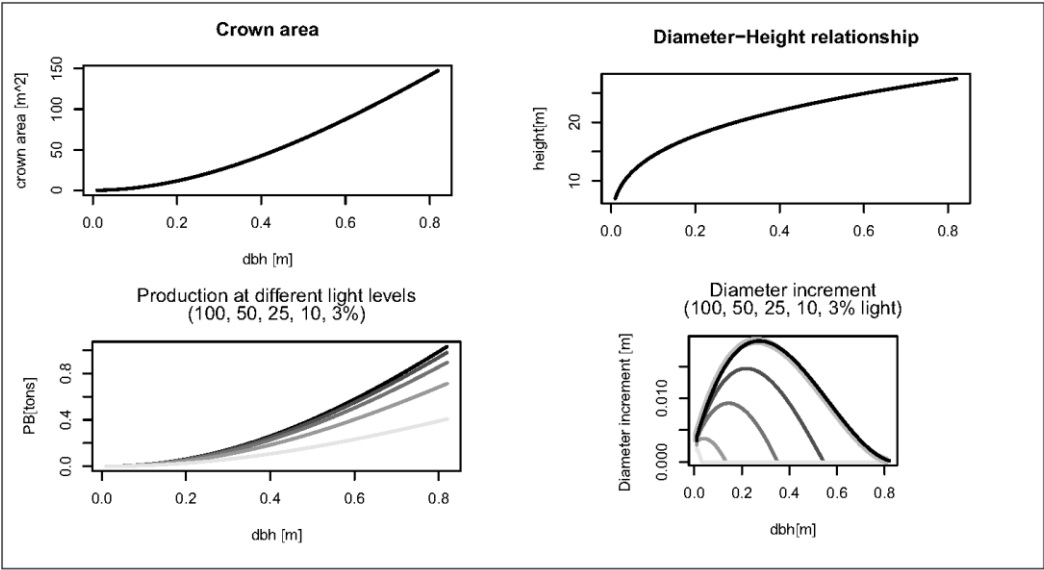
PFT4
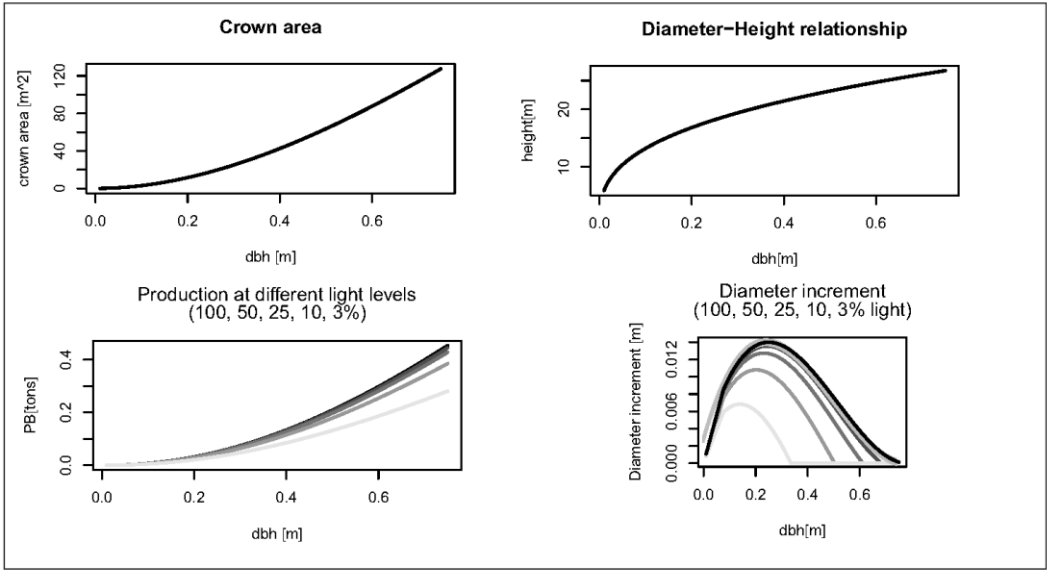
PFT5
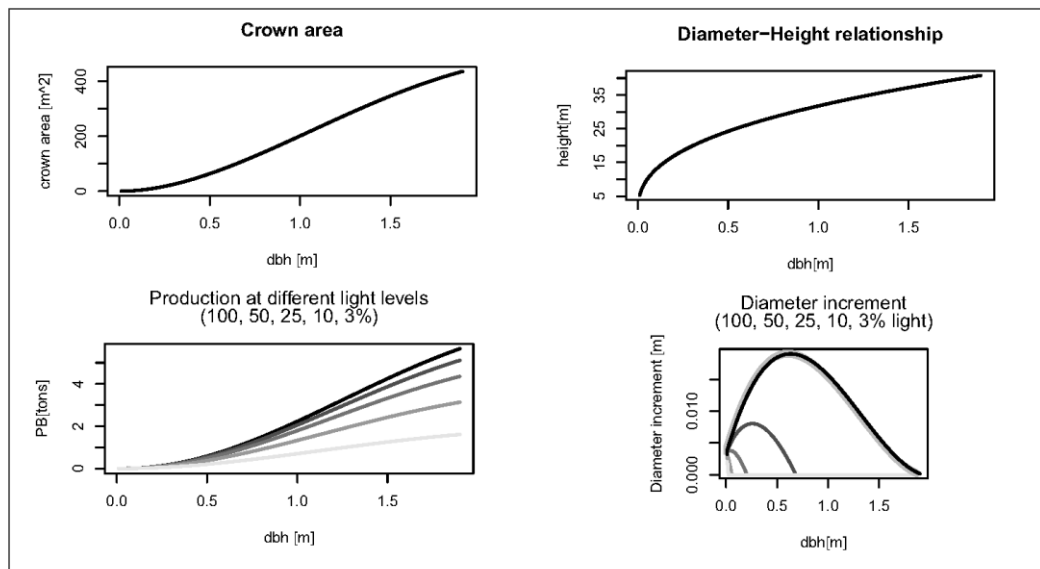
PFT6
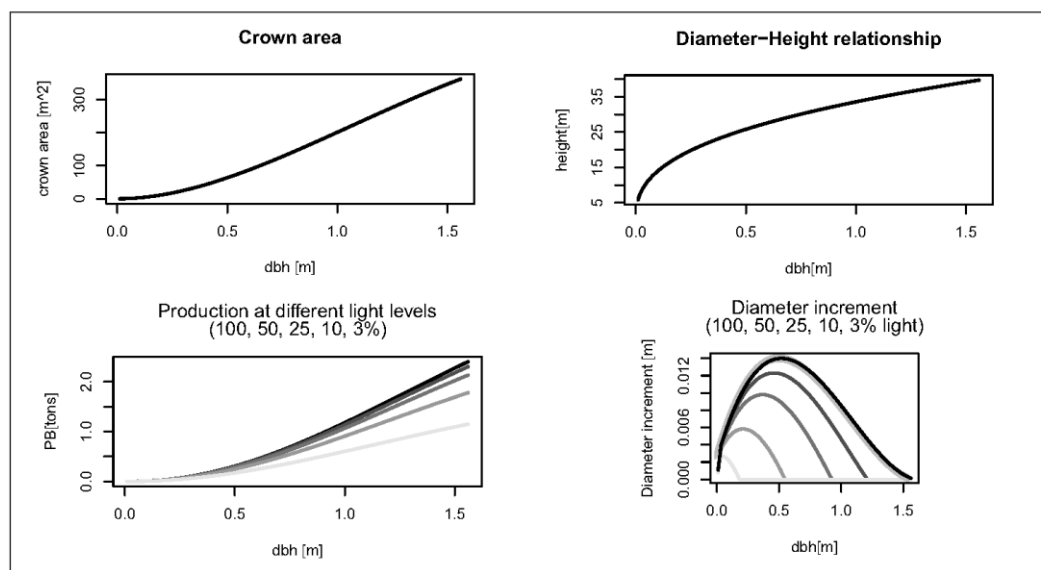
PFT7
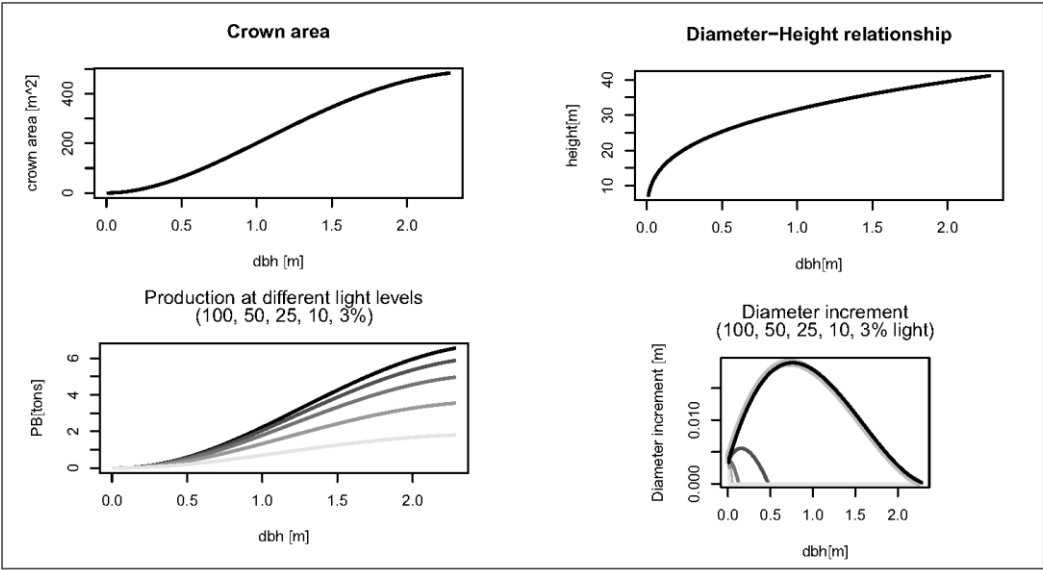
PFT8
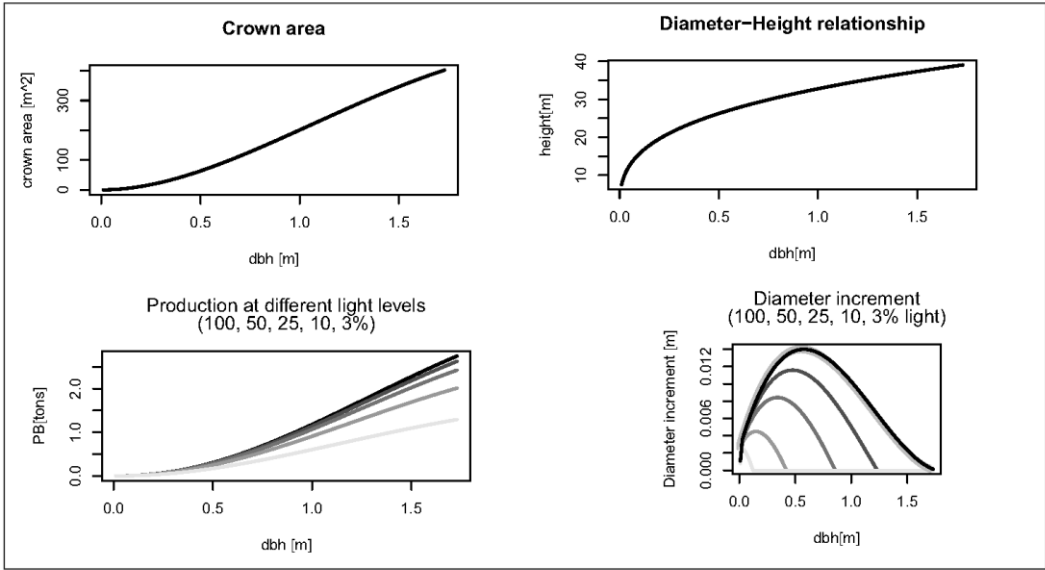
Figure A 9. Evaluation of different forest definition thresholds. The data used was from scene no. 9, Northern Brazil.
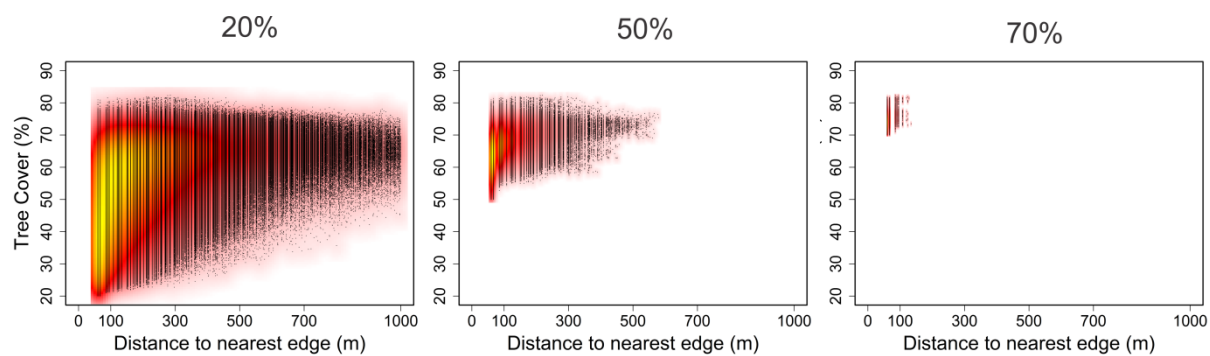
Figure A 10. Evaluation of window size influence for the tree cover neighborhood analysis. The data used for this comparison is scene no. 9, Northern Brazil
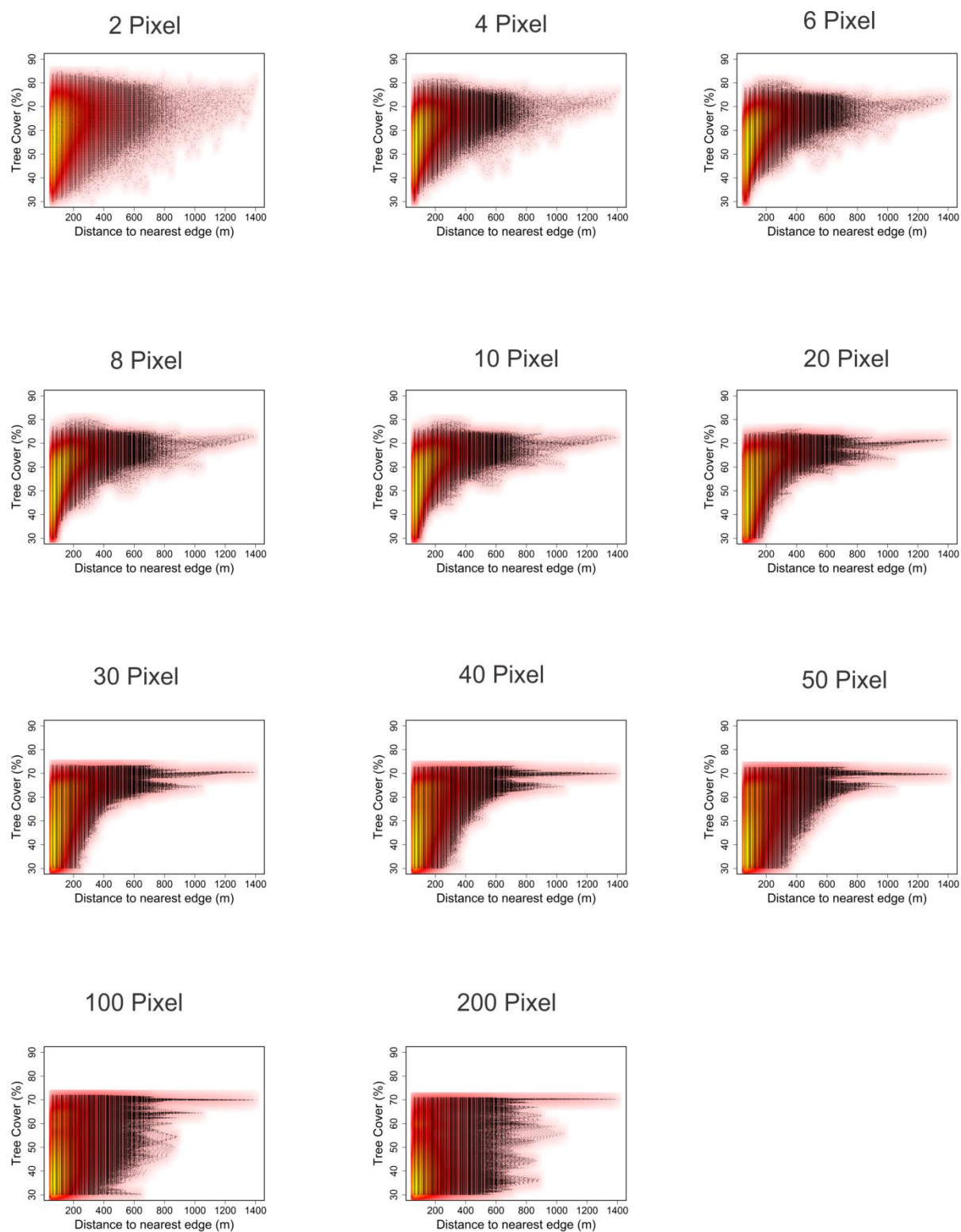
Table A 3. Parameters used in the FORMIND model. A complete overview of the Equations used in the model can be found in the FORMIND Handbook, available at http://formind.org. More details in (Dislich et al. 2009), and for the advanced climate in (Fischer et al. 2014)

Parameter	Description	Unit	PFT1	PFT2	PFT3	PFT4	PFT5	PFT6	Reference
TimeEnd	Total simulation time	y	1,000						
k	Light extinction coefficient	m^2 ground m^{-2} leaf	0.6						
I_0	Average irradiance above canopy	$\mu mol(photons)\ m^{-2}\ s^{-1}$	700						(Bendix et al. 2008)
I_{seed}	Minimum light intensity (relative to full light above canopy) required for	% of I_0	20	20	20	7	7	7	calibrated

Parameter	Description	Unit	PFT1	PFT2	PFT3	PFT4	PFT5	PFT6	Reference
	establishment of seeds								
M_{d0}	Mortality rate of individuals with less than 0.15 m (M_{d1}) DBH	y^{-1}	0.21	0.195	0.135	0.075	0.038	0.047	(Rüger et al. 2007)
H_{max}	Maximum size (height) of a tree	meters	40	40	40	40	40	40	Derived from inventory data
ΔD_{max}	Maximum yearly increment of stem diameter	mm/y	30	43.25	15.89	19.79	16.84	19.21	(Santos et al. 2008)
M_b	Background mortality rate	y^{-1}	0.041	0.041	0.025	0.037	0.025	0.01	
D_{stree}	Minimum	Meters	0.05	0.05	0.05	0.05	0.05	0.05	

Parameter	Description	Unit	PFT1	PFT2	PFT3	PFT4	PFT5	PFT6	Reference
	diameter for parent trees								
N_{seed}	Number of seeds thrown by each parent tree	y^{-1}	7660	16822	156	642	114	199	(Melo et al. 2006)
h_0	Diameter-Height relationship	-	31.39	37.67	31.39	37.67	31.39	37.67	Derived from inventory data
h_1			0.7	0.7	0.7	0.7	0.7	0.7	Derived from inventory data
C_{d0}	Crown diameter as function of diameter-curves	-	20						Estimated, based on (Goodman et al. 2014)
C_{d1}			-0.0004						
C_{d2}			0.5						
f_0	Form factor-	-	0.33611719						(Dislich et al.

Parameter	Description	Unit	PFT1	PFT2	PFT3	PFT4	PFT5	PFT6	Reference
f_1	Stem diameter-Relationship				-0.18				2009)
l_0	Parameter of Leaf Area Index-Stem diameter function of a single tree	-	1.58	1.58	1.58	1.58	1.58	1.58	estimated
l_1			0.1	0.1	0.2	0.2	0.3	0.3	
P_{max}	Maximum rate of photosynthesis	$\mu mol(CO2)$ $m^{-2}\ s^{-1}$	7	7	7	3.5	3.5	3.5	Calibrated
α	Slope of light response curve	mikromol(CO_2)/mikromol(photons)	0.6	0.6	0.6	0.8	0.8	0.8	Calibrated
ρ	Wood density	$t\ m^{-3}$	0.4	0.4	0.4	0.7	0.7	0.7	(Chave et al. 2006)

Parameter	Description	Unit	PFT1	PFT2	PFT3	PFT4	PFT5	PFT6	Reference
σ	Ratio of total aboveground biomass to stem biomass	-							(Stocks et al. 1996)

Table A 4. Reference field data for edge and small fragment (<100) plots of Brazilian Atlantic Forest in NE Brazil (Coimbra forest). Information from the field inventory data, with species grouped according to the 6 Plant Functional Types. Data represents trees larger than 0.1 m DBH.

Edge

PFT	Shade Tolerance	Seed Dispersal Category	Number of Stems	Basal Area (m²/ha)
1	Intolerant	Non-Animal	115	5.67
2	Intolerant	Small Seeds	332	9.16
3	Intolerant	Large Seeds	108	3.30
4	Tolerant	Non-Animal	1	0.06
5	Tolerant	Small Seeds	17	0.25
6	Tolerant	Large Seeds	21	0.37
Total	-	-	594	18.81

Fragments

PFT	Shade Tolerance	Seed Dispersal Category	Number of Stems	Basal Area (m²/ha)
1	Intolerant	Non-Animal	131.00	6.46
2	Intolerant	Small Seeds	283.33	9.32
3	Intolerant	Large Seeds	180.33	6.18
4	Tolerant	Non-Animal	13.67	0.37
5	Tolerant	Small Seeds	92.33	2.80
6	Tolerant	Large Seeds	65.00	2.18
Total	-	-	765.67	27.31

Figure A 11. Boxplot comparison of large and small seed species in relation to the corresponding adult wood density. Field data from (Oliveira et al. 2008, Santos et al. 2008).
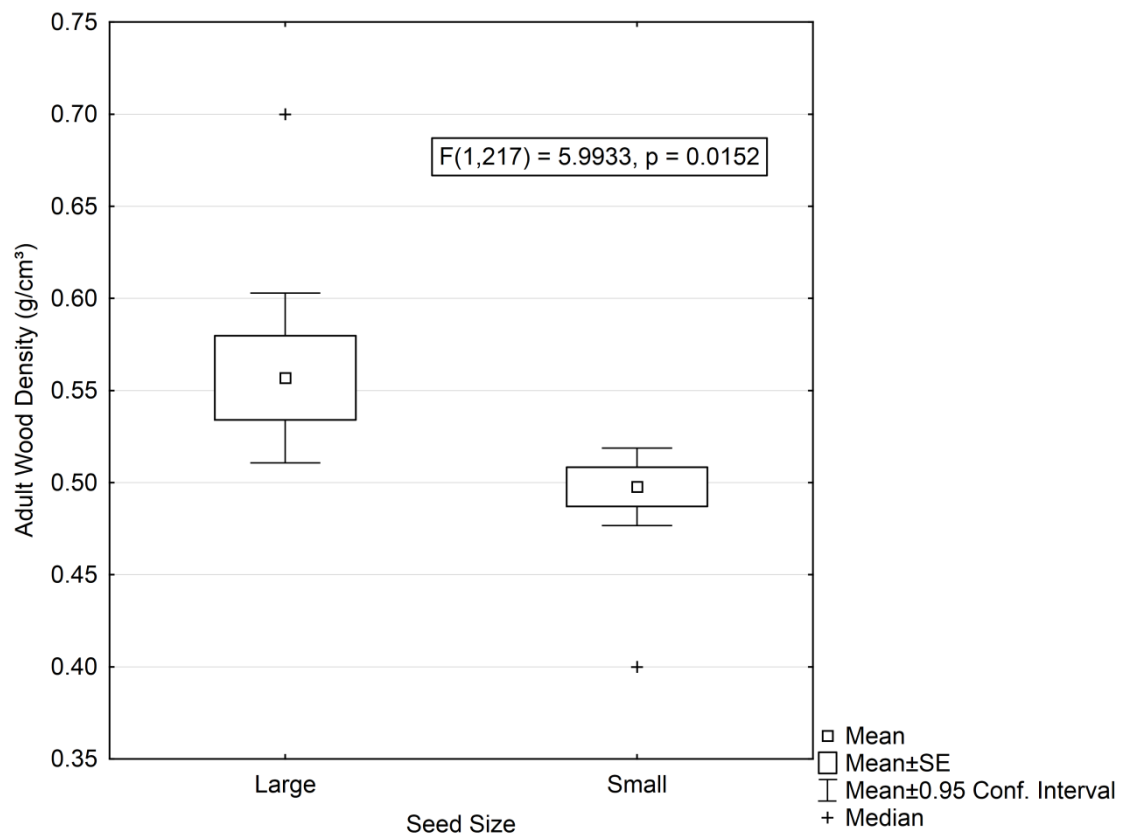
Table A 5. Reference simulation data for aboveground biomass, considering varying pos-dispersal predation and reduction of large seed dispersal, in an unfragmented and undisturbed forest. Values are relative to the reference (in red, average of last 100 years of simulation) 0% pre-dispersal predation and 1,000 post-dispersal predation factor (positives indicate relative gain and negative relative loss).

			Pre-Dispersal Predation Rate (PFT3 and PFT6)											
			0%	20%	30%	50%	70%	80%	90%	93%	95%	97%	98%	99%
	1,000	**PFT3**	**6.35**	20.7%	7.8%	-8.6%	-23.1%	-17.0%	-39.4%	-45.0%	-51.6%	-49.6%	-61.8%	-100.0%
		PFT6	**114.05**	-15.8%	2.5%	15.1%	-6.6%	-11.4%	-5.4%	-8.9%	-99.3%	-100.0%	-100.0%	-100.0%
		Total	**332.05**	-5.4%	1.5%	3.2%	-2.4%	-3.7%	-1.2%	-2.1%	-24.6%	-22.2%	-25.0%	-23.8%
	3,000	**PFT3**	4.0%	-8.1%	16.3%	-4.7%	-17.0%	-52.8%	-47.1%	-54.6%	-34.4%	-53.7%	-68.2%	-100.0%
		PFT6	-0.2%	1.0%	-11.7%	9.5%	-6.5%	10.3%	-35.4%	-94.4%	-99.9%	-100.0%	-100.0%	-100.0%
		Total	-1.8%	0.6%	-4.9%	3.3%	-2.3%	3.0%	-9.8%	-23.2%	-23.3%	-23.1%	-24.0%	-24.5%
	5,000	**PFT3**	15.1%	3.3%	0.9%	26.1%	10.2%	-22.5%	-34.1%	-37.1%	-46.1%	-65.5%	-72.5%	-100.0%
		PFT6	-17.3%	-14.7%	-16.8%	-39.0%	-26.4%	-32.2%	-81.2%	-97.6%	-100.0%	-100.0%	-100.0%	-100.0%
		Total	-6.3%	-5.3%	-6.2%	-13.1%	-9.7%	-8.6%	-21.4%	-27.2%	-25.1%	-26.4%	-26.4%	-25.2%
	10,000	**PFT3**	62.2%	52.6%	46.6%	66.2%	43.0%	1.0%	-41.0%	-58.1%	-36.0%	-87.0%	-87.6%	-100.0%
		PFT6	-59.1%	-59.0%	-59.6%	-65.8%	-67.9%	-71.3%	-94.5%	-99.7%	-100.0%	-100.0%	-100.0%	-100.0%
		Total	-21.1%	-20.7%	-19.8%	-23.2%	-23.3%	-22.8%	-26.7%	-28.6%	-28.6%	-28.9%	-27.4%	-29.3%

Post-Dispersal predation factor β

Table A 6. 121 ha fragment size simulation data for aboveground biomass, considering varying pos-dispersal predation and reduction of large seed dispersal, in an unfragmented and undisturbed forest. Values are relative to the reference (in red, average of last 100 years of simulation) 0% pre-dispersal predation and 1,000 post-dispersal predation factor (positives indicate relative gain and negative relative loss.

121 ha Fragment			Pre-Dispersal Predation Rate (PFT3 and PFT6)		
			0%	50%	95%
Post-Dispersal predation factor β	**1,000**	PFT3	8.21	-3.1%	-56.2%
		PFT6	77.63	1.1%	-94.2%
		Total	**271.64**	**0.5%**	**-17.3%**
	5,000	PFT3	5.8%	3.4%	-58.8%
		PFT6	-7.8%	-16.7%	-96.9%
		Total	**-2.1%**	**-4.5%**	**-19.3%**
	10,000	PFT3	20.1%	16.9%	-71.5%
		PFT6	-56.6%	-60.5%	-98.9%
		Total	**-15.6%**	**-16.7%**	**-22.2%**

Figure A 12. Sequence of 12 simulations with predation parameters parameter varying from 0% to 95% seed dispersal reduction for PFTs 3 and 6, and varying post-dispersal predation pressures. Biomass change graphs show percentual changes in relation to 0% pre-dispersal predation.

8. LIST OF FIGURES

9. LIST OF TABLES

10. REFERENCES

Alkama, R., and A. Cescatti. 2016. Biophysical climate impacts of recent changes in global forest cover. Science **351**:600-604.

Alonzo, M., B. Bookhagen, and D. A. Roberts. 2014. Urban tree species mapping using hyperspectral and lidar data fusion. Remote Sensing of Environment **148**:70-83.

Angelsen, A., and D. Kaimowitz. 1999. Rethinking the Causes of Deforestation: Lessons from Economic Models. The World Bank Research Observer **14**:73-98.

Aragão, L. E. 2012. The rainforest's water pump. Nature **489**:217-218.

Arroyo-Rodriguez, V., F. P. Melo, M. Martinez-Ramos, F. Bongers, R. L. Chazdon, J. A. Meave, N. Norden, B. A. Santos, I. R. Leal, and M. Tabarelli. 2015. Multiple successional pathways in human-modified tropical landscapes: new insights from forest succession, forest fragmentation and landscape ecology research. Biol Rev Camb Philos Soc.

Asner, G., and R. Martin. 2008. Spectral and chemical analysis of tropical forests: Scaling from leaf to canopy levels. Remote Sensing of Environment **112**:3958-3970.

Asner, G. P. 2009. Tropical forest carbon assessment: integrating satellite and airborne mapping approaches. Environmental Research Letters **4**:034009.

Asner, G. P. 2011. Painting the world REDD: addressing scientific barriers to monitoring emissions from tropical forests. Environmental Research Letters **6**:021002.

Asner, G. P., and R. E. Martin. 2009. Airborne spectranomics: mapping canopy chemical and taxonomic diversity in tropical forests. Frontiers in Ecology and the Environment **7**:269-276.

Asner, G. P., R. E. Martin, D. E. Knapp, R. Tupayachi, C. Anderson, L. Carranza, P. Martinez, M. Houcheime, F. Sinca, and P. Weiss. 2011. Spectroscopy of canopy chemicals in humid tropical forests. Remote Sensing of Environment **115**:3587-3598.

Asner, G. P., R. E. Martin, R. Tupayachi, C. B. Anderson, F. Sinca, L. Carranza-Jiménez, and P. Martinez. 2014. Amazonian functional diversity from forest canopy chemical assembly. Proceedings of the National Academy of Sciences **111**:5604-5609.

Avitabile, V., M. Herold, G. B. Heuvelink, S. L. Lewis, O. L. Phillips, G. P. Asner, J. Armston, P. S. Ashton, L. Banin, N. Bayol, N. J. Berry, P. Boeckx, B. H. de Jong, B. DeVries, C. A. Girardin, E. Kearsley, J. A. Lindsell, G. Lopez-Gonzalez, R. Lucas, Y. Malhi, A. Morel, E. T. Mitchard, L. Nagy, L. Qie, M. J. Quinones, C. M. Ryan, S. J. Ferry, T. Sunderland, G. V. Laurin, R. C. Gatti, R. Valentini, H. Verbeeck, A. Wijaya, and S. Willcock. 2016. An integrated pan-tropical biomass map using multiple reference datasets. Glob Chang Biol **22**:1406-1420.

Baccini, A., S. J. Goetz, W. S. Walker, N. T. Laporter, M. Sun, D. Sulla-Menasche, J. Hackler, P. S. A. Beck, R. Dubayah, M. A. Friedl, S. Samanta, and R. A. Houghton. 2012. Estimated carbon

dioxide emissions from tropical deforestation improved by carbon-density maps. Nat Clim Change **2**:182-185.

Bannari, A., D. Morin, F. Bonn, and A. R. Huete. 1995. A review of vegetation indices. Remote Sensing Reviews **13**:95-120.

Barlow, J., C. A. Peres, B. O. Lagan, and T. Haugaasen. 2003. Large tree mortality and the decline of forest biomass following Amazonian wildfire. Ecol Lett **6**:6-8.

Bawa, K., J. Rose, K. Ganeshaiah, N. Barve, M. Kiran, and R. Umashaanker. 2002. Assessing biodiversity from space: an example from the Western Ghats, India. Conservation Ecology **6**:7.

Bawa, K. S., S. H. Bullock, D. R. Perry, R. E. Coville, and M. H. Grayum. 1985. Reproductive Biology of Tropical Lowland Rain Forest Trees. II. Pollination Systems. American Journal of Botany **72**:346-356.

Baz, A., and A. Garcia-Boyero. 1996. The SLOSS dilemma: a butterfly case study. Biodiversity & Conservation **5**:493-502.

Beer, C., M. Reichstein, E. Tomelleri, P. Clais, M. Jung, N. Carvalhais, C. Rödenbeck, M. Altaf Arain, D. D. Baldocchi, G. B. Bonan, B. A., A. Cescatti, G. Lasslop, A. Lindroth, M. Lomas, E. Luyssaert, N. Viovy, C. Williams, F. I. Woodward, and D. Papale. 2010. Terrestrial Gross Carbon Dioxide Uptake: Global Distribution and Covariation with Climate. Science **329**:834-838.

Bello, M., M. Galetti, M. A. Pizo, L. F. S. Magnago, M. F. Rocha, R. A. F. Lima, C. A. Peres, O. Ovaskainen, and P. Jordano. 2015. Defaunation affects carbon storage in tropical forests. Science Advances **1**.

Bendix, J., R. Rollenbeck, M. Richter, P. Fabian, and P. Emck. 2008. Climate. Pages 63-73 *in* E. Beck, editor. Gradients in a Tropical Mountain Ecosystem of Ecuador. Springer, Berlin.

Berenguer, E., J. Ferreira, T. A. Gardner, L. E. Aragao, P. B. De Camargo, C. E. Cerri, M. Durigan, R. C. J. Oliveira, I. C. Vieira, and J. Barlow. 2014. A large-scale field assessment of carbon stocks in human-modified tropical forests. Glob. Chang. Biol. **20**:3713-3726.

Bossel, H., and H. Krieger. 1991. Simulation model of natural tropical forest dynamics. Ecological Modelling **59**:37-71.

Bossel, H., and H. Krieger. 1994. Simulation of multi-species tropical forest dynamics using a vertically and horizontally structured model. Forest Ecology and Management **69**:123-144.

Botkin, D., J. Janak, and J. Wallis. 1972. Some ecological consequences of a computer model of forest growth. Journal of Ecology **60**:849-872.

Brazhnik, K., and H. H. Shugart. 2016. SIBBORK: A new spatially-explicit gap model for boreal forest. Ecological Modelling **320**:182-196.

Briant, G., V. Gond, and S. G. W. Laurance. 2010. Habitat fragmentation and the desiccation of forest canopies: A case study from eastern Amazonia. Biological Conservation **143**:2763-2769.

Broadbent, E., G. Asner, M. Keller, D. Knapp, P. Oliveira, and J. Silva. 2008. Forest fragmentation and edge effects from deforestation and selective logging in the Brazilian Amazon. Biol. Cons. **141**:1745-1757.

Brooks, T. M., S. L. Pimm, and J. O. Oyugi. 1999. Time Lag between Deforestation and Bird Extinction in Tropical Forest Fragments. Conserv Biol **13**:1140-1150.

Brown, K. S., and R. W. Hutchings. 1997. Disturbance, Fragmentation, and the Dynamics of Diversity in Amazonian Forest Butterflies. Pages 91-110 *in* W. F. Laurance and R. O. Bierregaard, editors. Tropical Forest Remnants - Ecology, Management and Conservation of Fragmented Communities. The University of Chicago Press, Chicago.

Bugmann, H. 2001. A review of forest gap models. Climatic Change **51**:259-305.

Bugmann, H., and A. M. Solomon. 2000. Explaining Forest Composition and Biomass across Multiple Biogeographical Regions. Ecological Applications **10**:95-114.

Camargo, J. L., and V. Kapos. 1995. Complex edge effects on soil moisture and microclimate in central Amazonian forest. J. Trop. Ecol. **11**:205-221.

Carson, T. N., and D. A. Ripley. 1997. On the Relation between NDVI, Fractional Vegetation Cover, and Leaf Area Index. Remote Sens Environ **62**:241-252.

Ceballos, G., P. R. Ehrlich, A. D. Barnosky, A. García, R. M. Pringle, and T. M. Palmer. 2015. Accelerated modern human–induced species losses: Entering the sixth mass extinction. Science Advances.

Chaplin-Kramer, R., I. Ramler, R. Sharp, N. M. Haddad, J. S. Gerber, P. C. West, L. Mandle, P. Engstrom, A. Baccini, S. Sim, C. Mueller, and H. King. 2015. Degradation in carbon stocks near tropical forest edges. Nat. Commun. **6**:10158.

Chave, J. 2013. The problem of pattern and scale in ecology: what have we learned in 20 years? Ecol Lett **16 Suppl 1**:4-16.

Chave, J., H. C. Muller-Landau, T. R. Baker, T. A. Easdale, H. ter Steege, and C. O. Webb. 2006. Regional and phylogenetic variation of wood density across 2456 neotropical tree species. Ecological Applications **16**:2356-2367.

Chiarello, A. 1999. Effects of fragmentaion of the Atlantic forest on mammal communities in south-eastern Brazil. Biol. Cons. **89**:71-82.

Chiarello, A. 2000. Density and Population Size of Mammals in Remnants of Brazilian Atlantic Forest. Conserv Biol **14**:1649-1657.

Clark, M., D. Roberts, and D. Clark. 2005. Hyperspectral discrimination of tropical rain forest tree species at leaf to crown scales. Remote Sensing of Environment **96**:375-398.

Cochrane, M. A., and W. F. Laurance. 2008. Synergisms among Fire, Land Use, and Climate Change in the Amazon. AMBIO: A Journal of the Human Environment **37**:522-527.

Conde, D. A., F. Colchero, H. Zarza, N. L. Christensen, J. O. Sexton, C. Manterola, C. Chávez, A. Rivera, D. Azuara, and G. Ceballos. 2010. Sex matters: Modeling male and female habitat differences for jaguar conservation. Biol. Cons. **143**:1980-1988.

Costa, J. B. P., F. P. L. Melo, B. A. Santos, and M. Tabarelli. 2012. Reduced availability of large seeds constrains Atlantic forest regeneration. Acta Oecologica **39**:61-66.

Crowther, T. W., H. B. Glick, K. R. Covey, C. Bettigole, D. S. Maynard, S. M. Thomas, J. R. Smith, G. Hintler, M. C. Duguid, G. Amatulli, M. N. Tuanmu, W. Jetz, C. Salas, C. Stam, D. Piotto, R. Tavani, S. Green, G. Bruce, S. J. Williams, S. K. Wiser, M. O. Huber, G. M. Hengeveld, G. J. Nabuurs, E. Tikhonova, P. Borchardt, C. F. Li, L. W. Powrie, M. Fischer, A. Hemp, J. Homeier, P. Cho, A. C. Vibrans, P. M. Umunay, S. L. Piao, C. W. Rowe, M. S. Ashton, P. R. Crane, and M. A. Bradford. 2015. Mapping tree density at a global scale. Nature **525**:201-205.

Dalponte, M., H. O. Ørka, L. T. Ene, T. Gobakken, and E. Næsset. 2014. Tree crown delineation and tree species classification in boreal forests using hyperspectral and ALS data. Remote Sensing of Environment **140**:306-317.

Dantas de Paula, M., C. P. A. Costa, and M. Tabarelli. 2011a. Carbon storage in a fragmented landscape of Atlantic forest: the role played by edge-affected habitats and emergent trees. Trop. Conserv. Sci. **4**:349-358.

Dantas de Paula, M., J. Groeneveld, and A. Huth. 2015. Tropical forest degradation and recovery in fragmented landscapes - Simulating changes in tree community, forest hydrology and carbon balance. Global Ecology and Conservation **3**:664-677.

Dantas de Paula, M., J. Groeneveld, and A. Huth. 2016. The extent of edge effects in fragmented landscapes: Insights from satellite measurements of tree cover. Ecological Indicators **69**:196-204.

Dantas de Paula, M., M. A. Oliveira, C. I. R. Santos, and J. S. Almeida-Cortez. 2011b. Herbivory Rate on Woody Species of the Caatinga and NDVI as Indicators of Plant Stress. Revista Brasileira de Geografia Física **5**:909-921.

de Sherbinin, A. 2013. Climate change hotspots mapping: what have we learned? Climatic Change **123**:23-37.

DeFries, R. S., C. B. Field, I. Fung, C. O. Justice, S. Los, E. M. Matson, H. A. Mooney, C. S. Potter, K. Prentice, P. J. Sellers, J. R. Townshend, C. J. Tucker, S. L. Ustin, and P. M. Vitousek. 1995. Mapping the land surface for global atmosphere-biosphere models: Toward continuous distributions of vegetation's functional properties. J. Geophys. Res. **100**:20867-20882.

DeFries, R. S., J. R. G. Townshend, and M. C. Hansen. 1999. Continuous fields of vegetation characteristics at the global scale at 1-km resolution. J. Geophys. Res. **104**:16911.

Diamond, J. 1972. Biogeographic Kinetics: Estimation of Relaxation Times for Avifaunas of Southwest Pacific Islands. Proc. Nat. Acad. Sci. USA **69**:3199-3203.

Didham, R. K., and R. M. Ewers. 2012. Predicting the impacts of edge effects in fragmented habitats: Laurance and Yensen's core area model revisited. Biological Conservation **155**:104-110.

Didham, R. K., and J. H. Lawton. 2001. Edge Structure Determines the Magnitude of Changes in Microclimate and Vegetation Structure in Tropical Forest Fragments. Biotropica **31**:17-30.

Dirzo, R., E. Mendoza, and P. Ortíz. 2007. Size-Related Differential Seed Predation in a Heavily Defaunated Neotropical Rain Forest. Biotropica **39**:355-362.

Dirzo, R., H. S. Young, M. Galetti, G. Ceballos, N. J. B. Isaac, and B. Collen. 2014. Defaunation in the Anthropocene. Science **345**:401-406.

Dislich, C., S. Günter, J. Homeier, B. Schröder, and A. Huth. 2009. Simulating forest dynamics of a tropical montane forest in South Ecuador. Erdkunde **63**:347-364.

Dislich, C., and A. Huth. 2012. Modelling the impact of shallow landslides on forest structure in tropical montane forests. Ecological Modelling **239**:40-53.

Doyle, T. W., H. H. Shugart, and D. C. West. 1982. FORICO: Gap Dynamics Model of the Lower Montane Rain Forest in Puerto Rico. Oak Ridge National Laboratory, USA.

Dyer, L. A., and D. K. Letourneau. 1999. Relative strenghs of top-down annd bottom-up forces in a tropical forest community. Oecologia **119**:265-274.

Fahrig, L. 2003. Effects of habitat fragmentation on biodiversity. Annual Review of Ecology and Systematics **34**:487-515.

FAO. 2014. FAO assessment of forests and carbon stocks, 1990-2015.

FAO. 2015. Global Forest Resources Assessment 2015 - How are the world's forests changing? , Food and Agriculture Organization of the United Nations, Rome.

Fischer, R., A. Armstrong, H. H. Shugart, and A. Huth. 2014. Simulating the impacts of reduced rainfall on carbon stocks and net ecosystem exchange in a tropical forest. Environmental Modelling & Software **52**:200-206.

Fischer, R., F. Bohn, M. Dantas de Paula, C. Dislich, J. Groeneveld, A. G. Gutiérrez, M. Kazmierczak, N. Knapp, S. Lehmann, S. Paulick, S. Pütz, E. Rödig, F. Taubert, P. Köhler, and A. Huth. 2016. Lessons learned from applying a forest gap model to understand ecosystem and carbon dynamics of complex tropical forests. Ecological Modelling **326**:124-133.

Foley, J. A., S. Levis, I. C. Prentice, D. Pollard, and S. L. Thompson. 1998. Coupling dynamic models of climate and vegetation. Glob Chang Biol **4**:561-579.

Forman, R. T. T. 1995. Land Mosaics: The ecology of landscapes and regions. Cambridge University Press.

Foster, D. R. 1992. Land-Use History (1730-1990) and Vegetation Dynamics in Central New England, USA. Journal of Ecology **80**:753-771.

Foster, D. R., M. Fluet, and E. R. Boose. 1999. Human or natural disturbance: Landscape dynamics of the tropical forests of Puerto Rico. Ecological Applications **9**:555-572.

Foster, S. A. 1986. On the Adaptive Value of Large Seeds for Tropical Moist Forest Trees: A Review and Synthesis. The Botanical Review **52**:261-293.

Freitas, S. R., T. J. Hawbaker, and J. P. Metzger. 2010. Effects of roads, topography, and land use on forest cover dynamics in the Brazilian Atlantic Forest. Forest Ecology and Management **259**:410-417.

Friend, A. D., H. H. Schugart, and S. W. Running. 1993. A Physiology-Based Gap Model of Forest Dynamics. Ecology **74**:792-797.

Gagné, S. A., F. Eigenbrod, D. G. Bert, G. M. Cunnington, L. T. Olson, A. C. Smith, and L. Fahrig. 2015. A simple landscape design framework for biodiversity conservation. Landscape and Urban Planning **136**:13-27.

Gibson, L., T. M. Lee, L. P. Koh, B. W. Brook, T. A. Gardner, J. Barlow, C. A. Peres, C. J. Bradshaw, W. F. Laurance, T. E. Lovejoy, and N. S. Sodhi. 2011. Primary forests are irreplaceable for sustaining tropical biodiversity. Nature **478**:378-381.

Goodman, R. C., O. L. Phillips, and T. R. Baker. 2014. The importance of crown dimensions to improve tropical tree biomass estimates. Ecological Applications **24**:680-698.

Gorchov, D. L., F. Cornejo, C. Ascorra, and M. Jaramillo. 1993. The role of seed dispersal in the natural regeneration of rain forest after strip-cutting in the Peruvian Amazon. Vegetatio **107**:339-349.

Götmark, F., and M. Thorell. 2003. Size of nature reserves: densities of large trees and dead wood indicate high value of small conservation forests in southern Sweden. Biodiversity and Conservation **12**:1271-1285.

Gould, W. 2000. Remote Sensing of Vegetation, Plant Species Richness, and Regional Biodiversity Hotspots. Ecological Applications **10**:1861-1870.

Grace, J., E. Mitchard, and E. Gloor. 2014. Perturbations in the carbon budget of the tropics. Glob Chang Biol **20**:3238-3255.

Granier, A., N. Bréda, P. Biron, and S. Villete. 1999. A lumped water balance model to evaluate duration and intensity of drought constraints in forest stands. Ecological Modelling **116**:269-283.

Grimm, V., and S. F. Railsback. 2005. Individual-based Modeling and Ecology. Princeton University Press.

Groeneveld, J., L. F. Alves, L. C. Bernacci, E. L. M. Catharino, C. Knogge, J. P. Metzger, S. Pütz, and A. Huth. 2009. The impact of fragmentation and density regulation on forest succession in the Atlantic rain forest. Ecological Modelling **220**:2450-2459.

Groves, C. R., D. B. Jensen, L. L. Valutis, K. H. Redford, M. L. Shaffer, M. Scott, J. V. Baumgartner, J. V. Higgins, M. W. Beck, and M. G. Anderson. 2002. Planning for Biodiversity Conservation: Putting Conservation Science into Practice. BioScience **52**:499-512.

Haddad, N. M., L. A. Brudvig, J. Clobert, K. F. Davies, A. Gonzalez, R. D. Holt, T. E. Lovejoy, J. O. Sexton, M. P. Austin, C. D. Collins, W. M. Cook, E. I. Damschen, R. M. Ewers, B. L. Foster, C. N. Jenkins, A. J. King, W. F. Laurance, D. J. Levey, C. R. Margules, B. A. Melbourne, A. O. Nicholls, J. L. Orrock, D. X. Song, and J. R. Townshend. 2015. Habitat fragmentation and its lasting impact on Earth's ecosystems. Sci. Adv. **1**:1-9.

Hansen, M. C., P. V. Potapov, R. Moore, M. Hancher, S. A. Turubanova, A. Tyukavina, D. Thau, S. V. Stehman, S. J. Goetz, T. R. Loveland, A. Kommareddy, A. Egorov, L. Chini, C. O. Justice, and J. R. Townshend. 2013. High-resolution global maps of 21st-century forest cover change. Science **342**:850-853.

Hansen, M. C., D. P. Roy, E. Lindquist, B. Adusei, C. O. Justice, and A. Altstatt. 2008a. A method for integrating MODIS and Landsat data for systematic monitoring of forest cover and change in the Congo Basin. Remote Sens. Environ. **112**:2495-2513.

Hansen, M. C., Y. E. Shimabukuro, P. Potapov, and K. Pittman. 2008b. Comparing annual MODIS and PRODES forest cover change data for advancing monitoring of Brazilian forest cover. Remote Sens. Environ. **112**:3784-3793.

Hansen, M. C., J. R. G. Townshend, R. S. DeFries, and M. Carroll. 2005. Estimation of tree cover using MODIS data at global, continental and regional/local scales. Int. J. Remote Sens. **26**:4359-4380.

Hansson, L., and P. Angelstam. 1991. Landscape ecology as a theoretical basis for nature conservation. Landscape Ecology **5**:191-201.

Hartig, F., C. Dislich, T. Wiegand, and A. Huth. 2014. Technical Note: Approximate Bayesian parameterization of a process-based tropical forest model. Biogeosciences **11**:1261-1272.

Harvey, C. A., A. Medina, D. M. Sánchez, S. Vilchez, B. Hernández, J. C. Saenz, J. M. Maes, C. F., and F. L. Sinclair. 2006. Patterns of animal diversity in different forms of tree cover in agricultural landscapes. Ecol. Appl. **16**:1986-1999.

Hawkins, B. A., R. Field, H. V. Cornell, D. V. Currie, J. F. Guegan, D. M. Kaufman, J. T. Kerr, G. G. Mittelbach, T. Oberdorff, E. M. O'Brien, E. E. Porter, and J. R. G. Turner. 2003. Energy, water, and broad-scale geographic patterns of species richness. Ecology **84**:3105-3117.

He, K. S., J. Zhang, and Q. Zhang. 2009. Linking variability in species composition and MODIS NDVI based on beta diversity measurements. Acta Oecologica **35**:14-21.

Helm, A., I. Hanski, and M. Partel. 2006. Slow response of plant species richness to habitat loss and fragmentation. Ecol Lett **9**:72-77.

Hernandez-Ruedas, M. A., V. Arroyo-Rodriguez, J. A. Meave, M. Martinez-Ramos, G. Ibarra-Manriquez, E. Martinez, G. Jamangape, F. P. Melo, and B. A. Santos. 2014. Conserving tropical tree diversity and forest structure: the value of small rainforest patches in moderately-managed landscapes. PLoS One **9**:e98931.

Hiltner, U., A. Bräuning, A. Gebrekirstos, A. Huth, and R. Fischer. 2016. Impacts of precipitation variability on the dynamics of a dry tropical montane forest. Ecological Modelling **320**:92-101.

Houghton, R. A. 2005. Aboveground Forest Biomass and the Global Carbon Balance. Glob Chang Biol **11**:945-958.

Houghton, R. A., F. Hall, and S. J. Goetz. 2009. Importance of biomass in the global carbon cycle. Journal of Geophysical Research: Biogeosciences **114**:n/a-n/a.

Huang, C., S. N. Goward, K. Schleeweis, N. Thomas, J. G. Masek, and Z. Zhu. 2009. Dynamics of national forests assessed using the Landsat record: Case studies in eastern United States. Remote Sens. Environ. **113**:1430-1442.

Hunt, E. R., S. C. Piper, R. Nemani, C. D. Keeling, R. D. Otto, and S. W. Running. 1996. Global net carbon exchange and intra-annual atmospheric CO2concentrations predicted by an ecosystem process model and three-dimensional atmospheric transport model. Global Biogeochemical Cycles **10**:431-456.

Hurtt, G. C., J. Fisk, R. Q. Thomas, R. Dubayah, P. R. Moorcroft, and H. H. Shugart. 2010. Linking models and data on vegetation structure. Journal of Geophysical Research: Biogeosciences **115**:n/a-n/a.

Huston, M., D. L. DeAngelis, and W. Post. 1988. New Computer Models Unify Ecological Theory. BioScience **38**:682-691.

Huth, A., and T. Ditzer. 2000. Simulation of the growth of a lowland Dipterocarp rain forest with FORMIX3. Ecological Modelling **134**:1-25.

Huth, A., and T. Ditzer. 2001. Long-term impacts of logging in a tropical rain forest - a simulation study. Forest Ecology and Management **142**:33-51.

Huth, A., M. Drechsler, and P. Kohler. 2004. Multicriteria evaluation of simulated logging scenarios in a tropical rain forest. J Environ Manage **71**:321-333.

Ibáñez, I., D. S. W. Katz, D. Peltier, S. M. Wolf, B. T. Connor Barrie, and C. Lortie. 2014. Assessing the integrated effects of landscape fragmentation on plants and plant communities: the challenge of multiprocess-multiresponse dynamics. J. Ecol. **102**:882-895.

IBGE. 1985. Atlas Nacional do Brasil: Região Nordeste. IBGE, Rio de Janeiro.

Ilstedt, U., A. Malmer, E. Verbeeten, and D. Murdiyarso. 2007. The effect of afforestation on water infiltration in the tropics: A systematic review and meta-analysis. Forest Ecology and Management **251**:45-51.

Janzen, D. H. 1969. Seed-Eaters Versus Seed Size, Number, Toxicity and Dispersal. Evolution **23**:1-27.

Janzen, D. H. 1970. Herbivores and the Number of Tree Species in Tropical Forests. Am Nat **104**:501-528.

Janzen, D. H. 1986. The future of tropical ecology. Annual Review of Ecology and Systematics **17**:305-324.

Jeganathan, C., V. K. Dadhwal, K. Gupta, and P. L. N. Raju. 2009. Comparison of MODIS Vegetation Continuous Field - based Forest Density Maps with IRS-LISS III Derived Maps. J. Indian Soc. Remote Sens. **37**:539-549.

Joffre, R., and S. Rambal. 1993. How Tree Cover Influences the Water Balance of Mediterranean Rangelands. Ecology **74**:570-582.

Kammersheidt, L., P. Köhler, and A. Huth. 2002. Simulating logging scenarios in secondary forest embedded in a fragmented neotropical landscape. Forest Ecology and Management **170**:89-105.

Kapos, V. 1989. Effects of Isolation on the Water Status of Forest Patches in the Brazilian Amazon. Journal of Tropical Ecology **5**:173-185.

Kapos, V., G. Ganade, E. Matsui, and R. L. Victoria. 1993. $\partial^{13}\mathrm{C}$ as an Indicator of Edge Effects in Tropical Rainforest Reserves. Journal of Ecology **81**:425-432.

Kapos, V., E. Wandelli, J. L. Camargo, and G. Ganade. 1997. Edge-Related Changes in Environment and Plant Responses Due to Forest Fragmentation in Central Amazonia. Page 632 *in* W. F. Laurance and R. O. Bierregaard, editors. Tropical Forest Remnants - Ecology, Management, and Conservation of Fragmented Communities. The University of Chicago Press, Chicago.

Kazmierczak, M., T. Wiegand, and A. Huth. 2014. A neutral vs. non-neutral parametrizations of a physiological forest gap model. Ecological Modelling **288**:94-102.

Kerr, J. T., and M. Ostrovsky. 2003. From space to species: ecological applications for remote sensing. Trends Ecol. Evol. **18**:299-305.

Kitajima, K. 1994. Relative importance of photosynthetic traits and allocation patterns as correlates of seedling shade tolerance of 13 tropical trees. Oecologia **98**:419-428.

Kleidon, A. 2009. Nonequilibrium thermodynamics and maximum entropy production in the Earth system: applications and implications. Naturwissenschaften **96**:653-677.

Köhler, P. 2000. Modelling anthropogenic impacts on the growth of tropical rain forests. Universität Gesamthochschule Kassel, Der Andere Verlag, Osnabrück.

Köhler, P., J. Chave, B. Riéra, and A. Huth. 2003. Simulating the Long-term Response of Tropical Wet Forests to Fragmentation. Ecosystems **6**:114-128.

Köhler, P., and A. Huth. 1998. The effects of tree species grouping in tropical rainforest modelling: Simulations with the individual-based model FORMIND. Ecological Modelling **109**.

Köhler, P., and A. Huth. 2004. Simulating growth dynamics in a south-east Asian rainforest threatened by recruiting shortage and tree harvesting. Climatic Change **67**:95-117.

Köhler, P., and A. Huth. 2007. Impacts of recruitment limitation and canopy disturbance on tropical tree species richness. Ecological Modelling **203**:511-517.

Köhler, P., K. Reinhard, and A. Huth. 2002. Simulating anthropogenic impacts to bird communities in tropical rain forests. Biological Conservation **108**:35-47.

Kornig, J., and H. Balslev. 1994. Growth rates and mortality patterns of tropical lowland tree species and the relation to forest structure in Amazonian Ecuador. Journal of Tropical Ecology **10**:151-166.

Kosoy, N., M. Martinez-Tuna, R. Muradian, and J. Martinez-Alier. 2007. Payments for environmental services in watersheds: Insights from a comparative study of three cases in Central America. Ecological Economics **61**:446-455.

Kozak, J. 2003. Forest Cover Change in the Western Carpathians in the Past 180 Years. Mountain Research and Development **23**:369-375.

Kürpick, P., U. Kürpick, and A. Huth. 1997. The Influence of Logging on a Malaysian Dipterocarp Rain Forest: a Study Using a Forest Gap Model. J Theor Biol **185**:47-54.

Lamarque, P., F. Quetier, and S. Lavorel. 2011. The diversity of the ecosystem services concept and its implications for their assessment and management. C R Biol **334**:441-449.

Lambin, E. F., H. J. Geist, and E. Lepers. 2003. Dynamics of land-use and land-cover change In tropical regions. Annu. Rev. Environ. Resour. **28**:205-241.

Laurance, W. 2008. Theory meets reality: How habitat fragmentation research has transcended island biogeographic theory. Biological Conservation **141**:1731-1744.

Laurance, W. F. 1997. Biomass Collapse in Amazonian Forest Fragments. Science **278**:1117-1118.

Laurance, W. F. 2009. Hyperdynamism in fragmented habitats. J. Veg. Sci. **13**:595-602.

Laurance, W. F., J. L. C. Camargo, R. C. C. Luizão, S. G. Laurance, S. L. Pimm, E. M. Bruna, P. C. Stouffer, G. Bruce Williamson, J. Benítez-Malvido, and H. L. Vasconcelos. 2011. The fate of Amazonian forest fragments: A 32-year investigation. Biol. Cons. **144**:56-67.

Laurance, W. F., and T. J. Curran. 2008. Impacts of wind disturbance on fragmented tropical forests: A review and synthesis. Austral Ecology **33**:399-408.

Laurance, W. F., L. V. Ferreira, J. M. Rankin-De Merona, and S. G. Laurance. 1998. Rain forest fragmentation an the dynamics of Amazonian tree communities. Ecology **79**:2032-2040.

Laurance, W. F., T. E. Lovejoy, H. L. Vasconcelos, E. M. Bruna, R. K. Didham, P. C. Stouffer, C. Gascon, R. O. Bierregaard, S. G. Laurance, and E. Sampaio. 2002. Ecosystem Decay of Amazonian Forest Fragments: a 22-Year Investigation. Conserv. Biol. **16**:605-618.

Laurance, W. F., H. E. Nascimento, S. G. Laurance, A. Andrade, J. E. Ribeiro, J. P. Giraldo, T. E. Lovejoy, R. Condit, J. Chave, K. E. Harms, and S. D'Angelo. 2006. Rapid decay of tree-community composition in Amazonian forest fragments. Proc. Natl. Acad. Sci. U S A **103**:19010-19014.

Lefsky, M. A., W. B. Cohne, S. A. Acker, G. G. Parker, T. A. Spies, and D. Harding. 1999. Lidar Remote Sensing of the Canopy Structure and Biophysical Properties of Douglas-Fir Western Hemlock Forests.

Lehmann, S., and A. Huth. 2015. Fast calibration of a dynamic vegetation model with minimum observation data. Ecological Modelling **301**:98-105.

Leigh, E. G., P. Davidar, C. W. Dick, J. P. Puyravaud, J. Terborgh, H. Ter Steege, and S. J. Wright. 2004. Why Do Some Tropical Forests Have So Many Species of Trees? Biotropica **36**:447-473.

Liang, X., D. P. Lettenmaier, E. F. Wood, and S. J. Burges. 1994. A simple hydrologically based model of land surface water and energy fluxes for general circulation models. Journal of Geophysical Research **99**:14,415-414,428.

Lima, J. G. C., S. M. B. B. Schulze, M. R. Ribeiro, and S. B. Barreto. 2008. Mineralogia de um argissolo vermelho-amarelo da zona úmida costeira do Estado de Pernambuco. Revista Brasileira de Ciências do Solo **32**:881-892.

Lindenmayer, D. B., W. F. Laurance, and J. F. Franklin. 2016. Global Decline in Large Old Trees. Science **338**:1305-1306.

Liu, J., and P. S. Ashton. 1995. Individual-based simulation models for forest succession and management. For. Ecol. Manage. **73**:157-175.

Lôbo, D., T. Leão, F. P. L. Melo, A. M. M. Santos, and M. Tabarelli. 2011. Forest fragmentation drives Atlantic forest of northeastern Brazil to biotic homogenization. Diversity and Distributions **17**:287-296.

Loveland, T. R., B. C. Reed, J. F. Brown, D. O. Ohlen, Z. Zhu, L. Yang, and J. W. Merchant. 2010. Development of a global land cover characteristics database and IGBP DISCover from 1 km AVHRR data. Int. J. Remote Sensing **21**:1303-1330.

Magnanini, A., and C. Magnanini. 2002. Árvores gigantescas da Terra e as maiores assinaladas no Brasil.*in* C. N. d. R. d. B. d. M. Atlântica., editor. Cadernos da Reserva da Biosfera da Mata Atlântica. CETESB - Companhia de Tecnologia de Saneamento Ambiental, São Paulo.

Maidment, D. 1993. Handbook of Hydrology. McGraw-Hill Professional.

Martensen, A. C., M. C. Ribeiro, C. Banks-Leite, P. I. Prado, and J. P. Metzger. 2012. Associations of forest cover, fragment area, and connectivity with neotropical understory bird species richness and abundance. Conserv. Biol. **26**:1100-1111.

McConkey, K. R., S. Prasad, R. T. Corlett, A. Campos-Arceiz, J. F. Brodie, H. Rogers, and L. Santamaria. 2012. Seed dispersal in changing landscapes. Biological Conservation **146**:1-13.

Melo, F. P., V. Arroyo-Rodriguez, L. Fahrig, M. Martinez-Ramos, and M. Tabarelli. 2013a. On the hope for biodiversity-friendly tropical landscapes. Trends Ecol. Evol. **28**:462-468.

Melo, F. P., R. Dirzo, and M. Tabarelli. 2006. Biased seed rain in forest edges: Evidence from the Brazilian Atlantic forest. Biological Conservation **132**:50-60.

Melo, F. P., D. Lemire, and M. Tabarelli. 2007. Extirpation of large-seeded seedlings from the edge of a large Brazilian Atlantic forest fragment. Ecoscience **14**:6.

Melo, F. P. L., S. R. R. Pinto, P. H. S. Brancalion, P. S. Castro, R. R. Rodrigues, J. Aronson, and M. Tabarelli. 2013b. Priority setting for scaling-up tropical forest restoration projects: Early lessons from the Atlantic Forest Restoration Pact. Environmental Science & Policy **33**:395-404.

Mendes Pontes, A. R., A. C. Beltrao, I. C. Normande, A. J. Malta, A. P. Silva Junior, and A. M. Santos. 2016. Mass Extinction and the Disappearance of Unknown Mammal Species: Scenario and Perspectives of a Biodiversity Hotspot's Hotspot. PLoS One **11**:e0150887.

Menon, S., and K. S. Bawa. 1997. Applications of geographic information systems, remote-sensing, and a landscape ecology approach to biodiversity conservation in the Western Ghats. Current science **73**:134-145.

Menzel, S., and J. Teng. 2010. Ecosystem services as a stakeholder-driven concept for conservation science. Conserv Biol **24**:907-909.

Metzger, J. P., and H. Décamps. 1997. The structural connectivity threshold: an hypothesis in conservation biology at the landscape scale. Acta Oecol. **18**:1-12.

Mielke, D. L., H. H. Shugart, and D. C. West. 1978. A Stand Model for Upland Forests of Southern Arkansas. Tennessee, Oak Ridge, Tennessee.

Milton, K., and M. L. May. 1976. Body weight, diet and home range area in primates. Nature **259**:459-462.

Mitchard, E., T. R. Feldpausch, R. Brienen, G. Lopez-Gonzalez, A. Monteagudo, T. R. Baker, S. L. Lewis, J. Lloyd, C. A. Quesada, E. Gloor, H. Ter Steege, P. Meir, E. Alvarez, A. Araujo-Murakami, L. E. Aragao, L. Arroyo, G. Aymard, O. Banki, D. Bonal, S. Brown, F. Brown, C. E. Cerón, V. C. Moscoso, J. Chave, J. A. Comiskey, F. Cornejo, M. C. Medina, L. Da Costa, F. R. C. Costa, A. Di Fiore, T. F. Domingues, T. L. Erwin, T. Frederickson, N. Higuchi, E. Honorio Coronado, T. J. Killeen, W. F. Laurance, C. Levis, W. E. Magnusson, B. S. Marimon, B. H. Marimon Junior, I. M. Polo, P. Mishra, M. T. Nascimento, D. Neill, M. P. Nuñes Vargas, W. A. Palacios, A. Parada, G. P. Miolina, M. Peña-Claros, N. Pittman, C. A. Peres, L. Poorter, A. Prieto, H. Ramirez-Angulo, Z. R. Correa, A. Roopsing, K. H. Roucoux, A. Rudas, R. P. Salomão, J. Schietti, M. Silveira, P. F. de Souza, M. K. Steininger, J. Stroop, J. Terborgh, R. Q. Thomas, M. Toledo, A. Torres-Lezama, T. R. van Andel, G. Van der Heijden, I. C. Vieira, S. Vieira, E. Villanova-Torre, V. A. Vos, O. Wang, O. Zartman, C. E. Zartman, Y. Malhi, and H. R. Phillips. 2014. Markedly divergent estimates of Amazon forest carbon density from ground plots and satellites. Global Ecology and Biogeography **23**:935-946.

Montesano, P. M., R. Nelson, G. Sun, H. Margolis, A. Kerber, and K. J. Ranson. 2009. MODIS tree cover validation for the circumpolar taiga–tundra transition zone. Remote Sens. Environ. **113**:2130-2141.

Muraoka, H., and H. Koizumi. 2005. Photosynthetic and structural characteristics of canopy and shrub trees in a cool-temperate deciduous broadleaved forest: Implication to the ecosystem carbon gain. Agricultural and Forest Meteorology **134**:39-59.

Murcia, C. 1995. Edge effects in fragmented forests: implications for conservation. TREE **10**:58-62.

Myneni, R. B., and D. L. Williams. 1994. On the Relationship between FAPAR and NDVI. Remote Sens Environ **49**:200-211.

Nascimento, H. E., and W. F. Laurance. 2004. Biomass dynamics in Amazonian Fragments. Ecological Applications **14**:127-138.

Nathan, R., and R. Casagrandi. 2004. A simple mechanistic model of seed dispersal, predation and plant establishment: Janzen-Connell and beyond. Journal of Ecology **92**:733-746.

Nessimian, J. L., E. M. Venticinque, J. Zuanon, P. De Marco, M. Gordo, L. Fidelis, J. D'arc Batista, and L. Juen. 2008. Land use, habitat integrity, and aquatic insect assemblages in Central Amazonian streams. Hydrobiologia **614**:117-131.

Neumann, M., and A. Reigber. 2010. Estimation of Forest Structure, Ground, and Canopy Layer Characteristics From Multibaseline Polarimetric Interferometric SAR Data. IEEE T Geosci Remote **48**:1086-1104.

Newbold, T., L. N. Hudson, S. L. Hill, S. Contu, I. Lysenko, R. A. Senior, L. Borger, D. J. Bennett, A. Choimes, B. Collen, J. Day, A. De Palma, S. Diaz, S. Echeverria-Londono, M. J. Edgar, A. Feldman, M. Garon, M. L. Harrison, T. Alhusseini, D. J. Ingram, Y. Itescu, J. Kattge, V. Kemp, L. Kirkpatrick, M. Kleyer, D. L. Correia, C. D. Martin, S. Meiri, M. Novosolov, Y. Pan, H. R. Phillips, D. W. Purves, A. Robinson, J. Simpson, S. L. Tuck, E. Weiher, H. J. White, R. M. Ewers, G. M. Mace, J. P. Scharlemann, and A. Purvis. 2015. Global effects of land use on local terrestrial biodiversity. Nature **520**:45-50.

Niemann, K. O., D. G. Goodenough, and G. J. Hay. 1997. Effect of Scale on the Information Content in Remote Sensing Imagery. IEEE Geoscience and Remote Sensing **2**:664-666.

Nobre, A. D. 2014. o Futuro Climático da Amazônia: Relatório de Avaliação Científica.

Oindo, B. O., R. A. de By, and A. K. Skidmore. 2000. Interannual variability of NDVI and bird species diversity in Kenya. International journal of applied earth observation and geoinformation **2**:172-180.

Ojeda, M. I., A. S. Mayer, and B. D. Solomon. 2008. Economic valuation of environmental services sustained by water flows in the Yaqui River Delta. Ecological Economics **65**:155-166.

Oliveira, F. M., V. M. Lira, R. T. Dantas, and W. M. Souza. 2006. Variabilidade temporal da precipitação em municípios localizados em diferentes sub-regiões do Estado de Pernambuco. Caminhos de Geografia **6**:175-184.

Oliveira, M. A., A. M. M. Santos, and M. Tabarelli. 2008. Profound impoverishment of the large-tree stand in a hyper-fragmented landscape of the Atlantic forest. For. Ecol. Manage. **256**:1910-1917.

Ovaskainen, O. 2002. Long-Term Persistence of Species and the SLOSS Problem. J Theor Biol **218**:419-433.

Pagiola, S. 2008. Payments for environmental services in Costa Rica. Ecological Economics **65**:712-724.

Pan, Y., R. A. Birdsey, J. Fang, R. A. Houghton, P. E. Kauppi, W. A. Kurz, O. L. Phillips, A. Shvidenko, S. L. Lewis, J. G. Canadell, P. Ciais, R. B. Jackson, S. W. Pacala, A. D. McGuire, S. L. Piao, A. Rautiainen, S. Stich, and D. Hayes. 2011. A Large and Persistent Carbon Sink in the World's Forests. Science **333**:988-993.

Pascual-Hortal, L., and S. Saura. 2006. Comparison and development of new graph-based landscape connectivity indices: towards the priorization of habitat patches and corridors for conservation. Landscape Ecology **21**:959-967.

Peel, M. C., B. L. Finlayson, and T. A. McMahon. 2007. Updated world map of the Köppen-Geiger climate classification. Hydrol. Earth Syst. Sci. **11**.

Peres, C. A., T. Emilio, J. Schietti, S. J. M. Desmoulière, and T. Levi. 2016. Dispersal limitation induces long-term biomass collapse in overhunted Amazonian forests. Proc Natl Acad Sci U S A **113**:892-897.

Pérez-Hoyos, A., F. J. García-Haro, and J. San-Miguel-Ayanz. 2012. Conventional and fuzzy comparisons of large scale land cover products: Application to CORINE, GLC2000, MODIS and GlobCover in Europe. ISPRS J. Photogramm. Remote. Sens. **74**:185-201.

Pérez-Hoyos, A., B. Martínez, M. A. Gilabert, and F. J. García-Haro. 2010. A multi-temporal analysis of vegetation dynamics in the Iberian peninsula using MODIS-NDVI data. EARSeL eProc **9**:22-30.

Petit, C. C., and E. F. Lambin. 2002. Impact of data integration technique on historical land-use/land-cover change: Comparing historical maps with remote sensing data in the Belgian Ardennes. Landsc Ecol **17**:117-132.

Pettorelli, N. 2013. The normalized difference vegetation index. Oxford University Press.

Pettorelli, N., W. F. Laurance, T. G. O'Brien, M. Wegmann, H. Nagendra, W. Turner, and E. J. Milner-Gulland. 2014. Satellite remote sensing for applied ecologists: opportunities and challenges. Journal of Applied Ecology **51**:839-848.

Pettorelli, N., J. O. Vik, A. Mysterud, J. M. Gaillard, C. J. Tucker, and N. C. Stenseth. 2005. Using the satellite-derived NDVI to assess ecological responses to environmental change. Trends Ecol Evol **20**:503-510.

Pettorelli, N., M. Wegmann, A. Skidmore, S. Mücher, T. P. Dawson, M. Fernandez, R. Lucas, M. E. Schaepman, T. Wang, B. O'Connor, R. H. G. Jongman, P. Kempeneers, R. Sonnenschein, A. K. Leidner, M. Böhm, K. S. He, H. Nagendra, G. Dubois, T. Fatoyinbo, M. C. Hansen, M. Paganini, H. M. de Klerk, G. P. Asner, J. T. Kerr, A. B. Estes, D. S. Schmeller, U. Heiden, D. Rocchini, H. M.

Pereira, E. Turak, N. Fernandez, A. Lausch, M. A. Cho, D. Alcaraz-Segura, M. A. McGeoch, W. Turner, A. Mueller, V. St-Louis, J. Penner, P. Vihervaara, A. Belward, B. Reyers, G. N. Geller, and D. Boyd. 2016. Framing the concept of satellite remote sensing essential biodiversity variables: challenges and future directions. Remote Sensing in Ecology and Conservation:n/a-n/a.

Pinto, S., F. Melo, M. Tabarelli, A. Padovesi, C. Mesquita, C. de Mattos Scaramuzza, P. Castro, H. Carrascosa, M. Calmon, R. Rodrigues, R. César, and P. Brancalion. 2014. Governing and Delivering a Biome-Wide Restoration Initiative: The Case of Atlantic Forest Restoration Pact in Brazil. Forests **5**:2212-2229.

Pinto, S. R. R., G. Mendes, A. M. M. Santos, M. Dantas de Paula, M. Tabarelli, and F. P. Melo. 2010. Landscape attributes drive complex spatial microclimate configuration of Brazilian Atlantic forest fragments. Trop. Conserv. Sci. **3**:389-402.

Plummer, S. E. 2000. Perspectives on combining ecological process models and remotely sensed data. Ecol Model **129**:169-186.

Poiani, K. A., M. D. Merrill, and K. A. Chapman. 2001. Identifying Conservation-Priority Areas in a Fragmented Minnesota Landscape Based on the Umbrella Species Concept and Selection of Large Patches of Natural Vegetation. Conserv. Biol. **15**:513-522.

Poiani, K. A., B. D. Richter, M. G. Anderson, and H. E. Richter. 2000. Biodiversity Conservation at Multiple Scales: Functional Sites, Landscapes, and Networks. BioScience **50**:133-146.

Ponzoni, F. J., and Y. Shimabukuro. 2007. Sensoriamento Remoto no Estudo da Vegetação. Editora Parêntese, São Paulo.

Pôrto, C., J. S. Almeida-Cortez, and M. Tabarelli. 2006. Diversidade Biológica e Conservação da Floresta Atlântica ao Norte do Rio São Francisco. Ministério do Meio Ambiente, Brasília.

Prentice, I. C., and R. Leemans. 1990. Pattern and Process and the Dynamics of Forest Structure: A Simulation Approach. J Ecol **78**:340-355.

Pretzsch. 2009. Forest Dynamics, Growth and Yield. Springer, Berlin Heidelberg.

Putz, F. E., and C. D. Canham. 1992. Mechanisms of arrested succession in shrublands: root and shoot competition between shrubs and tree seedlings. For. Ecol. Manage. **49**:267-275.

Pütz, S., J. Groeneveld, L. F. Alves, J. P. Metzger, and A. Huth. 2011. Fragmentation drives tropical forest fragments to early successional states: A modelling study for Brazilian Atlantic forests. Ecological Modelling **222**:1986-1997.

Pütz, S., J. Groeneveld, K. Henle, C. Knogge, A. C. Martensen, M. Metz, J. P. Metzger, M. C. Ribeiro, M. Dantas de Paula, and A. Huth. 2014. Long-term carbon loss in fragmented Neotropical forests. Nat. Commun. **5**:5037.

Ranson, K. J., P. M. Montesano, and R. Nelson. 2011. Object-based mapping of the circumpolar taiga–tundra ecotone with MODIS tree cover. Remote Sens. Environ. **115**:3670-3680.

Ranson, K. J., G. Sun, J. F. Weishampel, and R. G. Knox. 1997. Forest Biomass from Combined Ecosystem and Radar Backscatter Modeling. Remote Sens Environ **59**:118-133.

Ribeiro, M. C., J. P. Metzger, A. C. Martensen, F. J. Ponzoni, and M. M. Hirota. 2009. The Brazilian Atlantic Forest: How much is left, and how is the remaining forest distributed? Implications for conservation. Biol. Conserv. **142**:1141-1153.

Rodrigues, R. R., S. Gandolfi, A. G. Nave, J. Aronson, T. E. Barreto, C. Y. Vidal, and P. H. S. Brancalion. 2011. Large-scale ecological restoration of high-diversity tropical forests in SE Brazil. For. Ecol. Manage. **261**:1605-1613.

Rodrigues, R. R., R. A. F. Lima, S. Gandolfi, and A. G. Nave. 2009. On the restoration of high diversity forests: 30 years of experience in the Brazilian Atlantic Forest. Biological Conservation **142**:1242-1251.

Rosindell, J., S. P. Hubbell, and R. S. Etienne. 2011. The unified neutral theory of biodiversity and biogeography at age ten. Trends Ecol Evol **26**:340-348.

Rüger, N., Á. G. Gutiérrez, W. D. Kissling, J. J. Armesto, and A. Huth. 2007. Ecological impacts of different harvesting scenarios for temperate evergreen rain forest in southern Chile—A simulation experiment. Forest Ecology and Management **252**:52-66.

Rüger, N., G. Williams-Linera, W. D. Kissling, and A. Huth. 2008. Long-Term Impacts of Fuelwood Extraction on a Tropical Montane Cloud Forest. Ecosystems **11**:868-881.

Saatchi, S. S., N. L. Harris, S. Brown, M. Lefsky, E. T. Mitchard, W. Salas, B. R. Zutta, W. Buermann, S. L. Lewis, S. Hagen, S. Petrova, L. White, M. Silman, and A. Morel. 2011. Benchmark map of forest carbon stocks in tropical regions across three continents. Proc. Natl. Acad. Sci. U S A **108**:9899-9904.

Sala, O. E. 2000. Global Biodiversity Scenarios for the Year 2100. Science **287**:1770-1774.

Sander, H., S. Polasky, and R. G. Haight. 2010. The value of urban tree cover: A hedonic property price model in Ramsey and Dakota Counties, Minnesota, USA. Ecol. Econ. **69**:1646-1656.

Sanderson, E. W., K. H. Redford, A. Vedder, P. B. Coppolillo, and S. E. Ward. 2002. A conceptual model for conservation planning based on landscape species requirements. Landsc. Urban Plan. **58**:51-56.

Santo-Silva, E. E., W. R. Almeida, F. P. Melo, C. S. Zickel, and M. Tabarelli. 2012. The Nature of Seedling Assemblages in a Fragmented Tropical Landscape: Implications for Forest Regeneration. Biotropica **45**:386-394.

Santos, B. A., C. A. Peres, M. A. Oliveira, A. Grillo, C. P. Alves-Costa, and M. Tabarelli. 2008. Drastic erosion in functional attributes of tree assemblages in Atlantic forest fragments of northeastern Brazil. Biol. Cons. **141**:249-260.

Satake, A., and T. K. Rudel. 2007. Modeling the forest transition: forest scarcity and ecosystem service hypothesis. Ecological Applications **17**:2024-2036.

Saunders, D. A., R. J. Hobbs, and C. R. Margules. 1991. Biological Consequences of Ecosystem Fragmentation: A Review. Conservation Biology **5**:18-32.

Saxton, K. E., and W. J. Rawls. 2006. Soil Water Characteristic Estimates by Texture and Organic Matter for Hydrologic Solutions. Soil Science Society of America Journal **70**:1569.

Schloss, A. L., D. W. Kicklighter, J. Kaduk, U. Wittenberg, T. Intercomparison, and P. O. T. P. N. Model. 1999. Comparing global models of terrestrial net primary productivity (NPP): comparison of NPP to climate and the Normalized Difference Vegetation Index (NDVI). Glob Chang Biol **5**:25-34.

Schmolke, A., P. Thorbek, D. L. DeAngelis, and V. Grimm. 2010. Ecological models supporting environmental decision making: a strategy for the future. Trends Ecol Evol **25**:479-486.

Seddon, A. W., M. Macias-Fauria, P. R. Long, D. Benz, and K. J. Willis. 2016. Sensitivity of global terrestrial ecosystems to climate variability. Nature **531**:229-232.

Sexton, J. O., P. Noojipady, A. Anand, X.-P. Song, S. McMahon, C. Huang, M. Feng, S. Channan, and J. R. Townshend. 2015. A model for the propagation of uncertainty from continuous estimates of tree cover to categorical forest cover and change. Remote Sensing of Environment **156**:418-425.

Sexton, J. O., X.-P. Song, M. Feng, P. Noojipady, A. Anand, C. Huang, D.-H. Kim, K. M. Collins, S. Channan, C. DiMiceli, and J. R. Townshend. 2013. Global, 30-m resolution continuous fields of tree cover: Landsat-based rescaling of MODIS vegetation continuous fields with lidar-based estimates of error. Int. J. Digit. Earth **6**:427-448.

Shugart, H. H. 1984. A Theory of Forest Dynamics: The Ecological Implications of Forest Succession Models. Springer.

Shugart, H. H. 1998. Terrestrial ecosystems in changing environments. Cambridge University Press.

Shugart, H. H., G. P. Asner, R. Fischer, A. Huth, N. Knapp, T. Le Toan, and J. K. Shuman. 2015. Computer and remote-sensing infrastructure to enhance large-scale testing of individual-based forest models. Frontiers in Ecology and the Environment **13**:503-511.

Shugart, H. H., and I. R. Noble. 1981. A computer model of succession and fire response of the high-altitude Eucalyptus forest of the Brindahella Range, Australian Capital Territory. Aust J Ecol **6**:149-164.

Silva, J. M. C., and M. Tabarelli. 2000. Tree species impoverishment and the future flora of the Atlantic forest of northeast Brazil. Nature **404**:72-74.

Skidmore, A., and N. Pettorelli. 2015. Agree on biodiversity metrics to track from space. Nature **523**:403-405.

Slik, J. W. 2015. Correction for Slik et al., An estimate of the number of tropical tree species. Proc Natl Acad Sci U S A **112**:E4628-4629.

Sloan, S., and J. A. Sayer. 2015. Forest Resources Assessment of 2015 shows positive global trends but forest loss and degradation persist in poor tropical countries. For. Ecol. Manage. **352**:134-145.

Sobrinho, J. V. 1971. As Regiões Naturais do Nordeste o Meio e a Civilização. CONDEPE, Recife.

Spracklen, D. V., S. R. Arnold, and C. M. Taylor. 2012. Observations of increased tropical rainfall preceded by air passage over forests. Nature **489**:282-285.

Stocks, B. J., B. W. van Wilgen, W. S. W. Trollope, D. J. McRae, J. A. Mason, F. Weirich, and A. L. F. Potgieter. 1996. Fuels and fire behavior dynamics on large-scale savanna fires in Kruger National Park, South Africa. Journal of Geophysical Research **101**:23541.

Su, Y., Q. Guo, B. Xue, T. Hu, O. Alvarez, S. Tao, and J. Fang. 2016. Spatial distribution of forest aboveground biomass in China: Estimation through combination of spaceborne lidar, optical imagery, and forest inventory data. Remote Sensing of Environment **173**:187-199.

Tabarelli, M., and A. V. Lopes. 2008. Edge-effects Drive Tropical Forest Fragments Towards an Early-Successional System. Biotropica **40**:657-661.

Tabarelli, M., C. A. Peres, and F. P. L. Melo. 2012. The 'few winners and many losers' paradigm revisited: Emerging prospects for tropical forest biodiversity. Biological Conservation **155**:136-140.

Tabarelli, M., J. M. C. Silva, and C. Gascon. 2004. Forest fragmentation, synergisms and the impoverishment of neotropical forests. Biodivers. Conserv. **13**:1419-1425.

Tamme, R., L. Götzenberger, M. Zobel, J. M. Bullock, D. A. P. Hooftman, A. Kaasik, and M. Partel. 2014. Predicting species' maximum dispersal distances from simple plant traits. Ecology **95**:505-513.

Terborgh, J., L. Lopez, P. V. Nuñez, M. Rao, G. Shahabuddin, G. Orihuela, M. Riveros, R. Ascanio, G. H. Adler, T. D. Lambert, and L. Balbas. 2001. Ecological Meltdown in Predator-Free Forest Fragments. Science **294**:1923-1926.

Thomson, F. J., A. T. Moles, T. D. Auld, and R. T. Kingsford. 2011. Seed dispersal distance is more strongly correlated with plant height than with seed mass. Journal of Ecology **99**:1299-1307.

Tilman, D., R. M. May, C. L. Lehman, and M. A. Nowak. 1994. Habitat destruction and the extinction debt. Nature **371**:65-66.

Townsend, A. R., G. P. Asner, and C. C. Cleveland. 2008. The biogeochemical heterogeneity of tropical forests. Trends Ecol Evol **23**:424-431.

Townshend, J. R., M. C. Hansen, M. Carroll, C. DiMiceli, R. Sohlberg, and C. Huang. 2011. User Guide for the MODIS Vegetation Continuous Fields product Collection 5 version 1.*in* U. o. Maryland, editor. University of Maryland, Maryland.

Trainor, A. M., J. R. Walters, W. F. Morris, J. Sexton, and A. Moody. 2013. Empirical estimation of dispersal resistance surfaces: a case study with red-cockaded woodpeckers. Landsc. Ecol. **28**:755-767.

Trancoso, R., A. Carneiro Filho, J. Tomasella, J. Schietti, B. R. Forsberg, and R. P. Miller. 2010. Deforestation and conservation in major watersheds of the Brazilian Amazon. Environmental Conservation **36**:277-288.

UNFCC. 2014. New York Declaration of Forests - Action Statements and Action Plans. United Nations, New York.

Urban, D. L., G. B. Bonan, T. M. Smith, and H. H. Shugart. 1991. Spatial applications of gap models. For. Ecol. Manage. **42**:95-110.

Ustin, S. L. 2004. Remote Sensing for Natural Resource Management and Environmental Monitoring. 3 edition. John Wiley and Sons, Hoboken, New Jersey.

van Daalen, J. C., and H. H. Shugart. 1989. OUTENIQUA - A computer model to simulate succession in the mixed evergreen forests of the southern Cape, South Africa. Landsc Ecol **2**:255-267.

van Dijk, A. I. J. M., and R. J. Keenan. 2007. Planted forests and water in perspective. Forest Ecology and Management **251**:1-9.

van Lierop, P., E. Lindquist, S. Sathyapala, and G. Franceschini. 2015. Global forest area disturbance from fire, insect pests, diseases and severe weather events. Forest Ecology and Management **352**:78-88.

van Oijen, M., C. Reyer, F. J. Bohn, D. R. Cameron, G. Deckmyn, M. Flechsig, S. Härkönen, F. Hartig, A. Huth, A. Kiviste, P. Lasch, A. Mäkelä, T. Mette, F. Minunno, and W. Rammer. 2013. Bayesian calibration, comparison and averaging of six forest models, using data from Scots pine stands across Europe. Forest Ecology and Management **289**:255-268.

Vellend, M., K. Verheyen, H. Jacquemyn, A. Kolb, H. V. Calster, G. Peterken, and M. Hermy. 2006. Extinction debt of forest plants persists for more than a century following habitat fragmentation. Ecology **87**:542-548.

Veríssimo, A., P. Barreto, R. Tarifa, and C. Uhl. 1995. Extraction of a high-value natural resource in Amazonia: the case of mahogany. For. Ecol. Manage. **72**:39-60.

Villard, M.-A., J. P. Metzger, and S. Saura. 2014. REVIEW: Beyond the fragmentation debate: a conceptual model to predict when habitat configuration really matters. J. Appl. Ecol. **51**:309-318.

Visser, M. D., M. Bruijning, S. J. Wright, H. C. Muller-Landau, E. Jongejans, L. S. Comita, H. de Kroon, and C. Merow. 2016. Functional traits as predictors of vital rates across the life cycle of tropical trees. Functional Ecology **30**:168-180.

Wade, T. G., K. H. Riiters, J. D. Wickham, and K. B. Jones. 2003. Distribution and Causes of Global Forest Fragmentation. Conserv. Ecol. **7**.

Walker, B., A. Kinzig, and J. Langridge. 1999. Plant Attribute Diversity, Resilience, and Ecosystem Function: The Nature and Significance of Dominant and Minor Species. Ecosystems **2**:95-113.

Wang, Q., S. Adiku, J. Tenhunen, and A. Granier. 2005. On the relationship of NDVI with leaf area index in a deciduous forest site. Remote Sensing of Environment **94**:244-255.

Wirth, R., S. T. Meyer, I. R. Leal, and M. Tabarelli. 2008. Plant Herbivore Interactions at the Forest Edge. Springer-Verlag, Berlin Heidelberg.

Wright, J. S. 2002. Plant diversity in tropical forests: a review of mechanisms of species coexistence. Oecologia **130**:1-14.

Wright, J. S., A. Hernández, and R. Condit. 2007. The Bushmeat harvest alterls seedling banks by favoring lianas, large seeds, and seeds dispersed by bats, birds and wind. Biotropica **39**:363-371.

Wright, J. S., H. Zeballos, I. Domínguez, M. M. Gallardo, M. C. Moreno, and R. Ibáñez. 2000. Poachers Alter Mammal Abundance, Seed Dispersal, and Seed Predation in a Neotropical Forest. Conserv Biol **14**:227-239.

Xiao, X. 2004. Modeling gross primary production of temperate deciduous broadleaf forest using satellite images and climate data. Remote Sensing of Environment **91**:256-270.

ZAAL. 2009. Zoneamento Agroecológico de Alagoas – Mapa de reconhecimento de baixa e média intensidade de solos. EMBRAPA.

Zheng, D., and J. Chen. 2000. Edge effects in fragmented landscapes: a generic model for delineating area of edge influences (D-AEI). Ecological Modelling **132**:175-190.

Zolkos, S. G., S. J. Goetz, and R. Dubayah. 2013. A meta-analysis of terrestrial aboveground biomass estimation using lidar remote sensing. Remote Sensing of Environment **128**:289-298.